CHARACTERISTICS AND EFFECTS OF METAL(II)−DOPED IRON OXIDES ON THE REACTIVITY OF THE ACTIVATED IRON MEDIA TREATMENT SYSTEM

A Dissertation

by

SIN-HONG LIN

Submitted to the Office of Graduate and Professional Studies of
Texas A&M University
in partial fulfillment of the requirements for the degree of

DOCTOR OF PHILOSOPHY

Chair of Committee,	Yongheng Huang
Committee Members,	Binayak Mohanty
	Hongbin Zhan
	Raghupathy Karthikeyan
Head of Department,	Steve Searcy

December 2016

Major Subject: Biological and Agricultural Engineering

ABSTRACT

The activated iron media (AIM) treatment system is an innovative ZVI-based water treatment technology for removing heavy metals, reactive oxyanions and nutrients from a contaminated water stream. The AIM treatment system consists of zero-valent iron (ZVI), iron oxides represented by magnetite and ferrous iron. When the AIM immobilizes heavy metals from wastewaters, the heavy metals are entrapped as impurities in the iron oxides. The metal impurities may alter the physical/chemical properties of the iron oxides, and thus affect the reactivity of the AIM system.

In this study, Mn^{2+} and Zn^{2+}, two heavy metals commonly found in industrial wastewaters, were chosen to evaluate their effect on the magnetite-coated ZVI for nitrate and selenate removal in batch experiments. The results demonstrated that a magnetite-coated ZVI system with Mn^{2+} additions could effectively reduce both nitrate and selenate. Mn^{2+} could substitute structural Fe(II) of the magnetite, releasing dissolved Fe^{2+}. The co-existence of Mn^{2+} and Fe^{2+} with magnetite-coated ZVI can retain the media reactivity for both nitrate and selenite reduction, and the inverse spinel crystal structure of magnetite is not altered by the introduction of Mn(II) into its structure.

Unlike Mn^{2+} additions, a magnetite-coated ZVI system with added Zn^{2+} effectively reduces selenate, but nitrate reduction is significantly inhibited. Zn^{2+} was incorporated into the iron oxide coating, but the original magnetite structure was altered. Both aqueous Zn^{2+} and structural Zn(II) could effectively suppress nitrate reduction in a

magnetite-coated ZVI system. The role of Zn^{2+} addition on nitrate reduction inhibition was also confirmed by the continuous stirred-tank reactor (CSTR) experiments.

The results showed that adding metal impurities into the AIM treatment system could significantly influence the removal performance for particular contaminants. The effect of metal ions other than Mn^{2+} and Zn^{2+} should be investigated to understand more potentials of the AIM treatment system for applications in the future research.

ACKNOWLEDGEMENTS

I am sincerely grateful to my committee chair, Dr. Yongheng Huang. Under his guidance, I learned the significance of research with the critical thinking skill for my successful achievements in academia. I am also thankful to Dr. Huang for his supports to provide me beneficial resources for research and for his research diversities to bring me an innovative technology with laboratory and field experiences for comprehensive understandings.

I am very appreciative to my committee members, Dr. Binayak Mohanty, Dr. Hongbin Zhan, and Dr. Raghupathy Karthikeyan for their guidance and support throughout the course of this research. I would like to thank Dr. Yordanos Birsrat and Dr. Jing Wu in Material Characterization Facility and Dr. Joseph H. Reibenspies in X-ray Diffraction Laboratory at Texas A&M University for their assistance for my research.

I also like to extend my gratitude to my friends and colleagues and the department faculty and staff for bringing me a great experience, life and journey at Texas A&M University. They are just like my partners to help me during my PhD life when necessary.

Lastly, thanks to my family for their selfless supports, patience, encouragement, and love. Without their help, I could not successfully have done my PhD degree. Furthermore, special thanks to my wife, Verna, and my little dog, Brownie for their company during my PhD life.

NOMENCLATURE

µm	microMeter
µM	microMolar
µS	microSiemens
AIM	Activated Iron Media
Al^{3+}	Aluminum Ion
As(III)	Arsenite
As(V)	Arsenate
BET	Brunauer, Emmett, and Teller
Cl^-	Chloride Ion
cm	Centimeter
Co^{2+}	Cobalt Ion
Cr^{6+}	Hexavalent Chromium Ion
Cs+	Cesium Ion
CSTR	Continuous Stirred-Tank Reactor
CT	Carbon Tetrachloride
Cu^{2+}	Copper Ion
d	Day(s)
DDI	Deoxygenated Deionized
DI	Deionized
EC	Electrical Conductivity

EDS	Energy Dispersive Spectroscopy
Fe^0	Elemental Iron
Fe^{2+}	Ferrous Iron
Fe^{3+}	Ferric Iron
Fe_3O_4	Magnetite
$FeCl_2$	Ferrous Chloride
FeOx	Iron Oxides
FE-SEM	Field Emission Scanning Electron Microscope
h	Hour(s)
H+	Hydrogen Ion
H_2O	Water
H_2O_2	Hydrogen Peroxide
HRT	Hydraulic Retention Time
IC	Ion Chromatography
L	Liter
M	Molarity
MCI	Magnetite-Coated ZVI
mg/L	Milligrams Per Liter
mM	milliMolar
$Mn(OH)_2$	Manganese Hydroxide
Mn^{2+}	Divalent Manganese
Mn_3O_4	Hausmannite

$MnFe_2O_4$	Manganese Ferrite
mV	millivolt
N_2	Nitrogen Gas
N_2O	Nitrous Oxide
Na^+	Sodium Ion
Na_2SeO_4	Sodium Selenate
NaCl	Sodium Chloride
$NaNO_3$	Sodium Nitrate
NH_4^+	Ammonium
NO	Nitric Oxide
NO_2^-	Nitrite
NO_3^-	Nitrate
nZVI	Nano Zero-Valent Iron
OH^-	Hydroxyl Ion
ORP	Oxidation-Reduction Potential
PCBs	Polychlorinated Biphenyls
PCE	Perchloroethene
PRB	Permeable Reactive Barriers
Pu(III)	Trivalent Plutonium
Pu(V)	Pentavalent Plutonium
PZC	Point of Zero Charge
Se	Selenium

Se^{2-}	Selenide
SeO_3^{2-}	Selenite
SeO_4^{2-}	Selenate
SO_4^{2-}	Sulfate
TCE	Tricholoroethylene
Ti^{4+}	Titanium Ion
U(IV)	Tetravalent Uranium
U(VI)	Hexavalent Uranium
UO_2^{2+}	Uranyl Ion
USEPA	U.S. Environmental Protection Agency
XPS	X-Ray Photoelectron Spectroscopy
XRD	X-Ray Diffraction
Zn^{2+}	Divalent Zinc
$ZnCl_2$	Zinc Chloride
ZVI	Zero-Valent Iron
α-Fe_2O_3	Hematite
α-FeOOH	Goethite
γ-Fe_2O_3	Maghemite
γ-Fe_2O_3	Maghemite
γ-FeOOH	Lepidocrocite

TABLE OF CONTENTS

Page

LIST OF FIGURES

Page

LIST OF TABLES

Page

CHAPTER I INTRODUCTION

Zero-Valent Iron Technology

Zero-valent iron (ZVI), a reactive media for groundwater remediation, has been widely used for treating both organic and inorganic contaminants including polychlorinated biphenyls (PCBs), perchloroethene (PCE), tricholoroethylene (TCE), carbon tetrachloride (CT), nitrobenzene, uranyl, chromate, selenate, nitrate, molybdate, arsenic, and lead (Cantrell et al., 1995, Siantar et al., 1996, Wang and Zhang, 1997, Zhang, 2003, Huang et al., 2003, Joo et al., 2004, Noubactep et al., 2005, Morrison et al., 2006, Li et al., 2006, Noubactep, 2008, Coelho et al., 2008, Sasaki et al., 2008, , Huang et al., 2012, Tang et al., 2014). ZVI, a relatively inexpensive material, is a moderate reducing agent with a standard redox potential of $E^0 = -0.44V$ for $Fe^{2+} + 2e^- \rightarrow Fe^0$, and $E^0 = -0.04V$ for $Fe^{3+} + 3e^- \rightarrow Fe^0$. The primary mechanism responsible for contaminants removal by ZVI is chemical reduction, in which electrons transfer from ZVI grains to the target contaminants. As a consequence, elemental iron is oxidized to divalent iron or trivalent iron, and contaminants are reduced to a lower oxidation state. Subsequently, contaminants are generally transformed to non- or less toxic species.

The permeable reactive barriers (PRBs) using ZVI as the reactive media, a remediation technology developed in early 1990s for containing or cleaning up groundwater contaminant plumes, have been extensively studied in laboratory and field tests for over two decades (Reynolds et al., 1990, Gillham and O'Hannesin, 1994, Gavaskar et al., 1998, Gu et al., 1999, Li et al., 2006). The main removal mechanisms of

ZVI-based PRBs include chemical reduction, adsorption, and precipitation. PRBs using ZVI is generally considered as a cost-effective technology and recommended by the U.S. Environmental Protection Agency as a viable technology for various environmental remediation applications (USEPA, 2002).

A recent development of ZVI technology is the use of nanoscale zero-valent iron (nZVI) that provides much larger specific surface area and can achieve a higher reactivity than traditional ZVI media (e.g., -100 mesh). nZVI with increased flexibility for in situ and ex situ application due to its fine size is very effective for detoxification and removal of common contaminants including chlorinated solvents, pesticides and PCBs (Liu and Lowry, 2006, Grieger et al., 2010, Kim et al., 2010, Jiemvarangkul et al., 2011, Mueller et al., 2012, O'Carroll et al., 2013, Gomes et al., 2015). However, nZVI is constrained by its high cost, short life-span, and high chemical risk associated with its fine size and high reactivity.

Iron corrosion may result in the decrease of ZVI reactivity. As the iron media interact with the environments including reactions with not only target contaminants but also dissolved oxygen or even water, iron is oxidized or corroded, producing corrosion products often being referred to as the iron rusts that form a coating on the ZVI surface. Depending on the aquatic chemistry and other conditions, the iron rusts could be in forms of iron oxides, hydroxides, or oxy-hydroxides (FeOx), such as magnetite (Fe_3O_4), goethite (α-FeOOH), lepidocrocite (γ-FeOOH), hematite (α-Fe_2O_3), and maghemite (γ-Fe_2O_3). When iron grains are covered by a thick FeOx film, the FeOx layer might act as an electron transfer barrier, especially in form of ferric oxides. Consequently, the

interaction between ZVI and contaminants is blocked by the FeOx coatings. Thus, ZVI will lose its reactivity and become passivated. ZVI passivation has been a major obstacle to the broader applications of the technology. Much of the past research had focused on how to overcome the passivation and rejuvenate ZVI surface to sustain the media's reactivity.

Enhancement of ZVI Reactivity with Metal Ion Additions

The reactivity of ZVI media could be improved by metal ion additions in ZVI systems. Huang et al., (2003) demonstrated that adding ferrous iron into a ZVI system could greatly facilitate nitrate reduction by ZVI. In the ZVI/Fe^{2+} system, aqueous Fe^{2+} was found to transform the passivated layer of an oxidized iron oxide film on ZVI surface to a reactive magnetite (Fe_3O_4) coating to support nitrate reduction reaction. Huang et al. (2003) also proved that other metal ions of Fe^{3+}, Al^{3+}, and Cu^{2+} could enhance nitrate removal in a Fe^0-H_2O system.

Tang et al. (2014) showed that adding Co^{2+} and Mn^{2+} into a ZVI system could significantly promote the iron reactivity for selenate reduction. During selenate reduction process, these metal ions could be incorporated into the structure of magnetite due to similar ionic radius and valence to Fe^{2+}. More Co^{2+} and Mn^{2+} in the structure of magnetite would significantly enhanced reactivity in the ZVI-H_2O_2 system (Costa et al., 2006). Tang et al. (2012) demonstrated that Fe^{3+}, Al^{3+}, and Cu^{2+} could improve the reaction kinetics of nitrate reduction in ZVI systems under alkaline condition with soils. Satapanajaru et al. (2003) proved that metolachlor destruction rate was enhanced with Fe^{2+}, Fe^{3+}, and Al^{3+} in ZVI systems.

The Activated Iron Media Treatment System

The activated iron media (AIM) treatment system, invented by Dr. Yongheng Huang at Texas A&M University, is a ZVI-based water treatment technology developed primarily for removing heavy metals, reactive oxyanions and nutrients from a contaminated water stream. The AIM treatment system consists of Fe^0, Fe_3O_4, and Fe^{2+}. Fe_3O_4 may exist as a coating on Fe0 surface or in form of discrete particles. Fe^{2+} may be introduced by adding ferrous salt into the reactor and present as dissolved Fe^{2+} and surface bound $Fe^{(II)}$. Fe^0 is the major electron donor. The primary mechanisms of contaminant removal in the AIM treatment system may include (1) chemical reduction, (2) physical/chemical adsorption, (3) co-precipitation, and (4) lattice substitution.

Fe^{2+} in the AIM treatment system plays a key role in overcoming the passivation of ZVI surface. Fe^{2+} could regulate the FeOx-water interfacial chemistry to facilitate the transformation of iron corrosion products towards magnetite. Adding Fe^{2+} into a ZVI system would enhance the ZVI reactivity, and significantly increase the removal kinetics with the presence of magnetite coatings (Huang et al., 2003, Huang et al., 2004, Huang et al., 2005, Huang and Zhang, 2006a).

Magnetite, with the lowest electrical resistivity among iron oxides, exhibits metal-like electron conductivity. For ZVI grains with a magnetite coating, electrons produced from iron grains could travel virtually freely in the structure of magnetite to reach the FeOx-water interface to support various redox reactions. . Magnetite not only plays an important key role in removing contaminants including selenate and molybdate by redox reaction (Huang et al, 2012, Tang et al, 2014), but also in immobilizing

contaminants including Co^{2+}, UO_2^{2+}, Cs^{+}, Cr^{6+}, Se^{4+}, As(III), and As(V) by adsorption mechanism (Petrova et al., 2011). Magnetite ($Fe^{II}Fe_2^{III}O_4$) is a mixed iron(II) and iron(III) oxide with an ideal stoichiometric ratio of Fe(II):Fe(III) = 1:2. In the AIM treatment system, however, magnetite could develop a nonstoichiometric ratio of $Fe^{(II)}$:$Fe^{(III)}$ of > 1:2, to become $Fe^{(II)}$-rich Fe_3O_4. Fe(II)-rich Fe_3O_4 could be an effective reductant for redox reaction. Furthermore, the ion diffusion capacity of magnetite would stimulate oxygen/hydroxyl ions to diffuse into the solid structure to react with Fe^{2+} and Fe^{3+} to constitute iron corrosion products that would transform to magnetite with Fe^{2+} addition.

The potential of the AIM treatment system has been effectively demonstrated in both the laboratory and field tests for treating nitrate, selenate, molybdate, mercury, and hexavalent chromium-contaminated industrial wastewaters including oil & gas co-produced water, refinery stripped sour water, mining drainage, and flue-gas-desulfurization (FGD) wastewater from several power plants (Huang et al., 2012, Huang et al., 2013a, Huang et al., 2013b, Huang et al., 2013c). These successful demonstrations proved that the AIM treatment system is a highly effective treatment platform with robustness and flexibilities for immobilization, transformation, and mineralization of various heavy metals and contaminants.

Knowledge Gap

Magnetite in the AIM treatment system shows a great capacity in the incorporation of various impurities into its structure due to its unique properties of non-stoichiometry and structural flexibility. When the AIM treatment system treats heavy

metal-contaminated wastewaters, heavy metals are removed primarily through redox reaction, immobilization, or lattice substitution. The immobilized/substituted heavy metals, such as selenium and molybdenum, are entrapped as impurities in the structure of magnetite coatings, resulting in the alteration of chemical composition of magnetite. The different chemical composition of magnetite may exhibit distinct physical/chemical properties of reactive surface sites, cation exchange capacity, and electrical and ionic conductivity other than pure magnetite, and thus standard redox potential of magnetite with impurities might be affected with respect to its reactivity for different contaminants. Consequently, the performance of the highly reactive AIM treatment system may be greatly influenced by metal ion incorporations into the magnetite structure. However, the effect of the magnetite coatings incorporated with impurities in the activated iron treatment system for contaminant removal is not extensively investigated.

For the ZVI-based treatment technology, nitrate reduction reveals unique challenges. First, most reliable literatures reported that nitrate was reduced by ZVI to ammonia, not nitrogen gas as in the process of biological denitrification. Ammonia as the final product, a pollutant considered by some worse than nitrate, is not desirable (Cheng et al., 1997, Alowitz and Scherer, 2002, Huang et al., 2004, Yang and Lee, 2005). In addition to ammonia production, nitrate reduction by ZVI greatly increases ZVI consumption and sludge production. For instance, when treating a typical FGD wastewater with 20 mg/L of nitrate–N (1.4 mM) and 2.0 mg/L of selenate–Se (25.3 μM), the amounts of ZVI consumed would be 3.8 mM (212.7 g/m^3) for nitrate reduction and 50.6 μM (2.8 g/m^3) for selenate reduction, respectively. For wastewaters with significant

nitrate level, nitrate reduction could be responsible for most of ZVI consumption. Last, nitrate in wastewater may slow reaction kinetics for other target contaminants as nitrate competes with other contaminants for the limited available electrons released from ZVI corrosion.

To mitigate the potential problems resulted from nitrate reduction by ZVI, one solution is to control the reaction system to achieve selective inhibition of nitrate reduction, in which other target metal oxyanions such as selenate could be reduced but not nitrate. The potential benefits of suppressing nitrate reduction in a ZVI system could include: (1) potentially increasing the contaminant removal kinetics without the competition of nitrate to other contaminants, (2) decreasing ZVI media consumption and the sludge production, (3) decreasing the cost of chemical usage, operation, and maintenance, and (4) preventing the formation of ammonia.

Anecdotal evidences from some of our previous tests suggested that selectively inhibiting nitrate reduction in the ZVI-based treatment may be achievable. In most field tests with the AIM treatment system to date, nitrate and selenate were found to be simultaneously reduced to below 0.1 mg/L as nitrogen and 10 μg/L as selenium, respectively. However, there were two occasions in which selenate removal was normal (>98% removal) but nitrate reduction was limited (<10% removal). We screened through the potential factors that might contribute to the unusual results, but due to the complexity of the FGD wastewater quality and the field operational conditions, we could not definitively identify the factors and mechanisms that triggered nitrate reduction inhibition. Moreover, the phenomenon of nitrate reduction inhibition could not be

reproduced in laboratory environments, even though the industrial wastewater from the same power plant was treated by the AIM treatment system in laboratory tests. The process and mechanism of nitrate reduction inhibition is still not clear.

Research Hypothesis

The reactivity of the AIM treatment system is dependent on the chemical compositions and impurities in the iron oxide phase in the reactive media. The different chemical compositions of iron oxide could impart distinct physical and chemical properties with unique morphology, pore structure, surface area, ion strength, electrical conductivity, adsorption capacity, and cation/anion exchange capacity. These properties could affect the system reactivity of the AIM treatment system for aqueous contaminants removal from polluted wastewater.

A conceptual model of $M^{(II)}$ modified iron oxides was shown in Fig. 1. Magnetite-coated ZVI refers to a layered structure with ZVI grains in the core and a magnetite coating on the surface. When a divalent metal ion, $M^{(II)}$, contacts the magnetite coating, surface adsorption and ion exchange/substitution might follow, resulting in the exchange between $M^{(II)}$ and structural $Fe^{(II)}/Fe^{(III)}$. As more $M^{(II)}$ ions are incorporated as impurities in the iron oxide phase, the morphology, structure, electron transfer capacity, redox potential, and other physical and chemical properties of the iron oxide phase could be altered. Consequently, electrons from ZVI core might not move as freely through $M^{(II)}$-doped magnetite as through a pure magnetite layer, shown in Fig. 1(b). When the outer layer of magnetite-coated ZVI was mostly replaced by $M^{(II)}$ oxides coating, shown in Fig. 1(d), the chemical properties of ZVI media with $M^{(II)}$-doped iron

oxide coating could be significantly altered; for example, electron transfer in $M^{(II)}$-doped iron oxides could be more constrained due to higher electrical resistivity, resulting in a slower redox reaction in the $M^{(II)}$ oxides-water interface.

The chemical redox potential of magnetite-coated ZVI, related to the physical/chemical properties, could be affected with the presence of $M^{(II)}$ impurities. The schematic diagram in Fig. 2 illustrated the conceptual chemical composition and redox potential profiles of $M^{(II)}$ doped magnetite-coated ZVI from the inner layer to the outer layer (Fe^0, Fe_3O_4, $M^{(II)}$- Fe_3O_4, and $M^{(II)}$-rich Fe_3O_4). The chemical redox potential of the magnetite coating is constant and high with the ideal stoichiometric ratio of $Fe^{(III)}$ and $Fe^{(II)}$ of 2:1, shown in Fig. 2(a) and 2(b). In the transition phase of $M^{(II)}$- Fe_3O_4, the chemical composition of metal ions could be varied with distance due to ion diffusion in a solid structure. In the meantime, the available redox potential could be greatly reduced because of the impurity incorporation. Once the outer layer of magnetite-coated ZVI becomes $M^{(II)}$-rich Fe_3O_4, the chemical composition turns into $M^{(II)}$ dominated. Subsequently, the available redox potential could be relatively lower than the magnetite coatings and might not be strong enough for supporting the specific contaminant reduction due to thermodynamically unfavorable conditions.

Base on the conceptual model that describes the effect of the impurities (M(II)) on the available redox potential on the media surface, we postulated that nitrate reduction might be inhibited by manipulating $M^{(II)}$ impurities in the magnetite-coated ZVI structure. When the available chemical redox potential of $M^{(II)}$ doped magnetite-coated ZVI with selected $M^{(II)}$ additions is lower than the required minimum redox

potential needed to trigger nitrate reduction on the solid-liquid interface, nitrate reduction would not occur. However, other contaminants that requires less strict redox conditions might still be reduced, such as selenate. The impurities, such as Mn^{2+} and Zn^{2+}, could be incorporated into the iron oxide phase due to the similar ionic radius and valence to iron. The reactivity of magnetite-coated ZVI with impurity M(II) incorporation would be altered with the changes in morphology, pore structure, surface area, and electrical and ionic conductivity. Due to the impurities incorporation, the modified magnetite-coated ZVI could selectively suppress nitrate reduction but still retain its capacity for reducing other contaminants in an aqueous system.

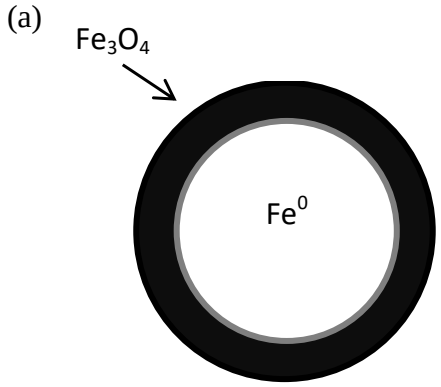

Figure 1. The conceptual model of modified iron oxides in the metal ion incorporation process for magnetite-coated ZVI transformation (a) pure magnetite-coated ZVI; (b) $M^{(II)}$-doped magnetite-coated ZVI; (c) $M^{(II)}$-rich doped magnetite-coated ZVI; (d) $M^{(II)}$ oxides coated magnetite-coated ZVI.

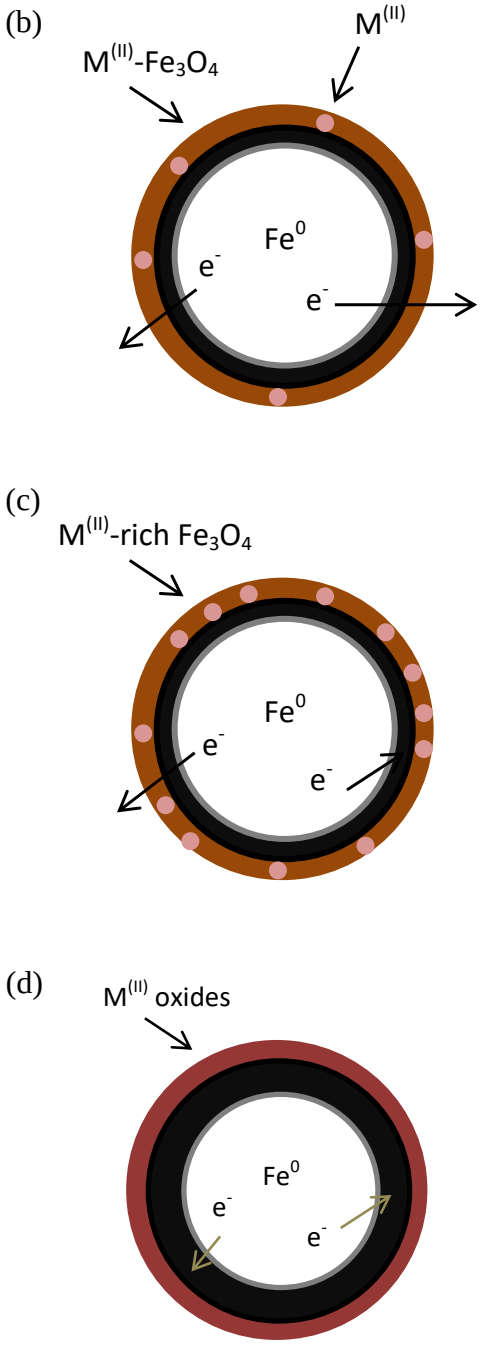

Figure 1. Continued.

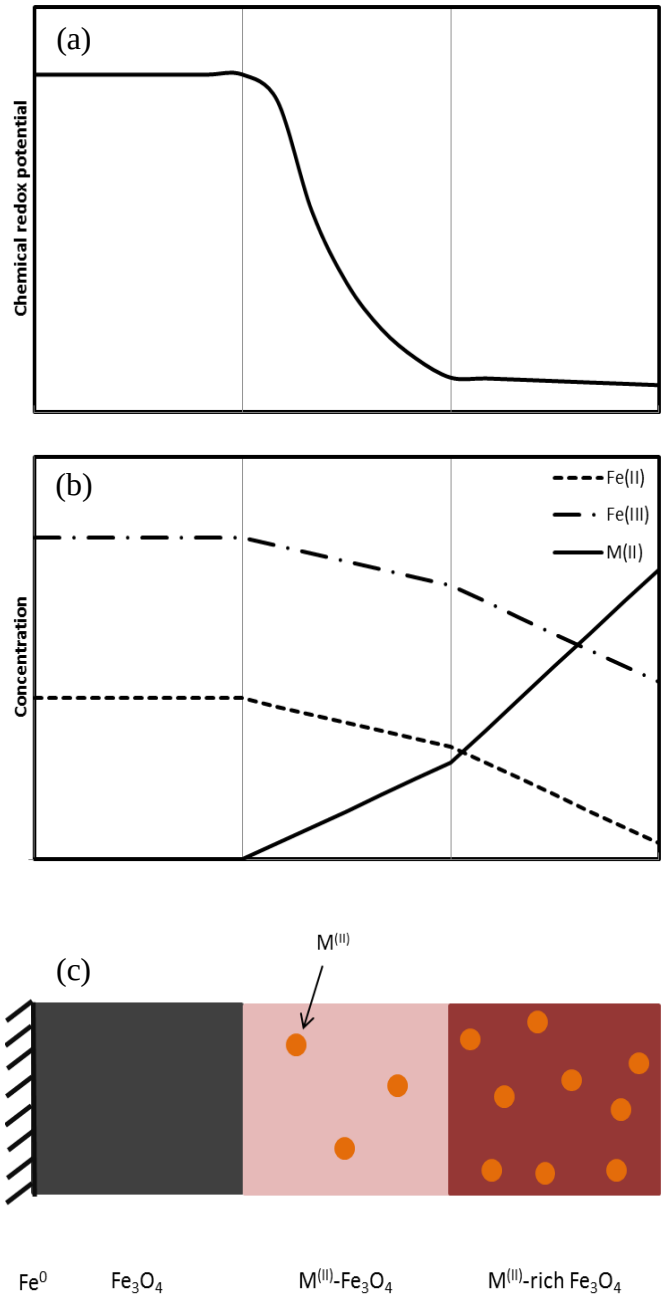

Figure 2. The conceptual model of the available chemical redox potential distribution over depth in a multiple layered $M^{(II)}$-Fe oxide coating structure. (a) The available chemical redox potential along the depth of the iron oxide coating; (b) Metal ions concentration profiles of Fe(II), Fe(III), and $M^{(II)}$; and (c) A layered structure of the oxide coating on ZVI grains.

Research Objectives

In this study, Mn^{2+} and Zn^{2+} were selected as metal cations to dope the iron oxide phase of the activated iron media. Both metallic Zn and Mn rank ahead of Fe in metal reactivity series, i.e., Zn and Mn exhibit lower standard electrode potentials than Fe. Thus, in a ZVI-based reactive system, Zn^{2+} and Mn^{2+} could not be thermodynamically reduced to Zn(0) and Mn(0); when Zn(II) and Mn(II) were incorporated into the iron oxide structure, they would not be reduced to Zn(0) or Mn(0) (as Cu(II) would become Cu(0)). In a ZVI/Fe_3O_4 media system, Zn^{2+} and Mn^{2+} could replace the structural $Fe^{(II)}/Fe^{(III)}$ of magnetite through isomorphic substitution due to the similarities in ionic radius and valance to iron ions. Thus, the introduction of Zn and Mn could form M(II)-doped iron oxides.

This study is to elucidate the interactions between the activated iron components (Fe^0, Fe_3O_4, Fe(II)) and the selected metal cations of Mn^{2+} and Zn^{2+} and how such interactions could alter the media's reactivity with respect to different contaminants. Magnetite-coated ZVI with Mn^{2+}/ Zn^{2+} modifications could affect the reactivity and kinetic reaction for the contaminant removal. The selected contaminants are nitrate (NO_3^-) and selenate (SeO_4^{2-}), which are common pollutants in agricultural, municipal and industrial wastewater. Nitrate and selenate has different reactivity with different redox behavior.

The research objectives are proposed:

(1) To evaluate the reactivity of subsequent FeOx coating process in the AIM treatment system with cations of Mn^{2+} and Zn^{2+} for nitrate and selenate removal.

(2) To characterize the composition of FeOx with Mn^{2+} and Zn^{2+} incorporations based on the qualitative and quantitative analysis, and to determine the reaction mechanism of nitrate and selenate removal in an AIM treatment system.

(3) To develop the specific iron oxide media with $M^{(II)}$ ions incorporation to selectively inhibit nitrate removal under certain chemical environment in AIM treatment system.

(4) To perform laboratory-scale continuous stirred tank reactors (CSTR) tests for the application of Zn^{2+} in activated reactive iron media systems for nitrate removal.

(5) To investigate the effect of electrical conductivity on the reactivity of AIM for nitrate reduction in the laboratory-scale reactor for both batch and CSTR experiments.

CHAPTER II EFFECT of MN^{2+} ON NITRATE REDUCTION BY MAGNETITE-COATED ZERO-VALENT IRON

Introduction

Nitrate (NO_3^-) is a common pollutant with toxicity and widespread occurrences in both groundwater and surface water, and in agricultural, municipal and industrial wastewaters. The main sources of nitrate contamination are from agricultural and industrial activities, such as nitrogen-contained fertilizer and irrigation with reclaimed wastewater (Soares, 2000; Su and Puls, 2004). To remediate nitrate-contaminated groundwater, ZVI-based permeable reactive barriers (PRBs) are successfully performed to remove nitrate and other heavy metals, and the mechanisms of nitrate removal are chemical reduction, adsorption and biological denitrification (Wilkin et al., 2003; Moore and Young, 2005; Della Rocca et al., 2007; Henderson and Demond, 2007; Su and Puls, 2007; Robertson et al., 2008; Statham et al., 2016). Moreover, zero-valent iron (ZVI) technology has been extensively studied for nitrate reduction in laboratory and filed tests since 1960s. The process of nitrate reduction in ZVI systems is an acid-driven process. Therefore, nitrate is able to be rapidly reduced to lower oxidation state of nitrogen products in a ZVI system under acidic conditions (pH < 4.0). Nitrate can be chemically reduced to nitrite (NO_2^-), nitric oxide (NO), nitrous oxide (N_2O), nitrogen gas (N_2) and ammonia (NH_4^+) (Young et al., 1964; Kapoor and Viraraghavan, 1997; Huang et al., 1998; Huang et al., 2003; Huang and Zhang, 2004; Yang and Lee, 2005; Huang and

Zhang, 2006a). For drinking water standards, U.S. EPA regulates that the maximum contaminant level of nitrate is 10 mg/L as nitrogen.

Iron oxides are produced when ZVI media interacts with environmental oxidants, such as oxygen and nitrate. The surface of ZVI grains is corroded and oxidized to produce iron corrosion products as a layer coating. Beside the formation on the ZVI surface, discrete iron oxides are able to be generated as intermediate/final products on liquid phase. The common iron corrosion products after nitrate reduction by ZVI systems are Fe_2O_3, Fe_3O_4 and FeOOH under environment conditions (Siantar et al., 1996; Huang and Zhang, 2005; Yang and Lee, 2005). Its composition may change to complex mixture of iron oxides, iron hydroxides or other precipitated minerals with time when coexisted different oxidants, salts and metal ions, such as oxygen, selenate, chloride, sulfate and aluminum, simultaneously reacts with ZVI grains or iron oxides. The iron oxide coating could contribute poor removal efficiency for pollution control in a ZVI system due to surface passivation. The passivated iron system without sustainability and longevity exhibits limited capacity of removing aquatic contaminants. The reason related to the surface passivation may be that iron corrosion products could provide less actively reactive site to attract contaminants or behave as an electron barrier to suppress electron transfer from ZVI grains to the solid/liquid interface to interact with aqueous pollutants for redox reaction (Luo et al., 2010; Chen et al., 2012; Zhang et al., 2016).

Magnetite ($Fe^{II}Fe^{III}{}_2O_4$), a mixed Fe^{2+}/Fe^{3+} oxides, has metal-like electrical conductivity, in contrast with poor electrical conductivities exhibited by other common

iron oxides of hematite (α-Fe_2O_3), maghemite (γ-Fe_2O_3), goethite (α-FeOOH) and lepidocrocite (γ-FeOOH). This unique property of magnetite among iron oxides could facilitate electron transfer in the structure of magnetite that may manifest as an electrical conductor. In addition, magnetite is an electron donor because the structural $Fe^{(II)}$ in magnetite is able to be utilized by some oxidants for chemical reduction. For example, magnetite could reduce radioactive substances of Pu(V) to Pu(IV) and U(VI) to U(IV) by structural $Fe^{(II)}$ with the formation of ferric oxides due to the oxidation of magnetite (Powell et al., 2004; Scott et al., 2005). However, magnetite alone has a limited capacity of reducing nitrate under acidic, neutral and alkaline conditions as well as magnetite precoated ZVI under neutral pH. For the enhancement of chemical reduction ability, co-presence of discrete magnetite and ZVI or magnetite-coated ZVI with specific catalytic metal ions (e.g. Fe^{2+}, Fe^{3+} or Al^{3+}) is performed to facilitate contaminant removal of nitrate, selenate and molybdate (Huang et al., 2003; Huang et al., 2012c; Tang et al., 2016). Therefore, the kinetic reaction of contaminant removal was significantly increased by ZVI/magnetite systems with the catalytic metal ions. Tang et al. (2014a) demonstrated that adding aqueous Mn^{2+} into a ZVI system could facilitate selenate reduction, implying that Mn^{2+} may also play an important role in enhancing iron reactivity as well as Fe^{2+}, Fe^{3+} or Al^{3+} in a ZVI system for water treatment. Nevertheless, the effect of aquatic Mn^{2+} in ZVI/magnetite systems for nitrate reduction is rarely investigated.

ZVI/magnetite systems with metal ion supplements provide an innovative solution for chemical wastewater treatment. The effect of specific metal ion could be

catalytic to enhance removal efficiency for pollution control in a ZVI/magnetite system. The objective of this study is to investigate the effect of aqueous Mn^{2+} on nitrate reduction in a ZVI or magnetite-coated ZVI system under anoxic conditions. Material characterization was conducted to identify the change of morphology, pore structure and crystalline materials of the reactive media before and after reaction through field emission scanning electron microscope (FE-SEM) with energy dispersive spectroscopy (EDS) and X-ray diffraction (XRD). The role of Mn^{2+} in ZVI and magnetite-coated ZVI systems was also discussed in order to evaluate the interaction among ZVI, iron oxides and the augmented metal ions.

Materials and Methods

Materials

All reagent solutions were made by deoxygenated deionized (DDI) water (E-pure, Barnstead, USA). Stock solution of 200 mM Fe^{2+}, 200 mM Mn^{2+}, and 150 mM NO_3^- were prepared with $FeCl_2 \cdot 4\ H_2O$ (J.T. Baker), $MnCl_2 \cdot 4\ H_2O$ (J.T. Baker), and $NaNO_3$ (>98%, Alfa Aesar), respectively. ZVI grains of -20 mesh (purity >99.2%, Alfa Aesar) has the specific surface area is around 0.073 m^2/g by BET nitrogen absorption analysis (Autosorb-6, Quantachrome, USA).

Production of Magnetite-Coated ZVI

A nitrate-Fe^{2+} pretreatment method was used to convert a traditional ZVI system into a hybridized ZVI/magnetite/Fe^{2+} system (Huang et al., 2012c). To create a hybrid ZVI system, 50 ml solution of 10 mM NO^{3-} with 6 mM Fe^{2+} was added into a 60 ml sampling bottle filled with 50 g ZVI in an anaerobic chamber, and then the bottle was

placed in a rotary tumbler at 30 rpm with 24 h reaction for nitrate reduction. NO_3^- would be rapidly reduced by ZVI with Fe^{2+}, and magnetite would be produced as an iron corrosion product (Huang et al., 2003). Produced magnetite would exist both in the form of the coating on the iron grain surface and in the form of discrete crystalline particles. To eliminate residual NO_3^-, Fe^{2+} and discrete magnetite particles in the reaction mixture, the top liquid with suspended particles were withdrawn and discarded with a syringe, and the remaining magnetite-coated ZVI (large grains settled on the bottom) would be rinsed 5 times with DDI water. The retained magnetite-coated ZVI would be dried by ultra-high purity of nitrogen gas flushing, and stored in an anaerobic chamber until used to conduct experiments.

Batch Experiments

Batch tests were conducted in 12 ml serum vials used as reactors. For each batch, multiple reactors were prepared in parallel under identical conditions. Each reactor was initially filled with ~0.5 g ZVI or magnetite-coated ZVI grains and then transferred into an anaerobic chamber (Coy Laboratory Products) to avoid potential interference of O_2 on iron chemistry. The anaerobic chamber, equipped with two unheated catalyst boxes to eliminate any trace oxygen, is filled with 95%N_2 and 5% H_2 gas. Once in the anaerobic chamber, a desired chemical concentration of 3mM NO_3^- as the target contaminant and 1, 2, or 3mM Mn^{2+} as supplementary metal ions are added into reactors with a total volume of 10 ml. Each reactor was sealed tightly with a rubber stopper and an aluminum cap. Sealed reactors were moved out of the anaerobic chamber and transferred into a tumbler rotating at 30 rpm under a dark environment for complete mixing. At selected

reaction times (1 h, 3 h, 6 h, 12 h and 24 h), one reactor (out of the dozen reactors) was withdrawn from the tumbler and sacrificed for measuring pH, cations of Fe^{2+} and Mn^{2+}, and anions of NO_3^-. The batch experiment was conducted in duplicate at room temperature ($21^oC \pm 2^oC$).

Analytical Methods

Filtrates from reactors were collected through 0.45 μm pore size of membrane filters for wet chemistry analysis by analytical instruments. An Ion Chromatography (IC, Dionex DX-500) equipped with an AS-22 separation column, a self-regenerating suppressor (AERS-4mm) and the CD-20 conductivity detector with a current of 50 mA was performed to analyze NO_3^-. For Mn^{2+} analysis, an IC equipped with an AD-20 absorbance detector and the MetPac^{TM} PAR diluent and MetPac^{TM} PDCA eluent were used following an established method (Huang et al. 2003). For dissolved Fe^{2+} measurement, a UV-Vis spectrophotometer (T80, PG Instruments) was used following the colorimetrical method of 1, 10-phenanthroline (APHA-AWWA-WEF, 2012).

Characterizations of Media

Morphology and pore structure were examined by FE-SEM (JEOL JSM-7500F), and XRD powder pattern was analyzed by X-ray powder diffractometer (Bruker-AXS D8) with copper X-ray radiations. Reactive media solids were prepared separately from the batch tests, and characterized by FE-SEM-EDS and XRD.

For preparing samples for FE-SEM analysis, reactors of the designed conditions were withdrawn from a rotary tumbler; the top liquid in the reactor were discarded; the bottom solid samples (large ZVI grains with surface coating) were collected after

washed with DDI water three times to remove residual salts (Na^+ and Cl^-) from the solid surface. The collected solid grains were then dried and stored in an anaerobic chamber with a N_2 environment until FE-SEM analysis.

For XRD analysis, batch reactors withdrawn from a rotary tumbler were first sonicated for 5 minutes to strip off the outer iron corrosion layer. The stripped suspended solids were collected and filtered through a membrane filter of 0.45 μm pore size, which formed a thin and uniform powder film on the filter paper. The membrane filter with solid samples was dried under an anaerobic environment. The filter paper with the dry solid sample film was mounted on the sample plate for XRD analysis.

Results and Discussions

ZVI Systems

A pure ZVI system has a very limited capacity for nitrate reduction under anoxic conditions with a near neutral (unadjusted) pH condition. pH value was varied between 7.9 to 8.3 and aqueous Fe^{2+} was not detected during the reaction. Nitrate was barely reduced during 24 h reaction time, indicating that ZVI lost its reactivity for nitrate reduction under neutral conditions. In neutral or alkaline conditions, the surface of ZVI grains could be oxidized and coated with a thin layer of iron oxides. These iron corrosion products could result in the passivation of ZVI surface that could suppress redox reaction between oxidants and ZVI grains.

Adding Mn^{2+} into a ZVI system exhibited no significant enhancement for nitrate reduction. With 1.0, 2.0 and 3.0 mM Mn^{2+} additions, an insignificant amount of nitrate was reduced in ZVI/Mn^{2+} systems with the initial pH at ~6.9 over 24 h reaction time.

Mn^{2+} concentration was only decreased in the first hour and remained steady to 24 h reaction time. Mn^{2+} concentration decreased by 0.04, 0.04 and 0.14 mM in the three tests with 1.0, 2.0 and 3.0 mM Mn^{2+}, respectively, suggesting that a small amount of Mn^{2+} was adsorbed or incorporated into the iron corrosion products, forming a mixed Mn-Fe oxides on the ZVI surface. Once the thin layer of Mn-Fe oxides was formed (e.g., after 1 h reaction time), the interaction between ZVI and aqueous reactants could be suppressed and the system became passivated. Fe^{2+} was gradually produced during 24 h reaction time. After 1 h reaction, Fe^{2+} concentrations in the tests with 1.0, 2.0 and 3.0 mM Mn^{2+} were 0.01, 0.04 and 0.04 mM, respectively. After 24 h reaction, Fe^{2+} in the three tests increased slightly to 0.06, 0.06 and 0.07 mM, respectively. The continued release of some Fe^{2+} from ZVI grains suggests that ZVI could be oxidized in the co-presence of aqueous Mn^{2+} and ZVI, which can be represented by $Fe^0 \rightarrow Fe^{2+} + 2e^-$. Since Mn^{2+} cannot be thermodynamically reduced by Fe^0, the oxidants responsible for ZVI oxidation could be either proton (H^+) from the acidity or ferric iron ($Fe^{(III)}$) from the iron oxides in the system. The acidity could be attributed to the added Mn^{2+} as $MnCl_2$ is a solution with some intrinsic acidity. Fe(III) may come from the surface iron rusts on the raw ZVI grains, as ZVI can be oxidized invariably by oxygen in the air and form a layer of ferric iron oxides. $Fe^{(III)}$ from the original surface rusts could be reduced to $Fe^{(II)}$ by ZVI. Subsequently, Mn^{2+} that could substitute structural $Fe^{(II)}$ in the iron oxides, resulting in the release of a small amount of aqueous Fe^{2+}.

Magnetite-Coated ZVI Systems

Fig. 3(a) illustrated nitrate concentration change during 24 h reaction time in a magnetite-coated ZVI system with or without Mn^{2+} additions. In the control test without Mn^{2+} addition, the magnetite-coated ZVI only media system achieved only an insignificant nitrate reduction (<10% removal out of the initial 3.0 mM nitrate) at near neutral pH. During 24 h reaction time, no Fe^{2+} was observed, and pH was varied from 7.1 to 8.0.

Adding aqueous Mn^{2+} into a magnetite-coated ZVI system significantly increase nitrate reduction. In general, nitrate reduction rate increased with increased Mn^{2+} dosages. The removal efficiency of nitrate in the tests with 1.0, 2.0 and 3.0 mM Mn^{2+} addition were 40%, 100% and 100%, respectively after 18 h reaction time. Nitrate was not further reduced between 18 h and 24 h in the test with 1.0 mM Mn^{2+} addition. During the first hour, with Mn^{2+} additions into a magnetite-coated ZVI system, no significant nitrate reduction was observed in all three tests. After 1 h, however, nitrate was rapidly reduced. The initial lag phase suggested that the raw surface of the magnetite-coated ZVI might be passive and could not support rapid nitrate reduction until it was activated through certain mechanism(s) after 1 hr. It is possible that the outer layer of magnetite coating on ZVI grains was actually oxidized by O_2 in the air to a ferric oxide layer (e.g., maghemite). The ferric oxide layer, considered a chemically passive layer, could not mediate nitrate reduction. However, in the aqueous system under anaerobic condition, the maghemite layer could be gradually reduced by ZVI and transformed to magnetite and thereafter, the media system could become reactive. With

the addition of Mn^{2+}, the magnetite coating could be transformed into mixed Mn-Fe oxides through the isomorphous substitution of the structural $Fe^{(II)}$ in magnetite by the added Mn^{2+}, resulting in the release of aqueous Fe^{2+}. Upon the reactivation of the surface, rapid nitrate reduction proceeded in the co-presence of magnetite-coated ZVI, Mn^{2+} and Fe^{2+}. pH increased from ~6.8 to ~9.5 by the end of test period in all three tests with Mn^{2+} addition (Fig. 3(b)), which is consistent with pervious observations that nitrate reduction in a ZVI system contributes to pH increase due to proton depletion (Alowitz and Scherer, 2002; Huang et al., 2003; Hwang et al., 2011). Nitrate reduction rate was in general proportional to the initial Mn^{2+} dosage after 6 h reaction time. The nitrate removal rates, however, were similar between the tests with 2.0 and 3.0 mM Mn^{2+} addition after 6 h. The test results showed that aqueous Mn^{2+} could interact with the preexisting magnetite coating on the ZVI that could activate the media to support nitrate reduction reaction.

Unlike the virgin ZVI systems in which the added Mn^{2+} was barely consumed, Mn^{2+} was gradually consumed with time in a magnetite-coated ZVI system, as shown in Fig. 3(c). When compared the profile of Mn^{2+} decrease with that of nitrate reduction, it appears that Mn^{2+} consumption could not be clearly related to nitrate reduction; for example, a significant decrease of Mn^{2+} was observed by t=1 h, but nitrate was barely reduced at the time. Over the entire reaction course, however, it was obvious that Mn^{2+} depletion proceeded concomitantly with nitrate reduction. Aqueous Mn^{2+} depletion might result from the incorporation of Mn^{2+} into the structure of the magnetite coating through cation exchanges between structural Fe(II)/Fe(III) and Mn^{2+} ions. In other

words, aqueous Mn^{2+} could substitute structural Fe(II) or Fe(III) in both tetrahedral and octahedral sites of the magnetite crystalline, and subsequently the structural Fe(II) or Fe(III) could be released from the magnetite coating into liquid phase. Dupuis and Beaudoin (2011) demonstrated that structural Fe(II)/Fe(III) in magnetite can be isomorphically replaced by multivalent metal cations, such as Zn^{2+}, Mn^{2+}, Al^{3+} and Ti^{4+} while still maintain the inverse spinel structure of magnetite. Significant increases of aqueous Fe^{2+} were observed during the reaction course, coincident with the decreases of aqueous Mn^{2+}, which could be explained as the isomorphous substitution of structural Fe(II)/Fe(III) by Mn^{2+}.

Fig. 3(d) showed the evolution profile of aqueous Fe^{2+} concentration in a magnetite-coated ZVI system with Mn^{2+} additions during nitrate reduction. Fe^{2+} was released rapidly and in a significant amount from the beginning of the test, but then gradually depleted along with nitrate reduction. The production of aqueous Fe^{2+} could be attributed to the isomorphous substitution of structural Fe(II) by the added Mn^{2+}. $Mn^{(II)}$-substituted magnetite was known capable of enhancing catalytic activity of magnetite for chemical reactions (Costa et al., 2006; Yang et al., 2009). Upon the reactivation of the magnetite coating after the initial lag time (e.g., 1 h), nitrate reduction by ZVI proceeded with the presence of both aqueous Fe^{2+} and Mn^{2+}. Consequently, aqueous Fe^{2+} could regulate the iron oxide-water interface that greatly facilitate electron transfer from ZVI core to the reactive surface site to support rapid nitrate reduction in a ZVI-based reactive system (Huang and Zhang, 2002; Huang et al., 2003; Xu et al., 2012). As a results of such a role, Fe^{2+} was consumed proportionally to nitrate reduction at a rate of 1 mol

nitrate to 0.75 mol Fe^{2+} consumption. Fe^{2+} consumption in this test could be more complicated due to the dynamic process of the isomorphic substitution between Mn^{2+} and Fe^{2+}. It would be reasonable to assume that aqueous Fe^{2+} and Mn^{2+} concentrations were dictated by certain equilibrium. Based on this assumption, we expect that once aqueous Fe^{2+} depletes, aqueous Mn^{2+} would also exhaust, which was observed in the test (Fig.3 (c) and (d)). When aqueous Fe^{2+} was completely consumed, nitrate reduction should halt. The fact that nitrate reduction continued for a few hours after both Fe^{2+} and Mn^{2+} exhausted could be explained as the presence of residual Fe^{2+} as surface–bound Fe^{2+} on the iron oxide coating continued to support nitrate reduction by ZVI. This is consistent with what was observed previously in a -ZVI/Fe^{2+} system (Huang et al. 2003). When surface-bound Fe^{2+} or Mn^{2+} was exhausted, nitrate reduction would be completely stopped, as is the case in the test with 1.0 mM Mn^{2+} addition after 16 h reaction time.

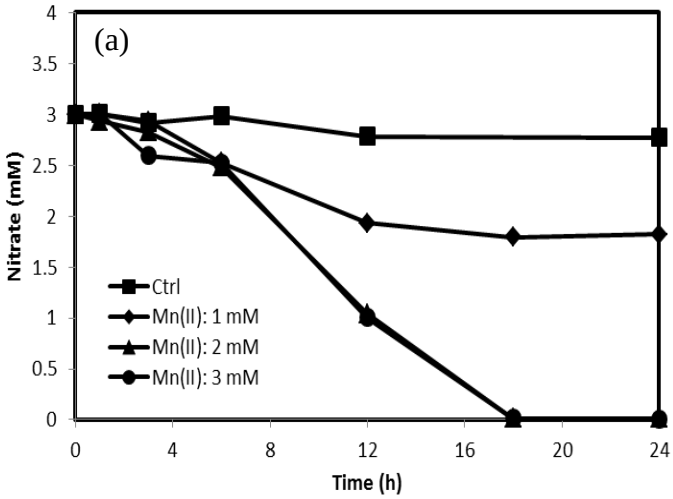

Figure 3. Time courses of (a) Nitrate, (b) pH, (c) Mn^{2+} and (d) Fe^{2+} in the batch reactors prepared with magnetite-coated ZVI (5% w/v) + 3.0 mM nitrate + various concentrations of Mn^{2+} (0, 1.0, 2.0, and 3.0 mM).

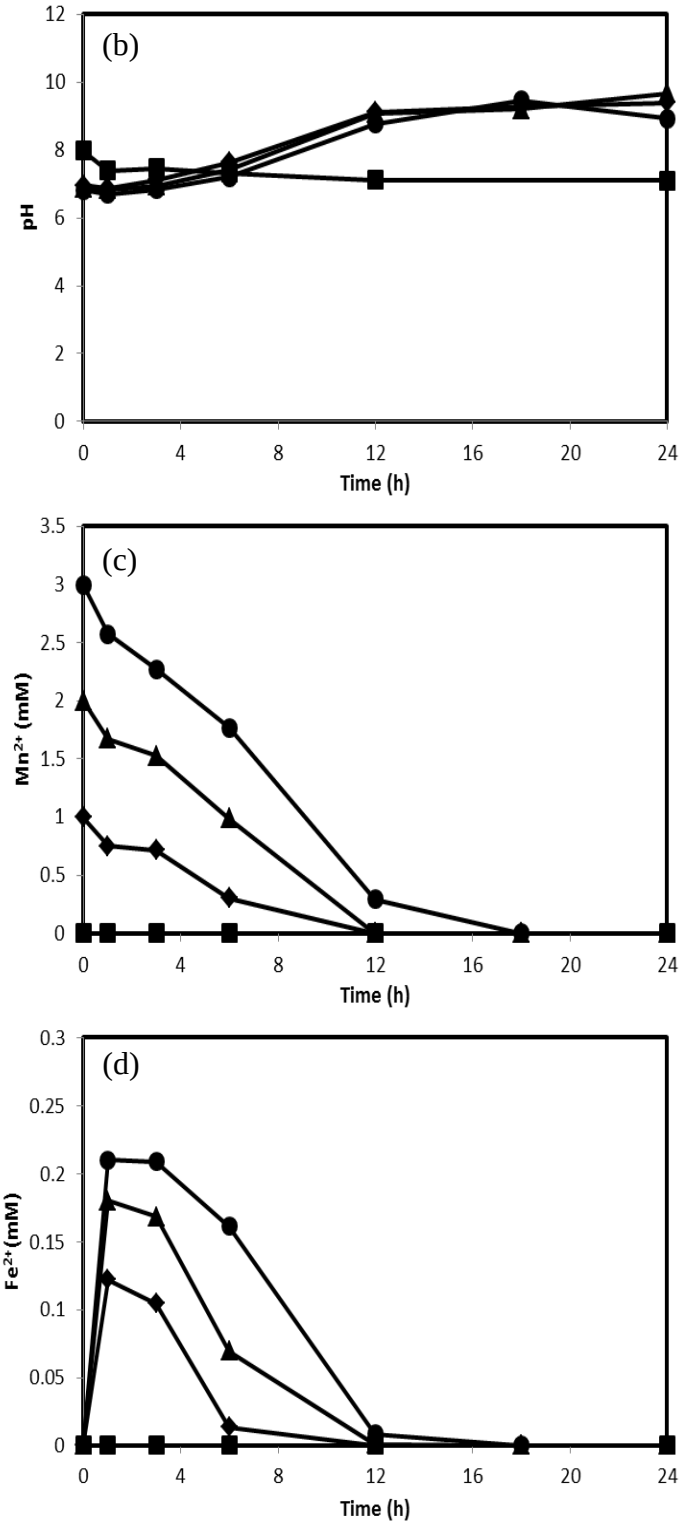

Figure 3. Continued.

XRD Results

XRD powder spectra indicated that magnetite and hausmannite (Mn_3O_4) are two major crystalline minerals in the solid structure, shown in Fig. 4. The major characteristic peaks of XRD results were 2 theta of 30.05^o, 35.28^o and 62.39^o. The powder spectrum of magnetite is similar with hausmannite but the peak intensity of the magnetite spectrum is relatively weaker than hausmannite. Based on the XRD results, magnetite could be the dominant crystalline mineral in the structure of spent media. During 12 h reaction time, the peak intensity in XRD spectra became stronger, suggesting that solid minerals were increasingly crystallized over time. Magnetite-coated ZVI media exhibited strong peak intensity to match the magnetite spectrum without obvious Fe^0 characteristic peaks. Thus, the surface of magnetite-coated ZVI grains is entirely covered by the magnetite coating. Nevertheless, in first hour, the XRD powder pattern of spent solid showed weak peaks on magnetite spectrum. The results implied that the partial magnetite coating could be initially transformed to another amorphous mineral through the interaction between the magnetite coating and Mn^{2+}, possibly Mn^{2+} incorporation. Subsequently, the surface of altered magnetite-coated ZVI could be deposited by magnetite that was formed during nitrate reduction process. The formation of amorphous mineral could provide a negative effect on the peak intensity of spent media but enhancement of the chemical environment for nitrate reduction. According to the XRD results, magnetite would be the final product of nitrate reduction in a magnetite-coated ZVI system with Mn^{2+} additions.

FE-SEM Analysis

Fig. 5 illustrated the morphology and pore structure of spent media and its surface coating during nitrate reduction process in a magnetite-coated ZVI system with Mn^{2+} additions. The surface of magnetite-coated ZVI media was covered with a thin layer of magnetite and several spots of magnetite crystal deposition. After 1 h reaction, another mineral with polygonal appearances (mostly in pentagon and hexagon) other than magnetite were produced with the average size of ~1 μm^2 and covered on the surface of magnetite-coated ZVI. The mineral would break down to smaller pieces with the average size of 0.25 μm^2 after 3 h reaction time. After 6 h reaction, the surface of magnetite-coated ZVI turned into accumulation of aggregated magnetite instead of polygonal shape of the amorphous mineral, because the XRD results indicated that magnetite was a major crystalline mineral in 6 h and 12 h solid samples. More magnetite was formed as small particles deposited on the surface of magnetite aggregation during nitrate reduction process in a magnetite-coated ZVI system with Mn^{2+} additions. According to the results of FE-SEM and XRD, the magnetite coating on the surface of ZVI grains would be initially transformed to another amorphous mineral with polygonal shape due to the interaction between magnetite-coated ZVI and aqueous Mn^{2+}. During nitrate reduction process, magnetite would be gradually produced as the final product, and deposited on the surface of solid media in the form of bulk aggregation and tiny particle deposition.

EDS spectra (data not shown) showed that manganese, iron and oxygen were present in the structure of the spent media at 12 h reaction time. The atomic ratio of

manganese, iron and oxygen in the bulk aggregation was 0.02: 0.68: 1. The content of manganese in the sample was relatively small compared to iron and oxygen. The ratio of (manganese + iron) to oxygen was ~ 0.7: 1, which was close to the stoichiometric ratio of iron to oxygen at 0.75: 1 in magnetite (Fe_3O_4), implying that bulk aggregate may be similar to magnetite in its composition. The results also supported that the final product after nitrate reduction by a magnetite-coated ZVI system with Mn^{2+} additions still retain the crystalline structure of magnetite based on the analyses of FE-SEM and XRD. In addition, the EDS results demonstrated that Mn^{2+} could diffuse into the bulk solid structure of magnetite coating, likely through isomorphic substitution of lattice Fe(II) or Fe(III) by Mn(II), which transforms an ideal magnetite structure into a mixed Mn-Fe inverse spinel crystalline structure, thus forming Mn^{2+}-doped magnetite on the surface of ZVI grains.

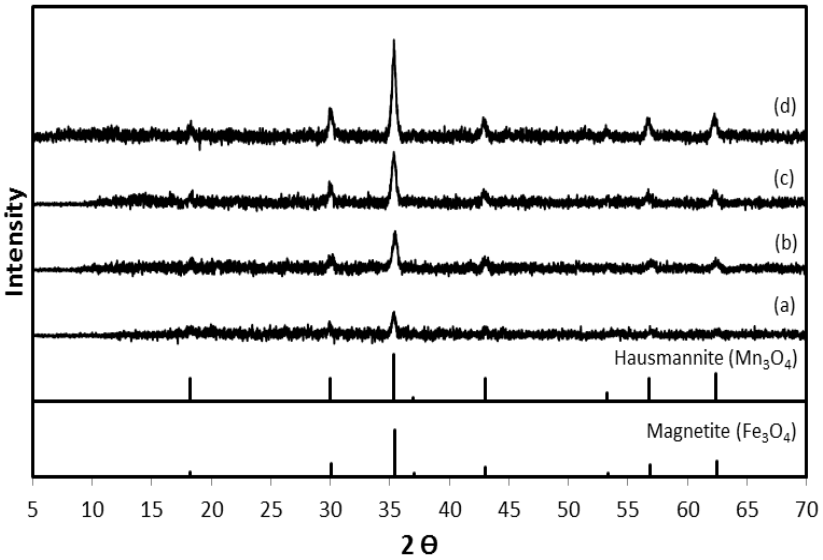

Figure 4. XRD powder patterns of the iron corrosion products collected from a batch test using magnetite-coated ZVI with Mn^{2+} addition for nitrate reduction after reaction time of (a) 1 h, (b) 3 h, (c) 6 h and (d) 12 h. The initial conditions were controlled as 5% w/v of magnetite-coated ZVI + 3mM Mn^{2+} + 3mM NO_3^-. The references of XRD spectra are magnetite (Fe_3O_4) and hausmannite (Mn_3O_4).

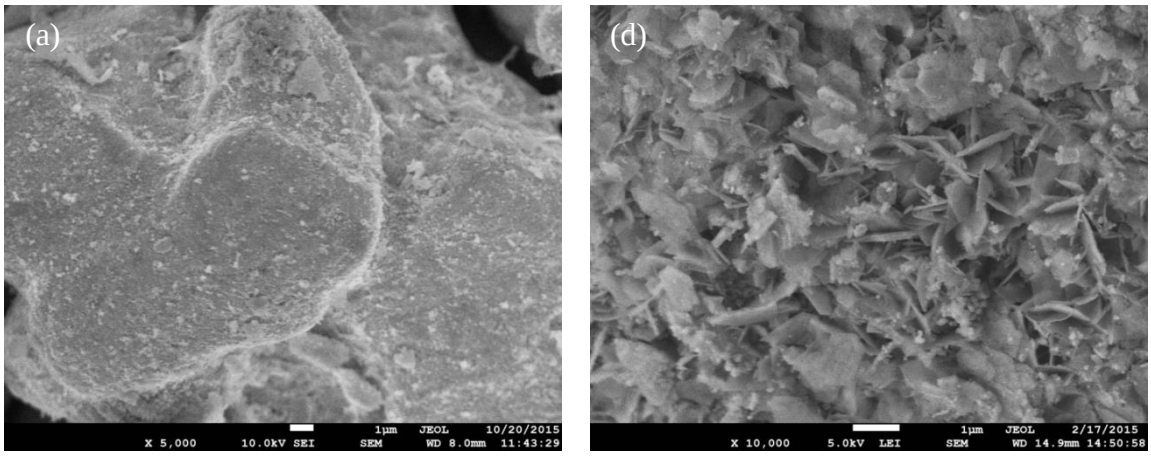

Figure 5. SEM images of the reactive media sampled at different stages from a batch test: (a) magnetite-coated ZVI, (b) 1 h, (c) 3 h, (d), 6 h and (e) 12 h. The initial conditions were controlled as 50g/L magnetite-coated ZVI + 3.0 mM Mn^{2+} + 3.0 mM NO_3^-.

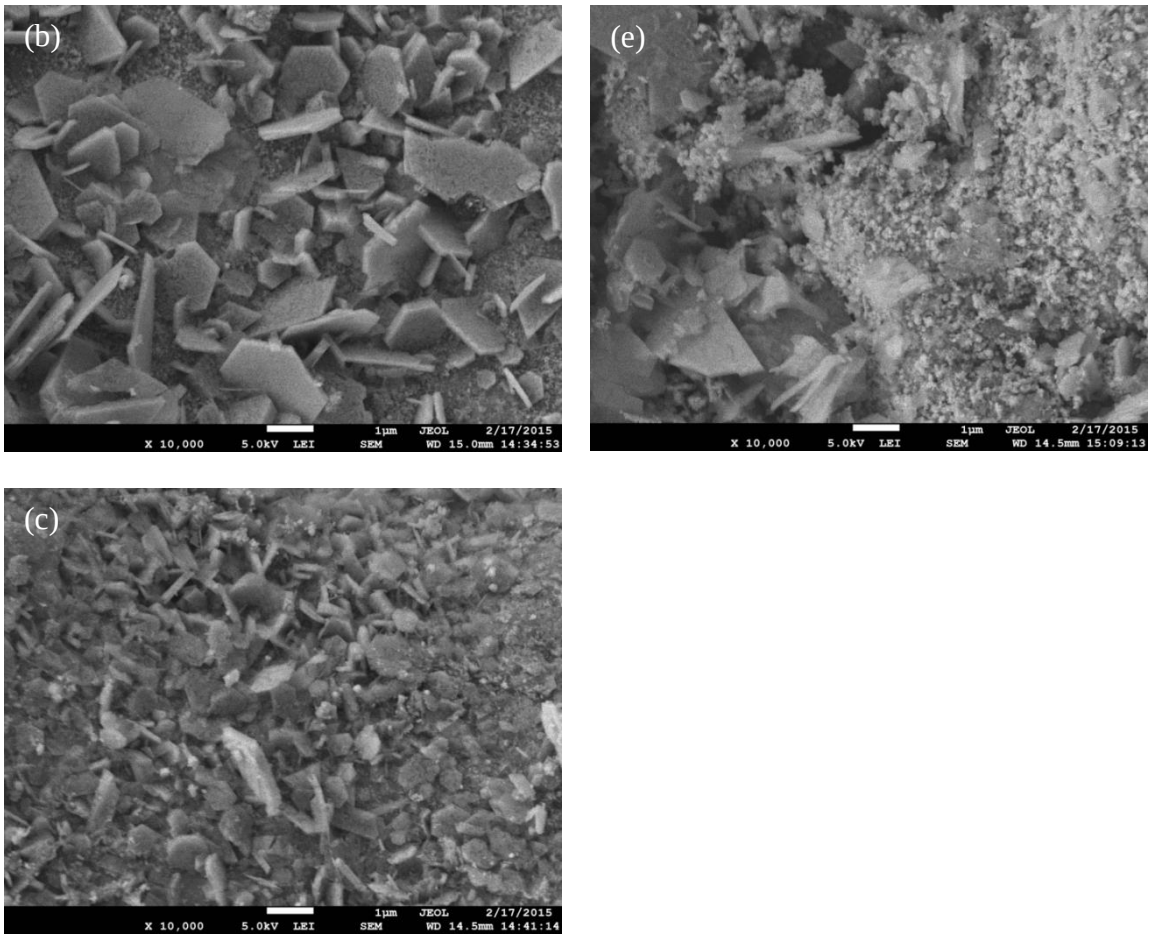

Figure 5. Continued.

The Effects of Mn^{2+}

The test with magnetite-coated ZVI system demonstrates that adding aqueous Mn^{2+} could facilitate nitrate reduction. Aqueous Mn^{2+}, however, doesn't directly result in nitrate reduction in the system as evident by the fact that negligible nitrate reaction occurred in the first hour even with the presence of aqueous Mn^{2+}. The role of Mn^{2+} could be complicated. Initially, Mn^{2+} would be incorporated into the magnetite coating to form $Mn^{(II)}$-doped iron oxides that were not a crystalline mineral with polygonal

appearances. $Mn^{(II)}$-doped iron oxides could act as a catalyst (Costa et al., 2006; Yang et al., 2009; Liang et al., 2012) for initiating nitrate reduction in the magnetite-coated ZVI system. Once nitrate reduction started, new magnetite was produced as a corrosion product, which would coat on the surface of the existing $Mn^{(II)}$-doped iron oxides. In the meantime, more Mn^{2+} would continuously adsorb onto and be integrated into the new magnetite coating, by which rapid nitrate reduction would be sustained until Mn^{2+} was completely consumed in liquid phase.

Fe^{2+} released from the media could be quantitatively related to Mn^{2+} incorporation into the iron oxide structure. The amount of Fe^{2+} released upon the introduction of Mn^{2+} into the system was proportional to the consumed Mn^{2+} at the first hour in all three tests with 1.0, 2.0 and 3.0 mM Mn^{2+} addition, as shown in Fig. 6. The stoichiometric ratio of Fe^{2+} increase to Mn^{2+} decrease is ~ 0.51:1. Therefore, 0.51 mol structural Fe(II) would be released from the magnetite coating when 1 mol aqueous Mn^{2+} was incorporated into the structure of magnetite. Due to the unbalanced total charge between Fe^{2+} released and Mn^{2+} consumed, excess anions in liquid phase might be balanced by the uptake of O^{2-} or OH^- from H_2O to form new oxides coupled with the release of H^+ into the liquid phase. Liang et al. (2013) demonstrated that Mn^{2+} could occupy the tetrahedral and octahedral sites in magnetite for the replacement of structural Fe(III) and Fe(II), respectively. Similarly, the possibility could not be excluded that not only structural Fe(II) but also structural Fe(III) in the magnetite coating might be exchanged with Mn^{2+}. Consequently, the released Fe^{2+} and Fe^{3+} from the magnetite

coating could subsequently contribute to facilitating nitrate reduction in magnetite-coated ZVI systems (Huang et al., 2003).

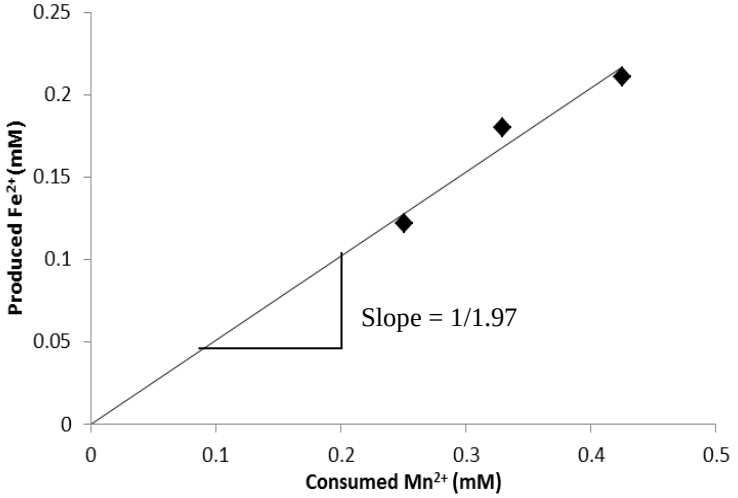

Figure 6. The linear relationship between consumed Mn^{2+} and produced Fe^{2+} observed in the tests with 1.0, 2.0 and 3.0 mM Mn^{2+} addition based on the change by the first hour reaction time. The ratio of produced Fe^{2+} to consumed Mn^{2+} is ~ 0.51 to 1.0 with a correlation coefficient of 0.99.

Table 1. Fe^{2+} production over time calculated based on the Mn^{2+} decrease observed during 12 h reaction time in the magnetite-coated ZVI systems with Mn^{2+} additions. The calculation is based on the ratio of 0.51 mol Fe^{2+} released to 1.0 mol Mn^{2+} consumed as observed in the first hour reaction time before nitrate reduction started.

Initial Mn^{2+} (mM)	Anticipated Fe^{2+} production (mM)			
	Reaction time			
	1 h	3 h	6 h	12 h
1	0.13	0.14	0.36	0.51
2	0.17	0.24	0.52	1.01
3	0.22	0.37	0.63	1.34

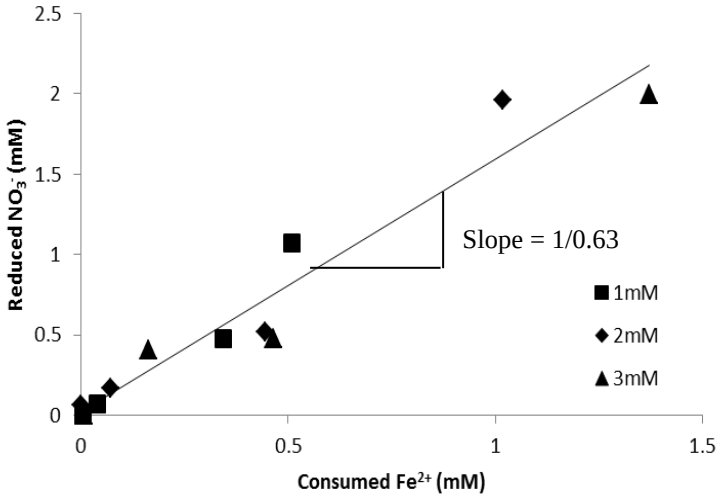

Figure 7. The concentration distribution of anticipated consumed Fe^{2+} versus reduced NO_3^- in the tests with 1.0, 2.0 and 3.0 mM Mn^{2+} during 12 h reaction time before nitrate complete depletion. The stoichiometric ratio of reduced NO_3^- to consumed Fe^{2+} is 1:0.63 with correlation coefficient of 0.97.

Adding aqueous Fe^{2+} had been previously demonstrated for its effectiveness in significantly enhancing kinetic reaction for the removal of nitrate, nitrite, selenate, molybdate, nitrobenzene, mercury and heavy metals in ZVI/magnetite systems in laboratory and field tests (Huang et al., 2003; Huang and Zhang, 2006a, b; Huang et al., 2013; Tang et al., 2016). Like externally-supplied Fe^{2+}, the internally-released Fe^{2+} could be performed as a catalyst in chemical reaction for contaminant removal in ZVI-based technology. It was understood that once nitrate reduction started in a ZVI system, the released Fe^{2+} would be gradually consumed at a ratio of 1 mol nitrate to 0.75 mol Fe^{2+} (Huang et al 2003). Such a quantitative relationship between Fe^{2+} decrease and nitrate reduction could not be directly obtained in this study due to the presence of Mn^{2+} and its apparent dynamic equilibrium with aqueous Fe^{2+}. However, upon manipulation, the relationship could still be estimated. Based on the mass ratio between Fe^{2+} released

and decreased Mn^{2+} observed at 1 h reaction time (before nitrate reduction started), Fe^{2+} production resulted from the observed Mn^{2+} decrease, assuming zero Fe^{2+} consumption due to nitrate reduction, was calculated in Table 1 for the three tests with 1.0, 2.0 and 3.0 mM Mn^{2+} addition. Thus, based on the ideal Fe^{2+} production and the actual concentration observed during the time course, we could calculate the amount of Fe^{2+} consumed by nitrate reduction. Fig. 7 illustrated the relationship between consumed Fe^{2+} and reduced NO_3^- in the three tests with 1, 2 and 3 mM Mn^{2+} addition before 12 h reaction, in which Mn^{2+} and NO_3^- were not completely depleted. The stoichiometric ratio of reduced NO_3^- to consumed Fe^{2+} was ~ 1:0.63.

To derive the chemical formula for nitrate reduction in a magnetite-coated ZVI system, ZVI (Fe^0) is assumed as the primary electron donor, and Fe^{2+} and magnetite are not responsible for redox reaction. In addition, both NH_4^+ and magnetite (Fe_3O_4) with the stoichiometric ratio of Fe^{2+} to Fe^{3+} of 1:2 are the final products from the reaction. For mass balance of Fe, the stoichiometric constant of Fe^0 is equal to 3X – 0.63 (assuming the stoichiometric constant of Fe_3O_4 as X and 0.63 from Fe^{2+} species). For the reaction, eight electrons are required to reduce nitrate to ammonia. In order to balance electrons of Fe_3O_4 from Fe^0, $2 \times (X - 0.63) + 3 \times (2X) = 8$ and X = 1.16. Therefore, 2.32 and 0.53 moles Fe^0 will become Fe^{3+} and Fe^{2+}, respectively. Consequently, the chemical formula with mass and charge balance for nitrate reduction in a magnetite-coated ZVI system with Mn^{2+} additions is theoretically suggested as the below:

$$NO_3^- + 2.85Fe^0 + 0.63Fe^{2+} + 2.36\ H_2O \rightarrow NH_4^+ + 1.16\ Fe_3O_4 + 0.72OH^- \quad [1]$$

When Fe^{2+} is considered as an electron donor as well as Fe^0, 0.63 mole Fe^{2+} would be converted to 0.63 mole Fe^{3+} and provides 0.63 mole electrons for magnetite formation. With repetitive calculation as above, the overall reaction would be the same as equation [1]. The results presented that the role of Fe^{2+} in a magnetite-coated ZVI system for nitrate reduction may be both a catalyst to enhance reaction kinetics for rapid removal or a reducing agent to provide electrons for redox reaction. Huang et al. (2003) proposed the formula of stoichiometric relationship for nitrate reduction in ZVI systems with Fe^{2+} additions, listing in the following:

$$NO_3^- + 2.82Fe^0 + 0.75Fe^{2+} + 2.25H_2O \rightarrow NH_4^+ + 1.19\ Fe_3O_4 + 0.50OH^- \quad [2]$$

The consumption of internally-released Fe^{2+} is less than externally-supplied Fe^{2+} for nitrate reduction to ammonia. The difference of internally-released and externally-supplied Fe^{2+} consumption is 0.12 mole for 1 mole nitrate reduction. Therefore, internally-released Fe^{2+} could exhibit stronger catalytic strength more than externally-released Fe^{2+} in a ZVI-based technology. The Fe^0 usage and Fe_3O_4 formation is similar with each other in ZVI and magnetite-coated ZVI systems, implying that nitrate reduction in ZVI-based technology with Fe^{2+} supplies follow the similar removal mechanism.

Summary

The experimental results showed that adding Mn^{2+} to a virgin ZVI system could not facilitate nitrate reduction by ZVI, which differs from the effectiveness of adding Fe^{2+}. When ZVI is pre-coated with a magnetite coating, adding aqueous Mn^{2+} could trigger rapid and sustained nitrate reduction. Mn^{2+} was found incorporated into the

structure of magnetite, likely through isomorphic substitutions of structure $Fe^{(II)}$ or $Fe^{(III)}$, resulting a significant release of dissolved Fe^{2+}. Like normal magnetite, the $Mn^{(II)}$-doped magnetite could effectively mediate redox activity of ZVI. Nitrate reduction occurred at a faster rate with a higher Mn^{2+} dosage. The FE-SEM and XRD analyses confirmed that an inverse spinel structure similar to magnetite was still the primary corrosion product from nitrate reduction in the magnetite-coated ZVI with Mn^{2+} addition. Like a ZVI/Fe^{2+} system for treating nitrate, with the addition of Mn^{2+} into a magnetite-coated ZVI system, nitrate reduction still consumed Fe^{2+} at a ratio of 1.0 mol NO_3^- reduction to 0.63 mol Fe^{2+} usage, even though Fe^{2+} was internally generated from Mn^{2+} substitution. The study showed that a magnetite-coated ZVI system with Mn^{2+} additions could be a viable system for nitrate reduction. Such difference showed that the importance of an inverse spinel structure.

CHAPTER III SELENATE REDUCTION BY MAGNETITE-COATED ZERO-VALENT IRON WITH MN^{2+}

Introduction

Zero-valent iron (ZVI), as a moderate reducing agent and inexpensive material, has been widely utilized to remediate inorganic and organic contaminants from water, such as nitrate, arsenate, selenate, lead, chromate, uranyl, molybdate and chlorinated solvents (Cantrell et al., 1995; Siantar et al., 1996; Huang et al., 1998; Huang and Zhang, 2002; Huang and Zhang, 2004; Noubactep et al., 2005; Yang and Lee, 2005; Morrison et al., 2006). For selenium treatment, oxidized selenium species can be reduced by ZVI to a lower oxidation state. For example, selenate (SeO_4^{2-}), a hexavalent selenium form commonly found in polluted water, can be reduced by ZVI to selenite (SeO_3^{2-}), elemental selenium (Se^0), or even to selenide (Se^{2-}) in a ZVI-based system under acidic conditions. The final products of iron corrosion from selenate reduction in a ZVI system are commonly magnetite and lepidocrocite, dependent on the initial concentration of selenate in the solution. When the initial selenate concentration is higher than 50 mg/L, lepidocrocite (γ-FeOOH) is the dominant iron corrosion product. In contrast, magnetite is predominant under other conditions (Zhang et al., 2005a; Zhang et al., 2005b; Olegario et al., 2010; Yoon et al., 2011). Reduction of oxidants (e.g. nitrate, oxygen, or selenate) by ZVI are invariably coupled with oxidation of ZVI and a release of electrons, in which iron is corroded to form iron oxides (or referred to iron rusts) as intermediate or final products. Overtime, the surface of ZVI grain would be inevitably covered by a

layer of iron corrosion products. Following the formation of a surface coating, all subsequent redox reaction would be mediated by the layer. Thus the physical chemical properties of this iron rust coating could greatly affect the reactivity of a ZVI system. Iron oxides exhibit different properties. Some, such as magnetite, possess metallic like electrical conductivity; others show little capacity for electron conduction.

In addition to chemical reduction, selenate could be removed through adsorption on the surface of iron (oxy)hydroxide of hematite, goethite, magnetite, ferric hydroxide, maghemite and green rusts (Su and Suarez, 2000; Peak and Sparks, 2002; Rovira et al., 2008; Hayashi et al., 2009; Gonzalez et al., 2012; Das et al., 2013; Jordan et al., 2013). Selenate adsorption by iron oxides is dependent on ionic strength and pH in the solution. Strong ionic strength in solution could result in less selenate removal due to competition between selenate and other ions for limited available adsorption sites on iron oxides. When pH is lower than the point of zero charge (PZC) of particular iron oxides, the surface of solid media could be dominated by positive charges, which could facilitate adsorption of ions with negative charges such as SeO_4^{2-}. Conversely, iron oxides with negative surface charges when pH is higher than their PZC could repulse selenate. Consequently, with an appropriate chemical environment, both reduction and adsorption may simultaneously occur and responsible for selenate removal in a ZVI-based system.

Magnetite-coated ZVI is recently developed as a reactive iron media for impaired water treatment. The magnetite coating on the surface of ZVI grains, as an electron conductor, could facilitate the electron transfer from ZVI core to the solid/liquid interface to support chemical redox reaction. Furthermore, the magnetite coating could

provide a protection on the ZVI surface to prevent the oxidation of ZVI to maintain its reactivity. Magnetite-coated ZVI augmented with selected metal ions of Fe^{2+}, Fe^{3+}, Al^{3+} or Mn^{2+} had been proven effective in significantly enhancing reaction rate for the removal of various contaminants including nitrate, selenate and molybdate in laboratory and pilot tests (Huang et al., 2003; Huang et al., 2012a, b; Huang et al., 2012c; Huang et al., 2013). The co-presence of ZVI, magnetite, and aqueous Fe^{2+} would create a highly effective media system that can achieve rapid removal of selenate through chemical reduction (Tang et al., 2016). Nitrate reduction rate in a magnetite-coated ZVI system with Fe^{2+} additions was much higher than in a ZVI system without augmented Fe^{2+} (Huang et al., 2003). All these previous results suggested that magnetite-coated ZVI as the reactive media in general possesses higher reaction potentials than a pure ZVI system for transforming and removing contaminants, in particular with the augmented of selected metal ions.

Magnetite-coated ZVI with Mn^{2+} additions for selenate removal has not been previously investigated yet. The objective of this study is to investigate the effect and role of adding Mn^{2+} into ZVI or magnetite-coated ZVI systems for selenate removal under anoxic conditions. The removal mechanism of selenate and the final iron corrosion products were validated through material characterization techniques like X-ray diffraction (XRD) and X-ray photoelectron spectroscopy (XPS). Field emission scanning electron microscope (FE-SEM) was used to elucidate the evolution of morphology and pore structures of the media during the reaction course.

Materials and Methods

Materials

All chemicals used were analytical reagent grade. All reagent solutions were prepared by deionized (DI) water (E-pure, Barnstead, USA) and stored in an anaerobic chamber that is filled with 95% N_2 and 5% H_2 and equipped with a catalytic oxygen gas removal system to maintain an oxygen-free environment (Coy Laboratory, USA). Stock solutions of 200 mM Fe^{2+}, 200 mM Mn^{2+}, and 2.53 mM SeO_4^{2-} were prepared with $FeCl_2 \cdot 4\ H_2O$ (J.T. Baker), $MnCl_2 \cdot 4\ H_2O$ (J.T. Baker), and Na_2SeO_4 (>99.8%, Alfa Aesar), respectively. ZVI grains of -20 mesh in size (>99.2%, Alfa Aesar) were used throughout the tests. The ZVI grains reported a specific surface area of 0.073 m^2/g based on the BET nitrogen absorption analysis (Autosorb-6, Quantachrome, USA). For batch experiments, deoxygenated DI (DDI) water was prepared by flushing DI water with ultra-high nitrogen (>99.999%) for 1 h to remove dissolved oxygen and transferred into the anaerobic chamber for storage until use.

Production of Magnetite-Coated ZVI

A nitrate-Fe^{2+} pretreatment method was used to convert virgin ZVI media into magnetite-coated ZVI. The detail of magnetite coating process was described in Chapter II.

Batch Experiments

Serum vials with 12 ml in volume were used as batch reactors to conduct batch experiments. For each run, multiple reactors were prepared with the same designed initial conditions. For an exemplary test run, each reactor was first filled with 0.50 g of

ZVI or magnetite-coated ZVI and then transferred into an anaerobic chamber that is strictly oxygen free to prevent oxygen from interfering ZVI chemistry. Designed amount of stock solutions and DDI water were filled in the reactor to a total volume of 10 mL with 3.0 mM NO_3^- and various concentrations of 1.0, 2.0, or 3.0 mM Mn^{2+}. The reactors were tightly sealed with rubber stoppers and aluminum caps, which were transferred from the anaerobic chamber to a rotary tumbler with 30 rpm for complete mixing. At a designed reaction time (1 h, 3 h, 6 h, or 12 h), one reactor was withdrawn from the tumbler and sacrifice for measuring pH, SeO_4^{2-}, Fe^{2+} and Mn^{2+}. Each batch experiment was repeated in duplicate at room temperature ($21^oC \pm 2^oC$).

Analytical Methods

For water chemistry analysis, filtrates were collected through 0.45 μm pore size of membrane filters after reactors were withdrawn and opened. Ion Chromatography (IC, Dionex DX-500) with AS-22 separation column, self-regenerating suppressor (AERS-4 mm) and CD-20 conductivity detector with the current of 50 mA was performed to analyze SeO_4^{2-}. For Mn^{2+} analysis, IC equipped with a CS-5A separation column, an AS-20 absorbance detector, MetPac™ PAR diluent and MetPac™ PDCA eluent was used. For dissolved Fe^2 measurement, UV-Vis spectrophotometer (T80, PG Instruments) was used through colorimetrical method of 1, 10-phenanthroline (APHA-AWWA-WEF, 2012).

Solid Characterizations

The morphology and pore structure were examined by FE-SEM (JEOL JSM-7500F). To collect solid sample for FE-SEM analysis, separate parallel batch tests were

conducted. One reactor was withdrawn from the rotary tumbler at a desired reaction time and transferred into the anaerobic chamber. Top liquid with suspended solids was discarded through a syringe. The iron media settled at the bottom was washed with DDI water for three times to remove residual salts (Na^+ and Cl^-) on the solids. The solid sample was then dried and stored in the anaerobic chamber until FE-SEM analysis.

Samples for XRD and XPS analyses were prepared following a process similar to SEM sample preparation. After withdrawn from the rotary tumbler, reactors were first sonicated for 5 minutes to strip off the outer layer of iron corrosion coatings. The top suspension with the stripped iron corrosion coatings was filtered with a membrane filter of 0.45 μm pore size, which formed a thin solid film on the paper; the solid cake together with the filter membrane was dried and stored under an anaerobic environment until used for XRD and XPS analyses.

XRD powder pattern was analyzed by X-ray powder diffractometer (Bruker-AXS D8) with copper X-ray radiations. An omicron XPS system equipped with 0.8 eV resolution Argus detector using Mg X-ray source was used for XPS measurement.

Results and Discussions

Selenate Reduction in a ZVI/Mn^{2+} System

No significant selenate removal was observed when virgin ZVI grains were used in both with and without externally added Mn^{2+}. Although adding Mn^{2+} into a ZVI system could result in Fe^{2+} production up to 5 mg/L by 12 h reaction time, selenate reduction was not enhanced through co-existence of ZVI, Fe^{2+} and Mn^{2+}. Tang et al. (2016) demonstrated that adding Fe^{2+} into a ZVI system could greatly accelerate reaction

rate of selenate removal in a ZVI system. Therefore, the result suggested that aqueous Mn^{2+} may disrupt the chemical interaction between selenate and ZVI/Fe^{2+}, resulting in the inhibition of selenate reduction in a ZVI/Fe^{2+} system. In the test, aqueous Mn^{2+} gradually decreased by around 0.2 mM by 12 h reaction time. The disappearance of aqueous Mn^{2+} could be attributed mainly to the incorporation into solid phase. Alternatively, Mn^{2+} decrease could result from the hydrolysis of Mn^{2+} to form mononuclear $MnOH^{+}$ complex or adsorb onto the iron oxide surface, both of which could result in H^{+} release and pH decrease in the solution (Perrin, 1962). The trend of pH decrease observed during the reaction course also supported that the hydroxyl ions were consumed.

Selenate Reduction in a Magnetite-Coated ZVI/Mn^{2+} System

Fig. 8(a) control test showed that without Mn^{2+} addition a magnetite-coated ZVI system is not reactive for selenate reduction, which is no different from a virgin ZVI system in the absence of externally-added Fe^{2+}. During the course, no aqueous Fe^{2+} was produced from magnetite-coated ZVI and pH was steady at ~8.2. The results showed that selenate could not be effectively reduced in both a virgin ZVI and a magnetite-coated ZVI system without an effective supplementary metal ion such as Mn^{2+} and Fe^{2+} at neutral pH.

Unlike a ZVI system, selenate could be rapidly reduced in a magnetite-coated ZVI system with Mn^{2+} addition. In all three tests with Mn^{2+} addition, no significant selenate reduction occurred in the first hour, but after the initial lag phase, selenate reduction accelerate quickly. Selenate was reduced to less than 0.02 mg/L (below the

detection limit of the IC method) within 6 h in the tests with 2.0 mM and 3.0 mM Mn^{2+}. In the test with 1.0 mM Mn^{2+}, selenate was completely removed after 12 h reaction. The initial 1 hour stagnant phase suggests that the media was not reactive initially for selenate removal, but with the presence of Mn^{2+}, the surface of the media could be gradually activated. Literature reported that magnetite crystalline exposed to air can be partially oxidized to form a thin layer of maghemite (γ-Fe2O3). Maghemite, although sharing a similar XRD spectrum or crystalline structure with magnetite, is a poor electron conductor. The initial lag phase might be due to the presence of a thin layer of maghemite on the outer surface of the magnetite coating on ZVI grains. The activation process may involve complicated interactions among ZVI, the magnetite coating and aqueous Mn^{2+}, which altered pH and released Fe^{2+}, and more importantly, changed the passive layer of maghemite into a reactive oxide coating on ZVI surface that allowed effective electron transfer and ion diffusion essential for mediating selenate reduction. Consequently, selenate could be rapidly reduced in the magnetite-coated ZVI system with Mn^{2+} addition.

Aqueous Mn^{2+} disappeared with time in all tests with Mn^{2+} as shown in Fig. 8(b). By 1 h reaction time, 0.18, 0.27 and 0.4 mM Mn^{2+} were consumed in the tests with 1.0, 2.0, and 3.0 mM Mn^{2+} tests, respectively. By 12 h reaction time, 0.31, 0.56 and 0.81 mM were decreased in the tests with 1.0, 2.0, and 3.0 mM Mn^{2+} tests, respectively. In conjunction with the Fe^{2+} release and decrease profiles observed during the tests, the results suggested that aqueous Mn^{2+} could be continuously incorporated into the solid phase that formed Mn(II)-doped iron oxides. The rate of Mn^{2+} decrease was similar and

time-independent in all cases, except for the initial 1 h lag phase. In the first one hour, Mn^{2+} decreased at a faster rate than the subsequent reaction time. The extra usage of Mn^{2+} might be related to the incorporation of Mn^{2+} into the outer passive maghemite layer into form a Mn(II)-doped magnetite layer. The incorporation of Mn(II) in the inverse spinel structure of maghemite with Fe(III) ion only might greatly improve its electron conductivity, just like the interaction between adjacent Fe(II) and Fe(III) enable efficient electron conduction in the magnetite structure where Fe(II) and Fe(III) are co-present.

In contrast to Mn^{2+} depletion, Fe^{2+} was gradually produced with time in all three tests with Mn^{2+} addition as shown in Fig. 8(c). By 12 h reaction time, 0.12, 0.21 and 0.27 mM aqueous Fe^{2+} were released in the tests with 1.0, 2.0 and 3.0 mM Mn^{2+}, respectively. Fe^{2+} could be generated from ZVI grains as the intermediate/final product during selenate reduction process. Nevertheless, in the first hour, selenate reduction was limited and only Mn^{2+} was consumed, implying that Fe^{2+} production was strongly pertinent to Mn^{2+} depletion. Therefore, Fe^{2+} could be released from the magnetite coating due to cation substitution by aqueous Mn^{2+}. In the test with 1.0 and 2.0 mM Mn^{2+}, the ratio of Fe^{2+} production to Mn^{2+} decrease were ~ 0.51, 0.41, 0.41 and 0.38 in 1 h, 3 h, 6 h and 12 h reaction time, respectively. In the test with 3.0 mM Mn^{2+}, the ratio of Fe^{2+} production to Mn^{2+} consumption were ~ 0.38, 0.4, 0.35 and 0.33 in 1 h, 3 h, 6 h and 12 h reaction time, respectively. In addition, Fe^{2+} production and Mn^{2+} consumption during the reaction time was linearly correlated, suggesting that the chemistry behind Fe^{2+} production and Mn^{2+} consumption are coupled.

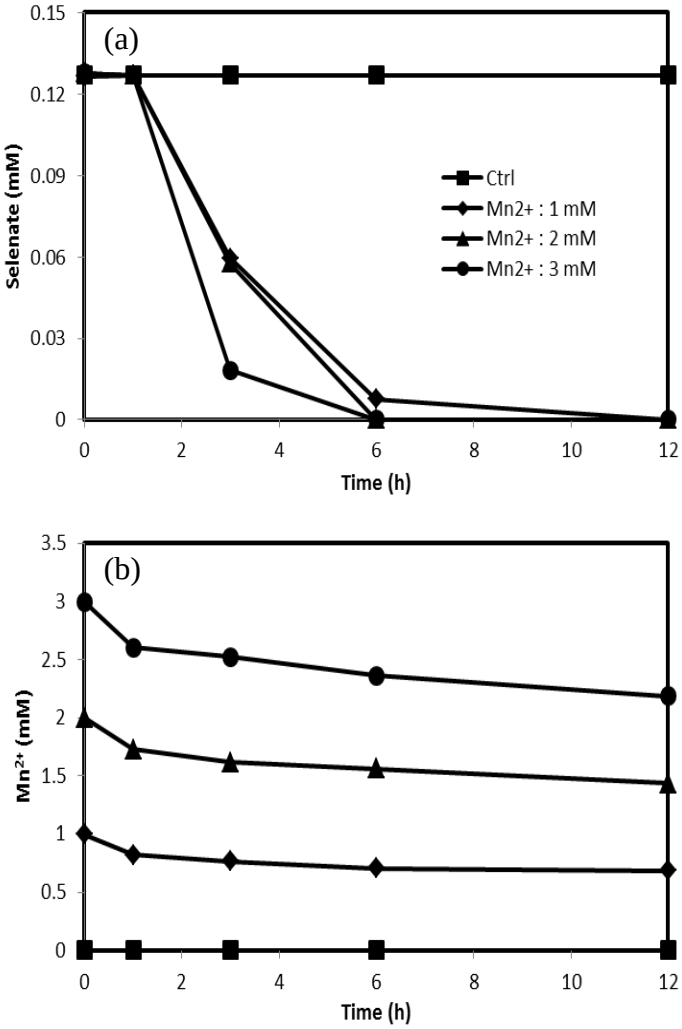

Figure 8. Change over time of (a) selenate, (b) Mn^{2+} and (c) Fe^{2+} concentration in a batch test with magnetite-coated ZVI system (5% w/v) + 0.127 mM (or 10 mg/L) selenate + various concentrations of Mn^{2+} (1.0, 2.0, or 3.0 mM, and 0 in the control).

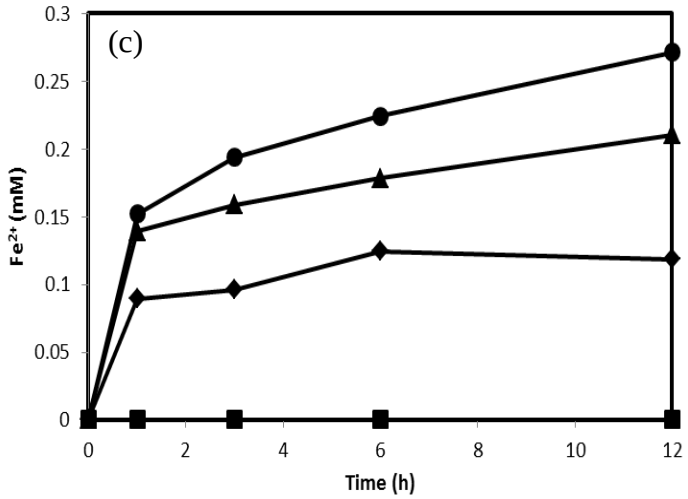

Figure 8. Continued.

XRD Results

The XRD results on the media sample collected from the batch test, shown in Fig. 9, confirm that magnetite and hausmannite (Mn_3O_4) are among the corrosion products. The major characteristic peaks of XRD powder spectra for both magnetite and hausmannite appears at 2 theta of 30.1^o, 35.3^o and 62.4^o (the strongest peak). The peak intensities were strengthened over time as reaction proceeded, suggesting that magnetite and hausmannite become better crystallized in structure during the reaction process.

Besides magnetite and hausmannite, nakauriite with the chemical formula of $Mn_8(SO_4)_4(CO_3)(OH)_6{\cdot}48(H_2O)$ or a similar material might also be produced during the reaction. The major characteristic peaks of nakauriite was at 2 theta of 12.1^o (the strongest peak), 24.4^o and 38.0^o. The peaks of nakauriite spectra were present in the media sample at 1 h and 3 h reaction time. The peak intensity of solid sample in 3 h reaction was stronger than the one in 1 h reaction. However, the nakauriite peaks

disappeared in the sample after 6 h reaction, implying that nakauriite might be an intermediate product during the reaction and could be transformed over time as the media aged when the interactions among ZVI, the magnetite coating and aqueous Mn^{2+} coupled with selenate reduction and ZVI corrosion in the system could result in the transformation of nakauriite into the more stable end product, e.g., magnetite or hausmannite or a mixture of both.

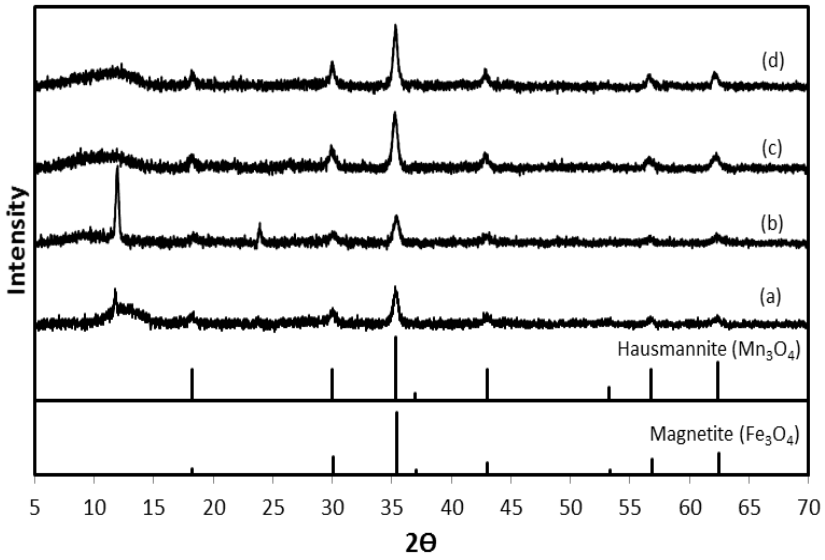

Figure 9. XRD spectra showed the evolution of the iron oxide phase collected from batch reactors with 5% w/v of magnetite-coated ZVI + 3.0 mM Mn^{2+} + 0.127 mM SeO_4^{2-} after (a) 1 h, (b) 3 h, (c) 6 h and (d) 12 h reaction time. XRD spectra of magnetite (Fe_3O_4) and hausmannite (Mn_3O_4) are provided as references.

To produce nakauriite, sulfate (SO_4^{2-}) ions have to essentially participate in the reaction. Sulfate, however, was not added into the system. It can be postulated that the formation of nakauriite might be related to selenate ions. Selenate is analogous to sulfate

due to the similarities in chemical structure, valence state and ionic radii. Selenate could not only directly substitute structural sulfate in crystallites but also could involve in the formation of sulfate minerals (Dutrizac et al., 1981; Hassett et al., 1990; Waychunas et al., 1995). Consequently, selenate could replace sulfate to participate in the reaction of nakauriite production to form a mineral of selenate-substituted nakauriite ($Mn_8(SeO_4)_4(CO_3)(OH)_6 \cdot 48(H_2O)$) in the reactive system. Thus, the XRD results suggested that one mechanism of selenate removal could be the direct use of selenate ion directly to form selenate-substituted nakauriite or the likes through a co-precipitation and crystallization process.

FE-SEM Analysis

The SEM micrographs in Fig. 10 recorded the morphological change of the media surface during selenate removal process in a magnetite-coated ZVI system with Mn^{2+} additions. The surface of the magnetite-coated ZVI was mostly covered by hexagonal shape of crystallites at 1 h reaction time. The crystallites with the average size of ~1 μm^2 could include hausmannite (Mn_3O_4) (Dhaouadi et al., 2012) according to the XRD results. Aqueous Mn^{2+} could be incorporated into the magnetite coating to substitute structural Fe(II) or Fe(III) to form hausmannite, resulting in the release of Fe^{2+} into aqueous phase as observed during the reaction. After 3 h reaction, significant selenate reduction occurred, and as a result, new corrosion products would be formed. SEM micrographs showed that aggregates of likely hausmannite and magnetite mixture with an average crystalline size of ~0.2 μm^2 were formed and accumulated over time.

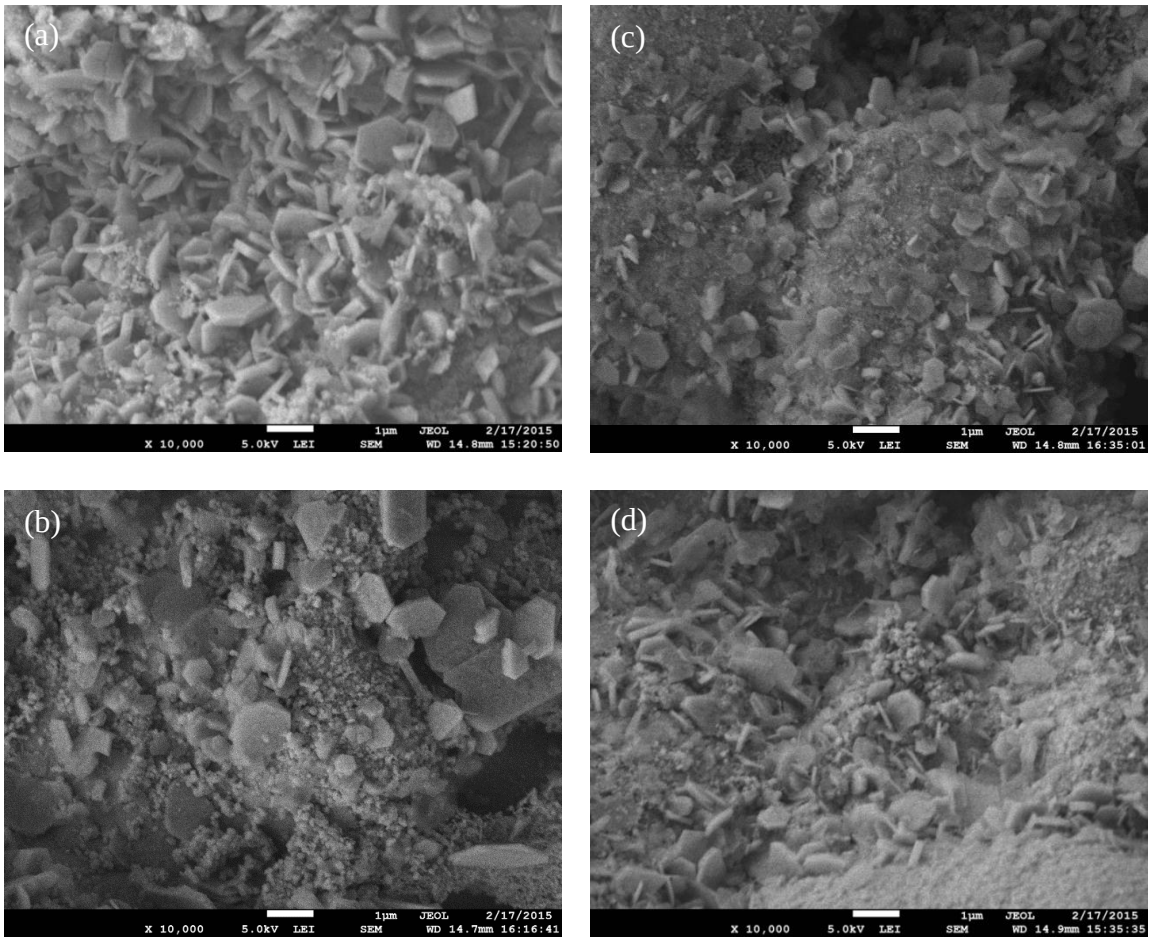

Figure 10. FE-SEM images of the media collected at (a) 1 h, (b) 3 h, (c) 6 h and (d) 12 h from the batch reactors with the initial conditions controlled as 50g/L magnetite-coated ZVI + 3.0 mM Mn^{2+} + 0.127 mM SeO_4^{2-}.

XPS Results

XPS scan (as shown in Fig. 11) were performed to illustrate the chemical status of Fe and Mn in the media collected from the batch test after 12 h reaction time. The spectra of XPS on element Fe indicated that magnetite was the final product from selenate reduction in a magnetite-coated ZVI system with Mn^{2+} additions. The result is consistent with the findings from SEM and XRD analyses. For element Mn, manganese

ferrite ($MnFe_2O_4$) was another manganese oxide other than hausmannite. The formation of manganese ferrite might not be directly attributed to selenate reduction in the system. Instead, it might be formed via the process of isomorphous substitution in which aqueous Mn^{2+} would replace structural Fe(II) in the magnetite coating without a significant change of the crystal structure, resulting in the same XRD powder spectrum to magnetite.

XPS scan in Fig. 12 showed the evolution of selenium species in the solid phase. In the first hour, selenate and elemental selenium were the two dominant species on the solid surface. By 12 h reaction time, selenium was found to exist only in selenide (Se^{2-}) form. Therefore, selenate and elemental selenium were reduced to selenide during the reaction. The XPS results implied that selenate could be removed through both adsorption by the reactive sites of the solid media and chemical reduction by magnetite-coated ZVI. In addition, the detection of selenate peak in the solid sample collected at 1 h reaction also corroborate the XRD results that selenate-substituted nakauriite was formed in 1 h and 3 h reaction.

The Roles of Mn^{2+}

A virgin ZVI with addition of Mn^{2+} is chemically passive for selenate reduction but a virgin ZVI with addition of Fe^{2+} can mediate rapid selenate reduction. Such different results suggest that the role of Mn^{2+} and Fe^{2+} are not fully substituted. The addition of Mn^{2+} is only effective when there is a preexisting magnetite coating on ZVI gains. In all tests, aqueous Mn^{2+} was found incorporated into the magnetite coating to replace structural Fe(II), resulting in the release of Fe^{2+} into aqueous phase, leading to

the formation of a mixed Mn(II)/Fe(II)/Fe(III) oxide layer that exhibit an inverse spinel structure similar to that of magnetite, the composition of which could range between hausmannite (Mn_3O_4) and manganese ferrite ($MnFe_2O_4$) as showed by the XPS and XRD spectra. Such mixed Mn(II)-Fe(II)-Fe(III) magnetite-like oxides appeared to be reactive for selenate reduction and also for nitrate reduction according to preious tests.

Aqueous Mn^{2+} alone could not directly trigger selenate removal as implied by the initial lag phase when selenate was barely removed even when all the key materials are present. The role of Mn^{2+} is complex and only functions through interactions with magnetite coating and ZVI and possibly aqueous Fe^{2+}. The fact that in the tests all Mn^{2+} was depleted while Fe^{2+} was still present suggested that Mn^{2+} might be the preferred metal ions over Fe^{2+} for activating the corrosion oxide layer to support selenate reduction. A quantitative relationship might exist between the amount of Mn^{2+} uptake and selenate reduction, but unfortunately, the current experimental design with a low selenate dosage (0.127 mM) used and high Mn^{2+} might not be the best design for deriving such quantitative relationship.

Removal Mechanisms of Selenate

The mechanisms for selenate removal in a magnetite-coated ZVI system with Mn^{2+} additions may include adsorption, mineral crystallization, and chemical reduction. XRD and XPS results suggested that selenate could interact with Mn^{2+} to form selenate-substituted nakauriite, possibly with the assistance of magnetite coating and/or ZVI, since no reaction would occur with Mn^{2+} and selenate alone. As selenate removal reaction proceeded, XRD results also indicated that selenate-substituted nakauriite was

not a stable end product and could be transformed as the structural selenate ions were gradually reduced by the ZVI towards Se(0) or Se(-II). The possible reactions of selenate removal by a magnetite-coated ZVI with Mn^{2+} additions may be represented by the following reaction equations:

$$8Mn^{2+} + 4SeO_4^{2-} + CO_3^{2-} + 54H_2O \rightarrow Mn_8(SeO_4)_4CO_3(OH_6) \cdot 48H_2O + 6H^+ \quad [3]$$

$$SeO_4^{2-} + 8H^+ + 6e^- \rightarrow Se^0 + 4H_2O \quad [4]$$

$$Se^0 + 2e^- \rightarrow Se^{2-} \quad [5]$$

Alternatively, selenate in aqueous phase could also be directly reduced to elemental selenium by magnetite-coated ZVI with ZVI as the electron source for the reduction of selenate to Se(0). This reaction could happen on the solid/liquid interface, but the resultant Se(0), existing as a fine crystalline, may be incorporated in the crystalline structure of magnetite or the porous bulk oxide coating on ZVI surface. Elemental selenium could be further reduced to selenide. Chemical reduction for selenate removal in both aqueous and solid phase could be occurred simultaneously in a magnetite-coated ZVI system with Mn^{2+} additions.

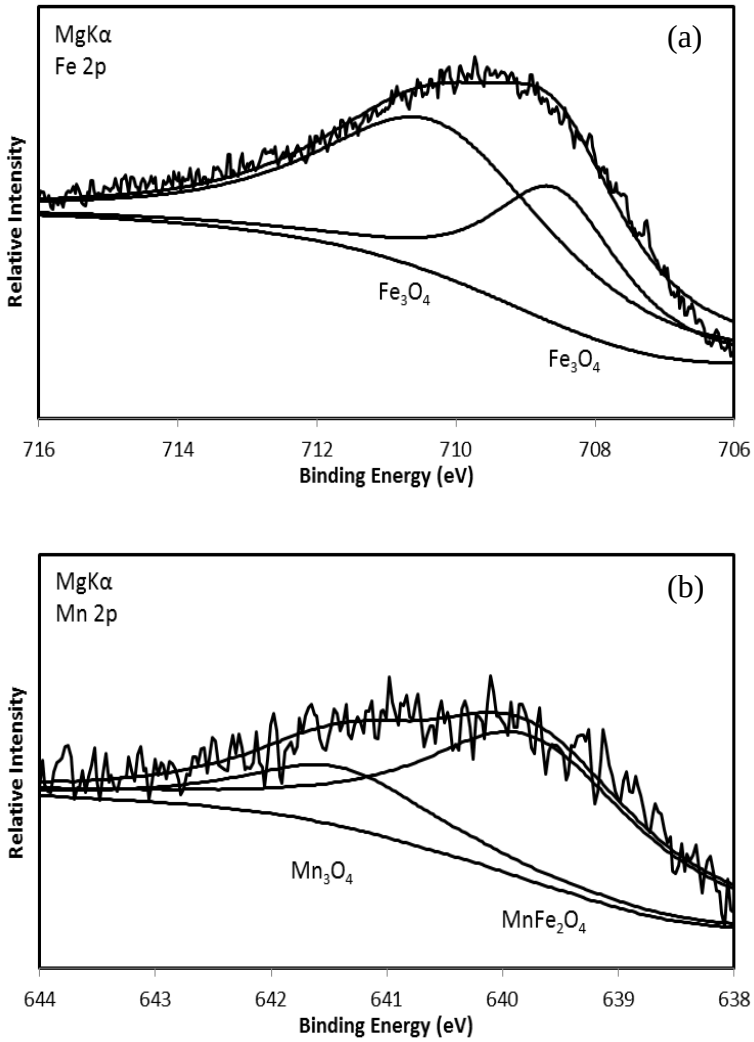

Figure 11. XPS scan profiles of the corrosion products on (a) Fe 2p and (b) Mn 2p regional binding energy. The spectra indicated the presence of Fe_3O4, $MnFe_2O_4$, and Mn_3O_4 in the corrosion products. Sample was collected from a batch test with initial conditions as 50g/L magnetite-coated ZVI + 3.0 mM Mn^{2+} + 0.127 mM SeO_4^{2-}.

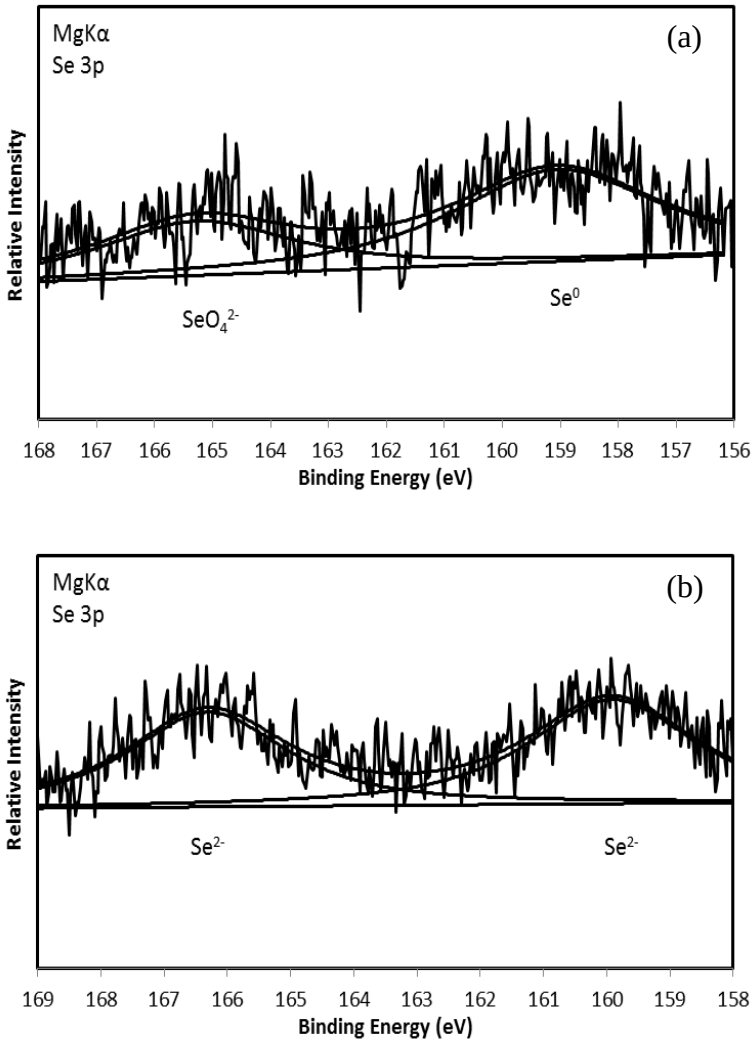

Figure 12. XPS high resolution spectra of the Se 3p binding energy on iron corrosion products collected after (a) 1 h and (b) 12 h reaction time from a batch test with initial conditions controlled as 50g/L magnetite-coated ZVI + 3.0 mM Mn^{2+} + 0.127 mM SeO_4^{2-}.

Summary

Selenate was effectively removed in a magnetite-coated ZVI system with Mn^{2+} additions under anoxic conditions. Although aqueous Mn^{2+} may not directly facilitate selenate reduction, Mn^{2+} could affect the chemistries in both aqueous and solid phase for

rapid selenate removal. In the presence of externally-added Mn^{2+}, selenate could be initially removed through co-precipitation process, in which both aqueous Mn^{2+} and selenate may participate in a chemical process that produce selenate-substituted nakauriite. In the solid phase, selenium was present in forms of selenate, elemental selenium and selenide. Selenide appeared to be the destined product as the immobilized selenate, existed first as a structural selenate component in nakauriite, was reduced stepwise over time by ZVI to elemental selenium and selenide. Mechanisms responsible for selenate removal in the system may include surface adsorption, mineral crystallization, and chemical reduction. The added Mn^{2+} would be incorporated into the magnetite structure to form Mn(II)-doped magnetite. The synergistic effect of magnetite-coated ZVI, Mn(II)-doped magnetite, Mn^{2+} and Fe^{2+} could play an important role in rapid selenate removal. More in-depth study will be needed to further our understandings on how ZVI, magnetite, Mn^{2+} and Fe^{2+} would interact with each other that could facilitate selenate removal.

CHAPTER IV EFFECT OF ZN^{2+} ON SELENATE REDUCTION BY MAGNETITE-COATED ZERO-VALENT IRON

Introduction

Selenium (Se), occurred naturally in environment, is an essential metalloid as micronutrients for the health of human being, fish, birds and animals. Therefore, the deficiency of Se can result in the biological dysfunction. Conversely, the overdose of Se can harm living organisms due to its toxicity, resulting in hair loss, circulatory problems and mortality. The anthropogenic sources of Se pollution are normally originated from irrigated agriculture, petrochemical refineries, mining, coal-fired power plants and industrial manufacturing operations (Lemly, 2004). Consequently, Se contamination is a worldwide problem with serious impacts on aquatic life. US EPA regulates that the maximum contamination level for Se in drinking water is 50 μg/L.

The common Se species in environment are selenate (Se(VI)), selenite (Se(IV)), elemental selenium (Se(0)), selenide (Se(-II)) and organic selenium. The oxidation state of Se significantly affect the solubility, mobility and toxicity of Se. For examples, Se(VI) and Se(IV) are predominantly mobile Se oxyanions, and Se(0) and Se(-II) are existed as solid with low solubility. Therefore, Se(VI) and Se(IV) exhibit more environmental risks than Se(0) and Se(-II) due to their high solubility and mobility (Zawislanski and Zavarin, 1996). Unlike Se(VI), Se(IV) is easily adsorbed onto oxides surface, especially onto iron oxides of magnetite, goethite, hematite and ferrihydrite (Martínez et al., 2006; Rovira et al., 2008; Chan et al., 2009; Das et al., 2013).

Therefore, Se(VI) is relatively stable and mobile Se species, resulting in difficult removal by traditional methods. Various treatments have been developed for removing Se in aqueous system, such as adsorption, chemical reduction and bioremediation (Zhang et al., 2005b; Morita et al., 2007; Zhang et al., 2008; Pettine et al., 2012; Szlachta and Chubar, 2013; Fu et al., 2016). However, these technologies could be costly in operation and maintenance and biological treatment may produce a large amount of sludge, resulting in unexpected cost by further post-treatment processes (Soda et al., 2011).

Zero-valent iron (ZVI), a moderately and inexpensive reducing agent, has been widely utilized to remove inorganic and organic contaminants for in situ and ex situ groundwater and wastewater remediation, such as nitrate, selenate, lead, chromate, molybdate and chlorinated solvents. (Siantar et al., 1996; Huang et al., 1998; Huang and Zhang, 2002; Huang and Zhang, 2004; Noubactep et al., 2005; Yang and Lee, 2005; Morrison et al., 2006; Della Rocca et al., 2007; Huang et al., 2012c; Tang et al., 2016). However, iron corrosion process could result in the formation of passive iron oxides on the surface of ZVI that tends to halt the reaction for contaminant removal. Besides ZVI, reactive iron oxides, such as magnetite, hematite, maghemite and green rust, can be used for Se removal (Su and Suarez, 2000; Rovira et al., 2008; Gonzalez et al., 2012; Jordan et al., 2013). Those iron oxides can provide active adsorption sites to chemically bond with aqueous Se species under certain conditions, but the removal efficiency would be sensitively influenced by chemical environments (e.g. pH and ionic strength). Therefore,

using ZVI or iron oxides only could significantly lead to poor performance of Se removal.

Magnetite-coated ZVI is a reactive iron media that can be used for water quality control. Among various iron oxides, only magnetite exhibits a metallic electron conductivity. The magnetite coating on the surface of ZVI not only directly provides reactive adsorption sites for pollutants but also prevent the loss of ZVI reactivity from the insulation of forming a passive iron rust coating. As a consequence, the ZVI core can more sustainably supply electrons to the solid/liquid interface to support redox reaction for chemical reductions mediated by the magnetite coating. Previous research has demonstrated that magnetite-coated ZVI can effectively enhance reaction rate for contaminant removal. With the augment of certain metal ions like Fe^{2+}, Fe^{3+}, Al^{3+} or Mn^{2+}, magnetite-coated ZVI could rapidly remove contaminants such as nitrate, selenate and molybdate (Huang et al., 2003; Huang and Zhang, 2006a; Huang et al., 2012a, b; Huang et al., 2012c; Huang et al., 2013; Tang et al., 2014b). These results showed that magnetite-coated ZVI has many potentials. However, magnetite-coated ZVI with other metal ion addition has not been investigated in depth. To fulfill the potentials of the new media and the chemistry behind its effectiveness, more studies are needed.

The purpose of this study is to evaluate the effect and role(s) of aqueous Zn^{2+} in a magnetite-coated ZVI system employed for removing selenate from water. The general approach is to conduct batch reactor tests to evaluate how selenate could be removed in the magnetite-coated ZVI media system under various control conditions. The morphology change of magnetite-coated ZVI during the reaction was characterized

through field emission scanning electron microscope (FE-SEM). In addition, X-ray diffraction (XRD) and X-ray photoelectron spectroscopy (XPS) were employed to determine iron corrosion products and the fate of selenium once immobilized from liquid phase and onto the solid media. The role and fate of Zn^{2+} in a magnetite-coated ZVI system was also analyzed.

Materials and Methods

Materials

All regent solutions were prepared by analytical reagent grade chemicals with deionized (DI) water (E-pure, Barnstead, USA). All prepared solutions were stored in the anaerobic chamber filled with 95% N_2 and 5% H_2 (Coy Laboratory, USA). The stock solution of 200 mM Fe^{2+}, 200 mM Zn^{2+}, and 2.53 mM SeO_4^{2-} were prepared with $FeCl_2 \cdot 4\ H_2O$ (J.T. Baker), $ZnCl_2 \cdot 4\ H_2O$ (J.T. Baker), and Na_2SeO_4 (>99.8%, Alfa Aesar), respectively.

Production of Magnetite-coated ZVI

To produce the magnetite coating, a nitrate-Fe^{2+} pretreatment method was utilized to transform pure ZVI to magnetite-coated ZVI. The detail of magnetite-coated ZVI production was described in Chapter II. ZVI grains of -20 mesh in size (>99.2%, Alfa Aesar) were used throughout the tests. The ZVI grains reported a specific surface area of 0.073 m^2/g based on the BET nitrogen absorption analysis (Autosorb-6, Quantachrome, USA). For batch experiments, deoxygenated DI (DDI) water was prepared by flushing DI water with ultra-high nitrogen (>99.999%) for 1 h to remove dissolved oxygen and transferred into the anaerobic chamber for storage until use.

Batch Experiments

All batch experiments were conducted using 12 ml serum vials as reactors. For each batch test, multiple reactors with identical initial conditions were prepared. For an exemplary test run, each reactor was first filled with 0.50 g of ZVI or magnetite-coated ZVI and then transferred into an anaerobic chamber that is strictly oxygen free to prevent oxygen from interfering ZVI chemistry. Designed amount of stock solutions and DDI water were filled in the reactor to a total volume of 10 mL with designed concentration of selenate (e.g., 0.127 mM) and Zn^{2+} (e.g., 1.0, 2.0, 3.0 mM). The reactors were tightly sealed with rubber stoppers and aluminum caps, which were transferred from the anaerobic chamber to a rotary tumbler with 30 rpm for complete mixing. At a designed reaction time (1 h, 2 h, 4 h, 8 h, 16 h or 24 h), one reactor was withdrawn from the tumbler and sacrifice for measuring pH, SeO_4^{2-}, Fe^{2+} and Zn^{2+}. Each batch experiment was repeated in duplicate at room temperature ($21^oC \pm 2^oC$).

Analytical Methods

For water chemistry analysis, filtrates were collected through 0.45 μm pore size of membrane filters after reactors were withdrawn and opened. Ion Chromatography (IC, Dionex DX-500) with AS-22 separation column, self-regenerating suppressor (AERS-4 mm) and CD-20 conductivity detector with the current of 50 mA was performed to analyze SeO_4^{2-}. For Zn^{2+} analysis, IC equipped with a CS-5A separation column, an AS-20 absorbance detector, MetPac™ PAR diluent and MetPac™ PDCA eluent was used. For dissolved Fe^{2+} measurement, UV-Vis spectrophotometer (T80, PG Instruments) was

used through colorimetrical method of 1, 10-phenanthroline (APHA-AWWA-WEF, 2012).

Solid Characterizations

The morphology and pore structure were examined by FE-SEM (JEOL JSM-7500F). To collect solid sample for FE-SEM analysis, separate parallel batch tests were conducted. One reactor was withdrawn from the rotary tumbler at a desired reaction time and transferred into the anaerobic chamber. Top liquid with suspended solids was discarded through a syringe. The iron media settled at the bottom was washed with DDI water for three times to remove residual salts (Na^+ and Cl^-) on the solids. The solid sample was then dried and stored in the anaerobic chamber until FE-SEM analysis.

Samples for XRD and XPS analyses were prepared following a process similar to SEM sample preparation. After withdrawn from the rotary tumbler, reactors were first sonicated for 5 minutes to strip off the outer layer of iron corrosion coatings. The top suspension with the stripped iron corrosion coatings was filtered with a membrane filter of 0.45 μm pore size, which formed a thin solid film on the paper; the solid cake together with the filter membrane was dried and stored under an anaerobic environment until used for XRD and XPS analyses.

XRD powder pattern was analyzed by X-ray powder diffractometer (Bruker-AXS D8) with copper X-ray radiations. An omicron XPS system equipped with 0.8 eV resolution Argus detector using Mg X-ray source was used for XPS measurement.

Results and Discussions

Selenate Removal

As shown in Fig. 13(a), selenate could not be effectively removed by magnetite-coated ZVI without the addition of Zn^{2+} (the control). With Zn^{2+} additions, however, selenate could be effectively removed. In fact the reaction achieved a remarkably high reaction rate in the early phase. For example, 84% of the added selenate had been removed after 1st hour reaction. The pattern of selenate removal in the three tests with Zn^{2+} was similar to each other before 3 h reaction time. Selenate was completely removed after 8 h, 16 h and 24 h reaction time in the three tests with 1.0, 2.0, and 3.0 mM Zn^{2+} additions, respectively. Higher Zn^{2+} dosage would increase reaction rate for selenate removal. The results demonstrated that aqueous Zn^{2+} could greatly accelerate selenate removal by magnetite-coated ZVI in an anaerobic environment.

As shown in Fig. 13(b), Zn^{2+} would be consumed during the reaction course. in For the tests with 1.0, 2.0, and 3.0 mM Zn^{2+} addition, aqueous Zn^{2+} concentration decreased by 0.72, 0.68, and 0.43 mM, respectively, after 24 h reaction time. The results showed that a high dosage of Zn^{2+} could achieve a better selenate removal with less Zn^{2+} consumed in a magnetite-coated ZVI system. Although Zn^{2+} decrease was not quantitatively related to selenate removal, Zn^{2+} consumption may still be linked to selenate removal. Zn^{2+} consumptions in the first hour in the three tests with 1.0, 2.0, and 3.0 mM Zn^{2+} addition were 0.25 mM, 0.14 mM and 0.07 mM, respectively, translating to a ratio of 3.6 : 2 : 1. The results suggested that Zn^{2+} consumption was inversely proportional to Zn^{2+} dosage. Zn^{2+} may interact with magnetite coating, likely being

incorporated into the lattice of the magnetite crystalline through an isomorphic substitution that barely changes the base structure.

Fe^{2+} was continuously produced during the reaction course, as shown in Fig. 13(c). Aqueous Fe^{2+} in the tests with 1.0, 2.0, and 3.0 mM Zn^{2+} addition were 0.54, 0.59, and 0.63 mM, respectively, after 24 h reaction. Because Fe^{2+} was not initially added into the system, Fe^{2+} could be a product from the selenate removal process. The amount and rate of Fe^{2+} release in the three tests with Zn^{2+} was not significantly different before 3 h reaction time despite the different dosage of Zn^{2+}. Overall, however, increased Zn^{2+} dosage would result in higher Fe^{2+} production. The coexistence of aqueous Fe^{2+} and Zn^{2+} in a magnetite-coated ZVI system may enhance selenate removal.

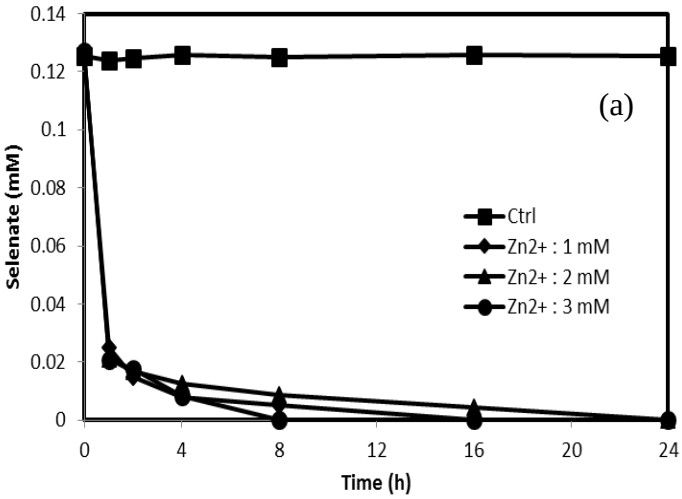

Figure 13. Change of (a) selenate, (b) Zn^{2+} and (c) Fe^{2+} concentration over time observed in a batch test with initial conditions controlled as 50 g/L magnetite-coated ZVI + 0.127 mM selenate + various concentrations of Zn^{2+} (1.0, 2.0, 3.0 mM).

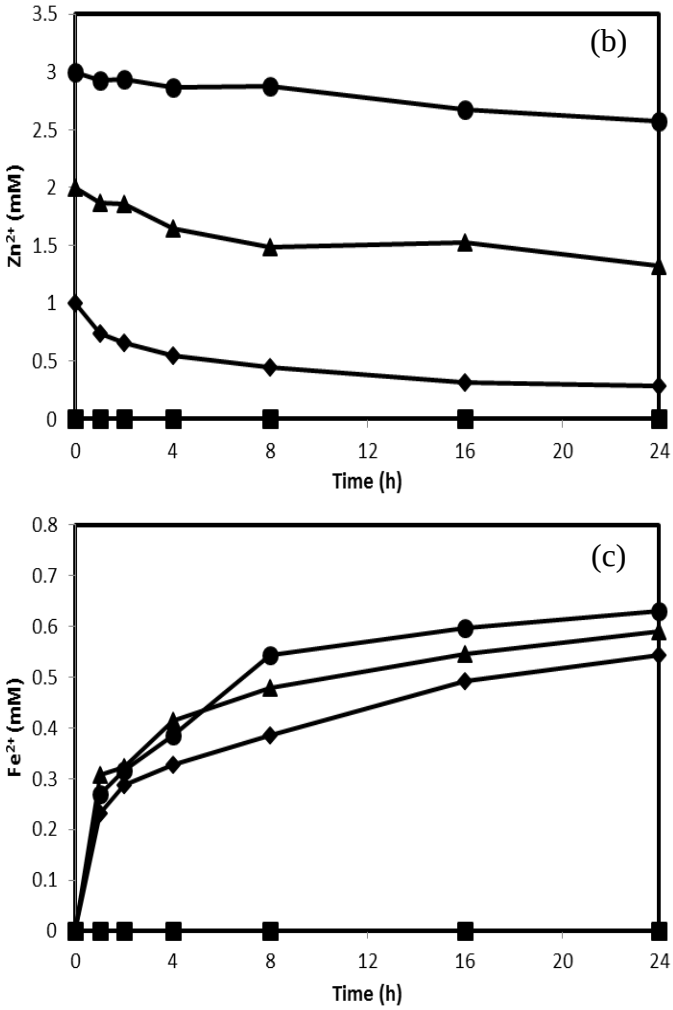

Figure 13. Continued

XRD Results

The XRD results (Fig. 14) showed that magnetite might still be the main iron corrosion products upon the reduction of selenate by a magnetite-coated ZVI in the presence of externally-added Zn^{2+}. The peak intensities of the XRD spectra, however, become weaker over time, suggesting that the initial crystalline magnetite coating was transformed to an amorphous form. After 2 h reaction, no obvious peak was detected in

the XRD spectrum. However, weak magnetite peaks re-appear after 4 h reaction. Unknown amorphous mineral could be formed after 2 h reaction, which could cover the initial magnetite coating and thus mask the magnetite peaks. Another possibility could be that chemistry responsible for selenate removal may also alter the magnetite, transforming a crystal structure into an amorphous one. The reappearance of magnetite after 4 h reaction suggests that the amorphous intermediate product could further evolved and be transformed to magnetite as the end stable product. After 24 h reaction, besides magnetite, two unknown peaks were detected at two theta of 21.0^{o} and 36.6^{o} degrees. XRD library search didn't produce any meaningful match with these two characteristic peaks, thus the crystalline could not be positively identified. The unknown peaks may be belonged to a composite mineral of Se, Fe, Zn and O.

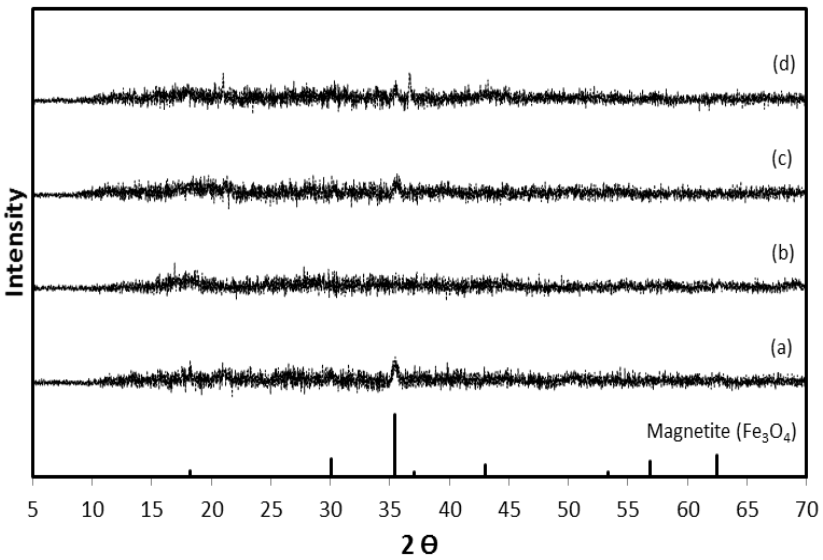

Figure 14. XRD powder patterns of the oxide samples collected at (a) 1 h, (b) 2 h, (c) 4 h and (d) 24 h reaction time from a batch reactor with initial conditions controlled as 50 g/L magnetite-coated ZVI + 3.0 mM Zn^{2+} + 0.127 mM SeO_4^{2-}. The reference is magnetite (Fe_3O_4).

FE-SEM Analysis

Fig. 15 illustrated the change of morphology and pore structure of the solid media collected from the batch test in a magnetite-coated ZVI system with Zn^{2+} additions. In the first hour, the surface of the magnetite coating was uniformly covered by a mineral with a hexagonal shape, which does not match with any of the common iron oxides (e.g. magnetite, hematite, maghemite, goethite or lepidocrocite). The mineral size was around 1 μm^2. However, the hexagonal shape of particular minerals disappeared after 2 h reaction from the surface, replaced instead by the massively aggregated structure. After 4 h reaction, the aggregated structure only partially covered the surface of the media. The results suggested that magnetite could be an intermediate product from selenate removal process. The surface of the media sample from 24 reaction was relatively smooth compared with the solid samples from 1, 2 and 4 h reaction time.

Energy-dispersive X-ray spectroscopy (EDS) showed that the elements of O, Fe and Zn were co-present in the media after reaction. Zn^{2+} was incorporated into the structure of the magnetite coating, accounting for an atomic ratio of 3.17% ~ 4.17% in the oxide coating. The ratio of chemical composition of O : Fe : Zn in the solid samples after 2 h, 4 h and 24 h reaction time were 17.8 : 11.7 : 1.0, 18.6 : 12.0 : 1.0 and 14.5 : 8.5 : 1.0, respectively. The chemical compositions in the samples from 2 h and 4 h reaction time were close, but at 24 h, Zn ratio increased. Moreover, The atomic ratio of (Fe + Zn) to element O in the media samples after 2 h, 4 h and 24 h reaction time were 0.71, 0.70 and 0.66, respectively, which is close to the ratio of Fe to O in the ideal magnetite

structure of 0.75. The results also support that aqueous Zn^{2+} could isomorphically substitute structural Fe(II) of the magnetite coating.

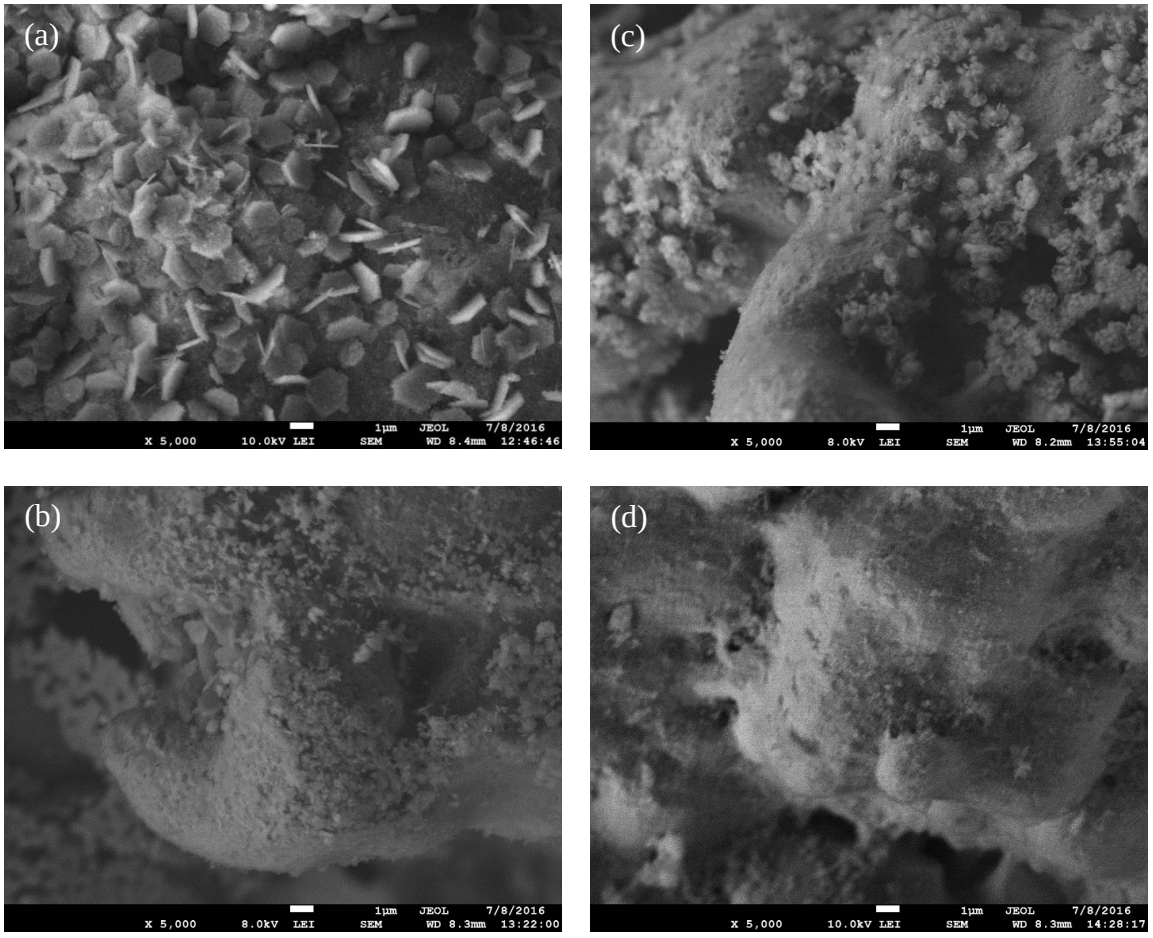

Figure 15. FE-SEM images on the media sample collected at (a) 1 h, (b) 2 h, (c) 4 h and (d) 24 h reaction time from a batch reactor with the initial test conditions controlled as 50 g/L magnetite-coated ZVI + 3.0 mM Mn^{2+} + 0.127 mM SeO_4^{2-} with various reaction times.

XPS Results

XPS analyses were performed to determine the chemical status of Fe, Zn, and Se on the oxide coating (Fig. 16). According to the Fe 2p regional binding energy spectrum,

Fe species were present in forms of both magnetite (Fe_3O_4) and Fe(II). Fe in the oxide coating include both divalent and trivalent iron. Therefore, magnetite could be the final product from selenate removal chemistry. No elemental iron was detected in all XPS scans, suggesting that no fresh ZVI surface existed and thus ZVI was fully coated with oxides. XPS spectrum in Zn 2p region indicated that zincs are present exclusively as zinc ferrite ($ZnFe_2O_4$), which is consistent with SEM-EDS and XRD results that together proved that the added Zn^{2+} could replace structural Fe(II) to form zinc ferrite through an isomorphous substitution process.

The XPS spectrum in the Se 3P binding energy region showed that selenide (Se(-II)) dominate after 24 h reaction, suggesting that chemical reduction is responsible for the removal of selenate by the media system. Selenate would require 8 electrons from ZVI in order to be fully reduced to Se(-II). The finding of selenate reduction to Se(-II) is not different from what previously reported in ZVI related research (Olegario et al., 2010; Yoon et al., 2011; Tang et al., 2014b, a; Fu et al., 2016).

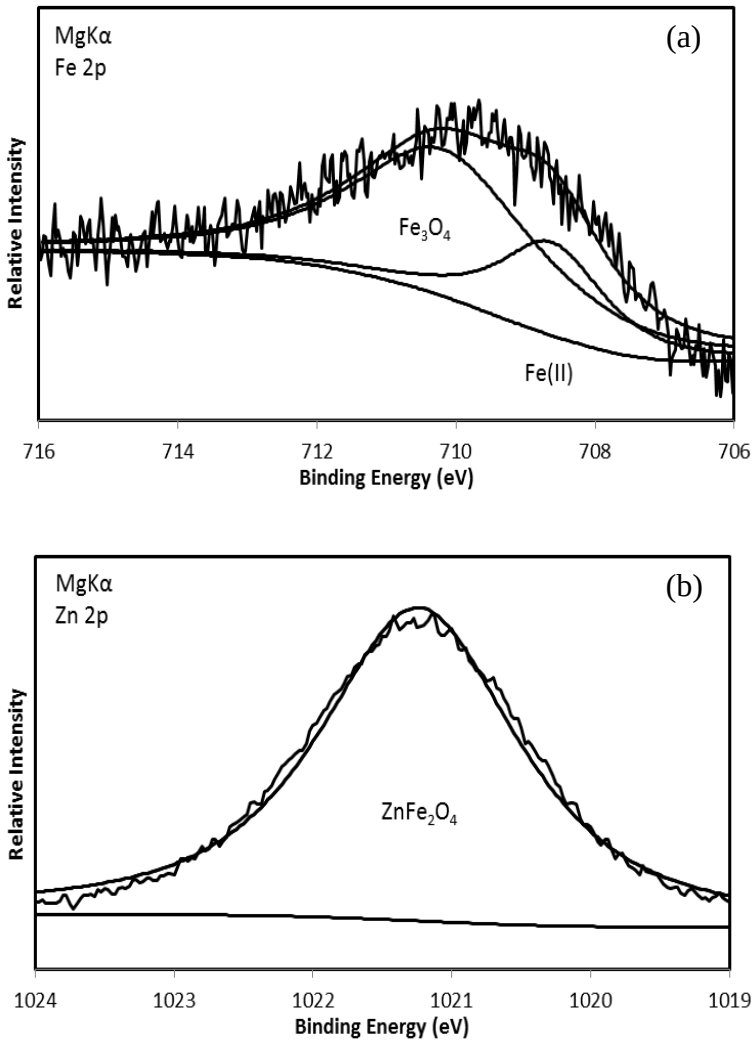

Figure 16. XPS spectra of the iron corrosion products on (a) Fe 2p, (b) Zn 2p and (c) Se 3p regional binding energy. The solid samples were collected after 24 h reaction time from a batch reactor with the initial test conditions controlled as 50g/L magnetite-coated ZVI + 3.0 mM Mn^{2+} + 0.127 mM SeO_4^{2-}.

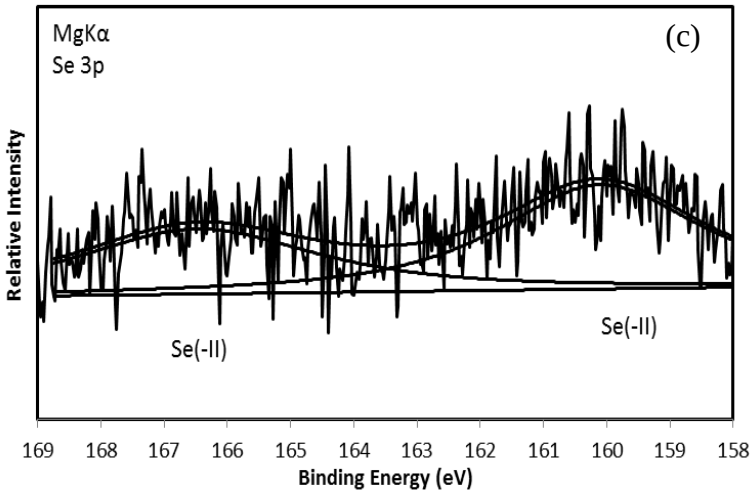

Figure 16. Continued.

Tests with Consecutive Selenate Dosing

Selenate could be completely reduced after 8 h reaction in a magnetite-coated ZVI system with 2.0 mM Zn^{2+} additions. To evaluate whether or not the reactivity of magnetite-coated ZVI + Zn^{2+} system could be sustained, a second dose of 0.127 mM selenate was added into the system after 24 h reaction when the initial 0.127 mM selenate were completely removed. The result showed that the second selenate dose was partially (83%) removed by 24 reaction time (Fig. 17(a)). The overall reaction rate was slower than what was observed in the first dose. The changes in the composition of the magnetite coating after the first dose treatment might be a factor. Upon the complete removal of the first selenate dose, the resultant unidentified amorphous oxide material could have partially covered on the reactive magnetite surface, which could slow or halt the interaction between the magnetite coating and selenate ions. Besides, as Zn^{2+} was increasingly incorporated into the oxide coating, the Zn-rich iron oxide coating could

exhibit distinct physical and chemical properties from the original magnetite coating. Consequently, the altered magnetite coating could become less reactive for selenate removal in the system even with sufficient Zn^{2+}.

As in the first 24 h reaction period, aqueous Zn^{2+} in the system was gradually consumed during the second 24 h reaction period, which is accompanied by a gradual release of aqueous Fe^{2+} [Fig. 17(b) and 17(c)]. Upon addition of the second selenate dose, aqueous Zn^{2+} increased slightly before gradually decreased. Such temporary slight increase in aqueous Zn^{2+} might come from unstable structural Zn(II) or surface-adsorbed Zn^{2+}, when the chemical equilibrium between solid and water was disrupted by the addition of second selenate dose. Similar to Zn^{2+}, a sudden slight increase of aqueous Fe^{2+} was observed at 24 h as a result of second selenate dose.

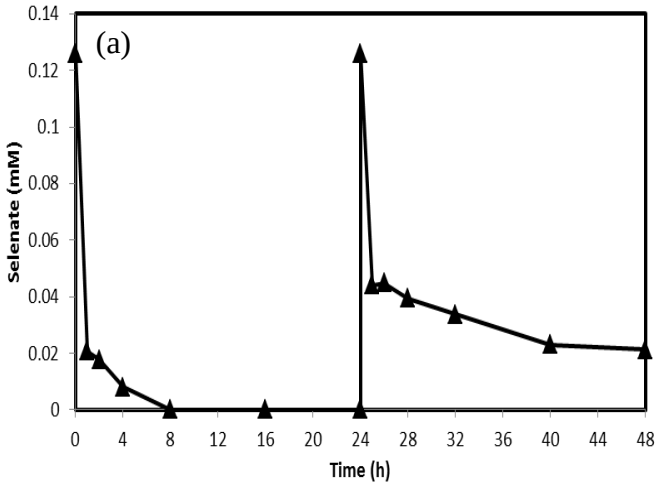

Figure 17. Time course of (a) selenate, (b) Zn^{2+} and (c) Fe^{2+} concentration change in a batch reactor with the initial conditions controlled as 50 g/L magnetite-coated ZVI system + 2.0 mM Zn^{2+} + an initial dose of 0.127 mM selenate, followed by a second dose of 0.127 mM selenate added at time 24 h.

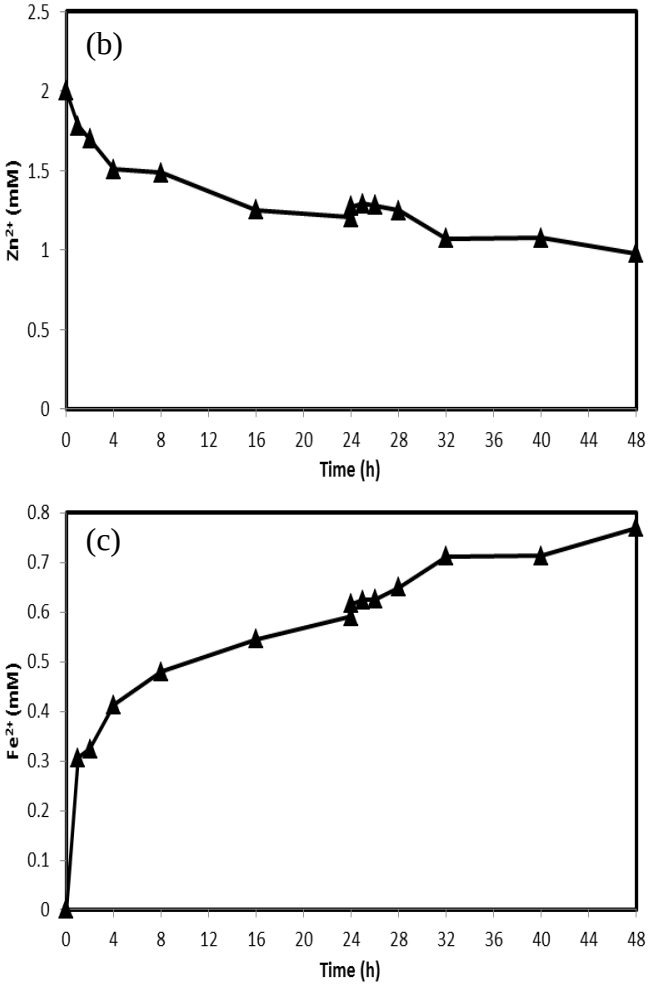

Figure 17. Continued.

Summary

Without aqueous Zn^{2+}, a magnetite-coated ZVI system could barely remove selenate under an anoxic condition. Adding Zn^{2+} into the system, however, could significantly enhance the reactivity of magnetite-coating ZVI for the removal of selenate. Zn^{2+} in the system may play an important role in triggering the reaction and promoting the reaction kinetics for selenate removal in a magnetite-coated ZVI system.

Zn^{2+} may involve in the selenate removal chemistry, likely participating in the formation of iron corrosion oxides. The incorporation of Zn^{2+} into the iron oxide coating likely proceeded mainly through an isomorphic substitution process that results in the formation of a zin ferrite structure, resulting in the release of aqueous Fe^{2+}. With the co-presence with aqueous Zn^{2+}, the process of selenate removal may be greatly accelerated initially, but under certain conditions, the reactivity of ZVI could be compromised when a less reactive, amorphous Zn-bearing oxide coating was formed in substitute of more reactive magnetite-structured oxide coating.

CHAPTER V INHIBITION OF NITRATE REMOVAL BY ZN^{2+} IN A MAGNETITE-COATED ZVI SYSTEM

Introduction

One drawback of the ZVI-based technologies for treating nitrate-contaminated wastewater is the reduction of nitrate to ammonia. Discharge of ammonia into a receiving water boy could be problematic due to its toxicity to many aquatic animals. Ammonia is neurotoxic that may chronically damage brain cells to cause brain edema, astrocytic swelling and abscesses (Görg et al., 2013; Rangroo Thrane et al., 2013; Dahlberg et al., 2016). Ammonia could interfere with the transport and neurotransmitter metabolism of amino acids, causing over-activated immune response. With a high level of ammonia, human being and aquatic animals may experience physiological disorder from oxidative stress and immune injury (Xing et al., 2016).

High nitrate in the wastewater may result in excess consumption of ZVI. Reduction of nitrate (N in +5 oxidation state) to ammonia (N in -3 oxidation state) requires 8 electron transfer. According to reaction stoichiometry, reduction of 1 mmol nitrate (14 mg as N) will require 2.67 mmol Fe0 (150 mg) if Fe0 is oxidized to form magnetite as the end product. Considering that nitrate in many wastewater are in concentration much higher than heavy metals (such as selenate), much of ZVI consumption would result from nitrate reduction, not heavy metal removal.

Furthermore, high nitrate level in water could compete with other target contaminants (such as selenate, chromate) for limited electrons released from ZVI

corrosion process, and thus effectively become a chemical inhibitor in a Fe^0-based treatment systems, and thereby potentially resulting in slow removal reaction kinetics for other key target pollutants. As a result, the treatment system has to be designed with longer reaction time, larger reaction tanks, increasing both the capitol and operational costs. Consequently, treating heavy metal contaminated wastewater with high nitrate level could become a challenge for the ZVI-based technologies in real world applications.

Nitrate could be effectively converted to nitrogen using biological treatment system (denitrification processes). The bio-denitrification technologies are well established, but the applications also pose a challenge due to the increase of the cost. In many industrial applications, due to the complexity and variations of water quality, operating a biological process could be a major challenge that many users want to avoid. One alternative or maybe better solution to overcome the challenges associated with high nitrate wastewater is through the selective inhibition of nitrate reduction in the ZVI-based technology while maintaining high reactivity for other target contaminants such as heavy metals. In addition to avoid ammonia production and increase ZVI's reactivity, inhibition of nitrate reduction could also decrease sludge production, reduce chemical usage and thus the O&M costs.

Achieving selective inhibition of nitrate is possible based on anecdotal evidences observed from this group field activities related to the use of the activated iron media system for treating heavy metals in the flue-gas-desulfurization wastewater. In two occasions, we observed that the activated iron media stopped converting nitrate to

ammonia while continued to efficiently remove selenium and mercury from the contaminated wastewater with high nitrate level (>100 mg/L nitrate-N). The mechanism behind the nitrate inhibition however was not studied thoroughly and remained unclear so far.

The objective of this study is to investigate the inhibition of nitrate removal in a magnetite-coated ZVI system through Zn^{2+} additions. According to previous chapter, aqueous Zn^{2+} could be incorporated into the structure of magnetite-coated ZVI to form Zn^{2+} doped magnetite-coated ZVI. In this study, we aim to evaluate the effect of structural Zn(II) in the magnetite coating on nitrate reduction. For the purpose, both batch tests and a flow-through system using continuous stirred-tank reactor (CSTR) was investigated to evaluate the chemistry and the potential application of aqueous Zn^{2+} as a nitrate reduction inhibitor in a magnetite-coated ZVI system.

Materials and Methods

The chemicals, the preparation of magnetite-coated ZVI and batch experiments were the same as the previous chapters. The analytical methods for pH, Fe^{2+}, Zn^{2+} and NO_3^- analyses were also described in previous chapters. For CSTR experiments, 325-mesh ZVI grains, which reported nominal particle size of less than 44 μm in diameter, were used to prepare magnetite-coated ZVI media that were used throughout the tests in this chapter.

Synthesis of ZVI Media with a Zn^{2+}-Doped-Magnetite Coating

To prepare Zn^{2+}-doped magnetite-coated ZVI, 4 mM Zn^{2+} was firstly added into a batch reactor with 0.5 g magnetite-coated ZVI and DDI water with 10 ml in total in the

anaerobic chamber. The reactors were then transferred into a tumbler rotating with 30 rpm for complete mixing and reaction. At designed reaction time of 1 h, 2 h, 3 h and 24 h, reactors were withdrawn from the tumbler and transferred into the anaerobic chamber for manipulations or tests. The top liquid with fine suspensions in batch reactors were discarded; the remaining media that settled quickly at the bottom was washed with DDI water for three times; the washed media were dried in the anaerobic chamber and stored until being used for batch experiments.

During the Zn^{2+} pretreatment, aqueous Zn^{2+} would be gradually incorporated into the structure of the magnetite coating (shown in Table 2). Increased reaction time could result in elevated Zn^{2+} incorporation into the solid phase, resulting in more Zn(II) in the magnetite-coated ZVI. The calculation of the ratio of Zn(II) to total Fe (Fe(II) + Fe(III) was based on the amount of incorporated Zn^{2+} divided by the amount of structural Fe (the content of Fe in solid – the release of Fe in liquid). After 24 h reaction, the content of structural Zn(II) was significantly larger than total Fe. Therefore, Zn(II) was dominant in the structure of Zn^{2+} doped magnetite-coated ZVI.

Table 2. Zn^{2+} concentration in aqueous and solid phase after Zn^{2+} incorporation into the structure of magnetite-coated ZVI at 1 h, 2 h, 3 h and 24 h.

Reaction Time	1 h	2 h	3 h	24 h
Aqueous Zn^{2+} (mM)	3.43	3.34	3.33	3.09
Incorporated Zn^{2+} (mM)	0.57	0.66	0.67	0.91
Zn(II) to Total Fe in solid	0.7	0.71	0.75	1.77

Continuous Stirred-Tank Reactor

The bench-top flow through treatment system using CSTR reactor with reaction zone (6 L) and settling zone was made from stainless steel (Fig. 18). The magnetite-coated ZVI were created by operating the CSTR system in batch mode: essentially adding 300 g virgin ZVI grain (with a relatively fresh surface) to mix with 10 mM NO_3^- and 6 mM Fe^{2+} for overnight reaction. The media would be fluidized fully in the reaction zone by controlling the overhead electric at 1000 rpm. Due to an engineering design of separate reaction and settling zones, the media can be mostly retained in the reaction zone to interact with aqueous pollutants. The simulated wastewater contained 3.0 mM nitrate and 0.127 mM selenate, which were introduced into the reactor to test the media reactivity for the removal performance. At a treatment flow rate of 1.0 L/h, the hydraulic reaction time (HRT) in the reactor was 6 h. Treated effluent were sampled from the top of the settling zone at a frequency of 1 sample per day (i.e., 4 HRT intervals). Water samples were analyzed for NO_3^-, SeO_4^{2-} and metal ions of Fe^{2+} and Zn^{2+}.

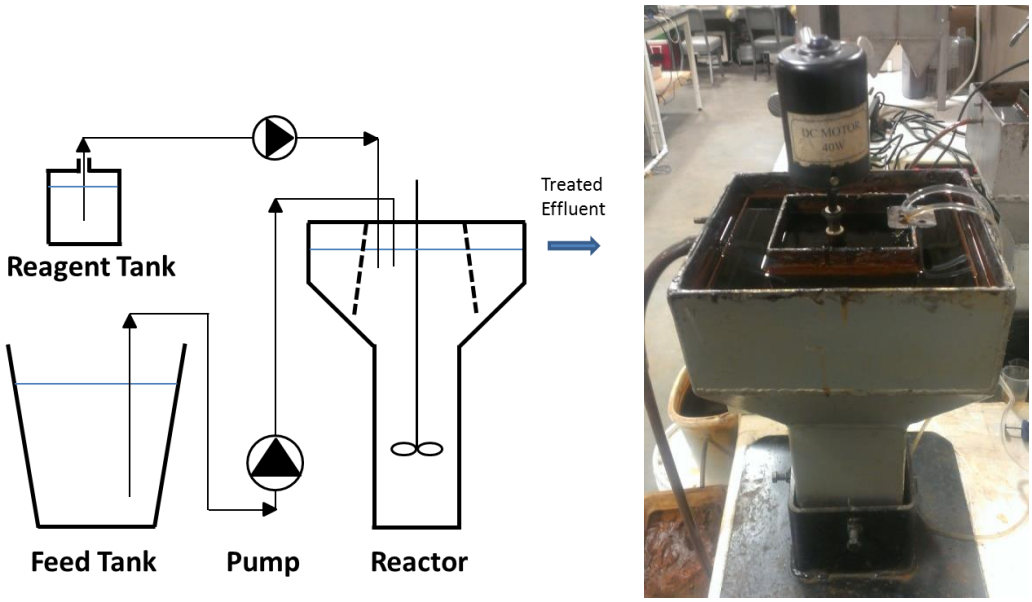

Figure 18. Schematic representation (left) of the CSTR flow-through treatment system (not to scale) and a photo of the CSTR reactor with an inner reaction zone (6 L effective volume) and an outer settling zone (also 6 L in volume) (right).

Results and Discussions

Zn^{2+} Doped Magnetite-Coated ZVI

As shown in Fig. 19(a), nitrate removal could be significantly inhibited by aqueous Zn^{2+} in a magnetite-coated ZVI system. With Fe^{2+} additions, nitrate could be removed in a magnetite-coated ZVI system. With Zn^{2+} additions, however, magnetite-coated ZVI lost its reactivity for nitrate reduction: nitrate was barely removed in the system over extended period. The presence of aqueous Zn^{2+} in a magnetite-coated ZVI system could adversely affect the interaction between magnetite-coated ZVI and nitrate that could halt nitrate reduction. The concentration change of aqueous Fe^{2+} and Zn^{2+} implied that aqueous Zn^{2+} could be incorporated into the structure of the magnetite coating to substitute structural Fe(II), resulting in Fe^{2+} production in aqueous phase.

Both aqueous Zn^{2+} and structural Zn(II) could play important roles in the inhibition of nitrate reduction in a ZVI-based technology.

Zn^{2+}-doped magnetite-coated ZVI could suppress the reaction of nitrate reduction in the system. With Fe^{2+} additions, unlike pure magnetite-coated ZVI, nitrate was barely removed after 2 h reaction time. The Zn^{2+}-doped magnetite coating could not support electron transfer and reactivity for nitrate reduction despite the presence of Fe^{2+}. Aqueous Fe^{2+} remained little change after 2 h reaction, but increased by 10% in all Zn^{2+} incorporation tests. Like Fe^{2+}, Zn^{2+} was detected in liquid after 2 h reaction and the concentration of Zn^{2+} in 1 h, 2 h, 3 h and 24 h Zn^{2+}-doped magnetite-coated ZVI tests were less than 0.01 mM, implying that the structure of Zn^{2+} doped magnetite-coated ZVI could be fragile, especially the lattice including structural Zn(II), resulting in the dissolution of structural Fe(II) and Zn(II) to aqueous phase.

With Zn^{2+} additions, nitrate could not be effectively removed in both magnetite-coated ZVI and Zn^{2+}-doped magnetite-coated ZVI system. Zn^{2+} could continuously occupy the lattice of structural Fe(II), resulting in Zn^{2+} consumption and Fe^{2+} production, as shown in Fig. 19(c) and (d). The results suggested that aqueous Zn^{2+} may rapidly incorporate into the magnetite coating to form Zn^{2+} doped magnetite-coated ZVI. When Zn^{2+} was present in the structure of magnetite-coated ZVI, the interaction between magnetite-coated ZVI and nitrate would be halted. Consequently, nitrate would not be effectively reduced by magnetite-coated ZVI.

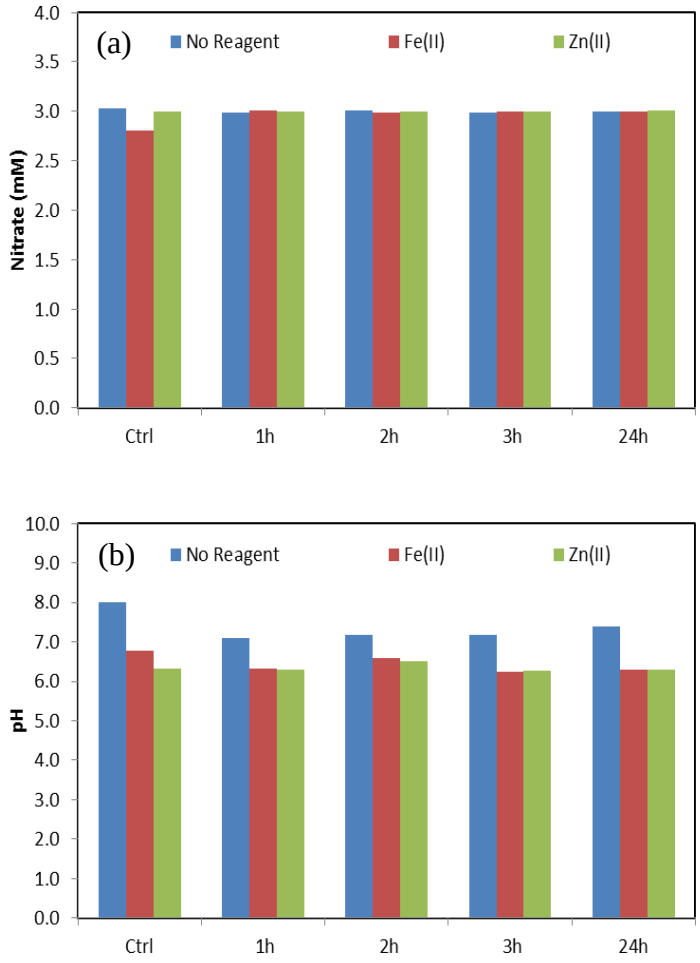

Figure 19. Results from the batch tests on nitrate reduction in magnetite-coated ZVI vs. Zn^{2+}-doped magnetite-coated ZVI systems, in which 0.2 mM Fe^{2+} or Zn^{2+} was added after 2 h reaction. (a) nitrate concentration, (b) pH, (c) aqueous Fe^{2+} and (d) aqueous Zn^{2+}. (Note: Ctrl: magnetite-coated ZVI; 1 h, 2 h, 3 h and 24 h in x axis: reaction time for Zn^{2+} incorporation into the magnetite-coated ZVI).

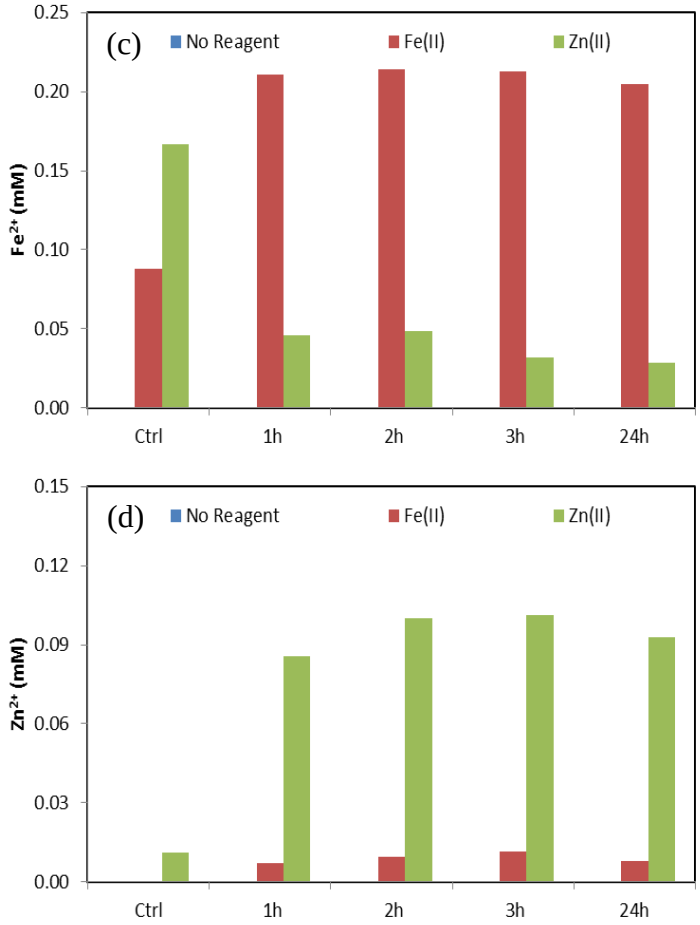

Figure 19. Continued.

Contrast to nitrate inhibition observed with a Zn^{2+}-doped magnetite-coated ZVI system, Fig. 20 illustrated that the same system could effectively remove selenate with Fe^{2+} or Zn^{2+} additions, proving that magnetite-coated ZVI with Zn^{2+} incorporation was a reactive iron media for impaired water treatment. Zn^{2+} doped magnetite-coated ZVI without reagents remained reactive with respect to selenate removal, just like a pure magnetite-coated ZVI system. Zn^{2+} doped magnetite-coated ZVI could provide active adsorptive sites for selenate removal, possibly through physical attraction by positive

charge due to its surface frangibility. The removal performance of selenate, however, became poor as reaction time of Zn^{2+} incorporation extended. The results confirmed that Zn^{2+} doped magnetite-coated ZVI could selectively suppress nitrate reduction but effectively remove selenate with/without Fe^{2+} or Zn^{2+} additions.

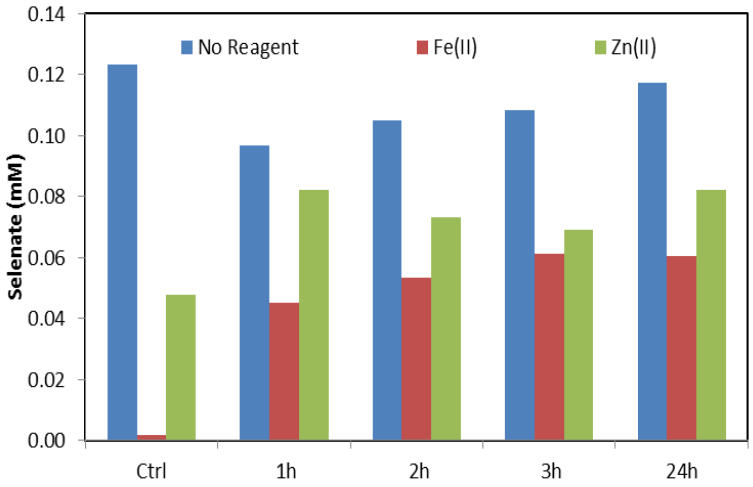

Figure 20. Selenate removal in both magnetite-coated ZVI (Ctrl) and Zn^{2+}-doped magnetite-coated ZVI systems (1, 2, 3, 24 h) with Fe^{2+} or Zn^{2+} additions.

Aqueous Zn^{2+} in a Magnetite-Coated ZVI Systems

Nitrate could be reduced in a magnetite-coated ZVI system with aqueous Zn^{2+} additions but the removal performance of nitrate was limited, as shown in Fig. 21(a). In the test with 1.0 mM Zn^{2+} addition, nitrate was slightly reduced from 3.0 mM to 2.8 mM. In the test with 3 mM Zn^{2+} additions, however, nitrate was barely removed during 12 h reaction. Therefore, more Zn^{2+} dosage in the system could inhibit nitrate removal. The results supported that Zn^{2+} could significantly suppress nitrate reduction in a

magnetite-coated ZVI system, similar to what was observed with a Zn^{2+}-doped magnetite-coated ZVI system.

Fig. 21(b) illustrated that the pH change during 12 h reaction in the system. pH would be initially decreased and then increased in all tests with Zn^{2+}.

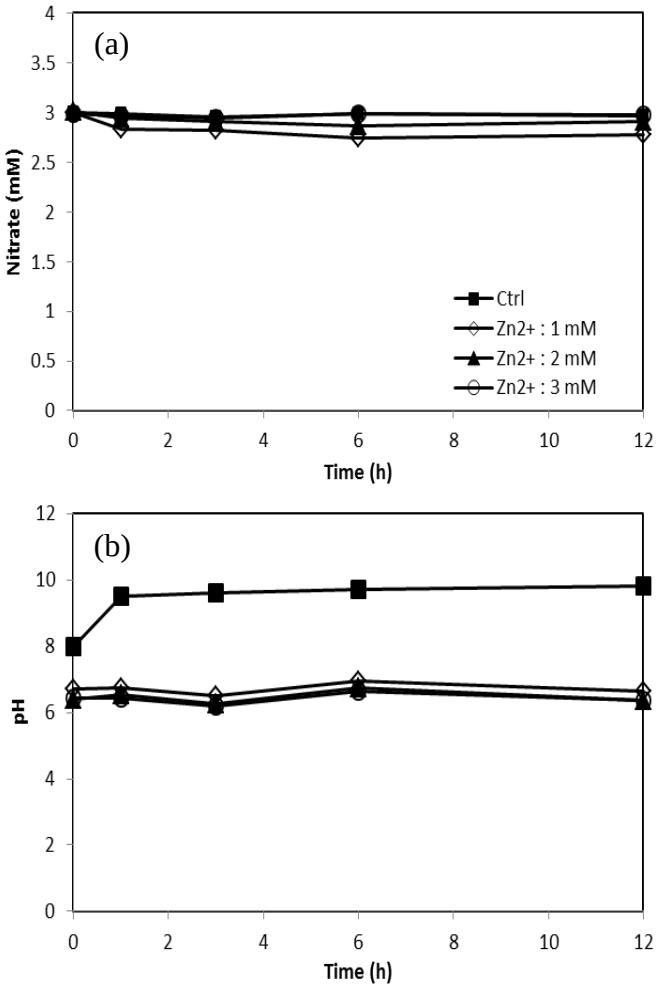

Figure 21. Time course of (a) selenate, (b) pH, (c) Fe^{2+} and (d) Zn^{2+} changes observed in a batch reactor with initial conditions controlled as 50g/L magnetite-coated ZVI system (5% w/v) + 3 mM selenate + various concentrations of Zn^{2+} (1.0, 2.0, and 3.0 mM).

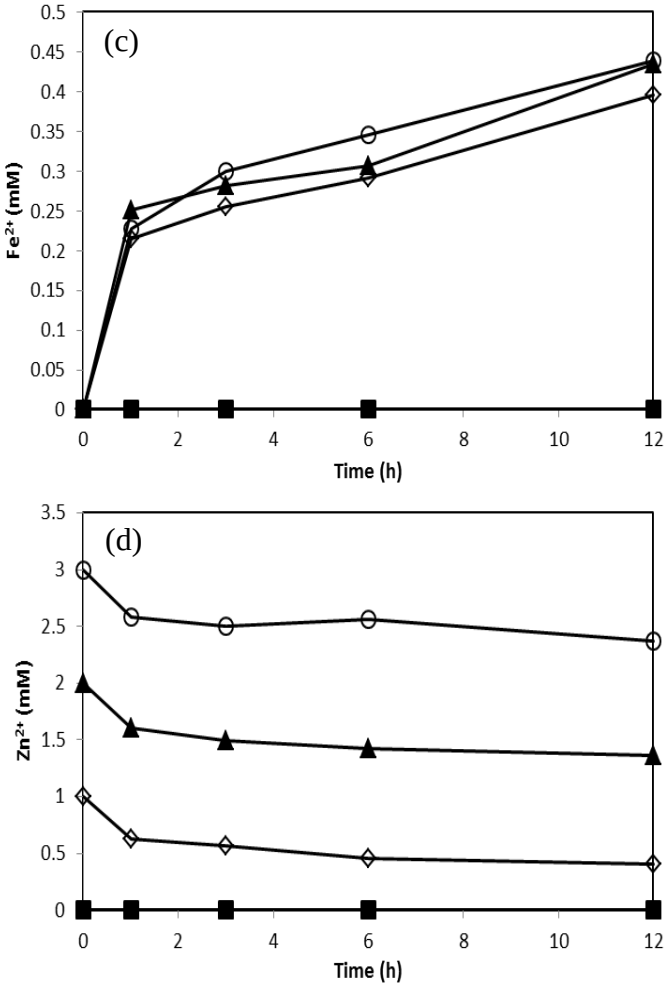

Figure 21. Continued.

Fig 21(c) and (d) illustrated changes of dissolved Fe^{2+} and Zn^{2+} concentration. In the first hour, aqueous Zn^{2+} rapidly decreased in all tests, but thereafter Zn^{2+} decrease much slowly. Conversely, Fe^{2+} increased rapidly in the first hour, but thereafter such increase slowed significantly. It appears that Zn^{2+} consumption can be correlated well in quantity with Fe^{2+} production, which strongly suggested that substitution of structural Fe(II) by Zn^{2+} are the main dynamic occurred in the system. Zn^{2+} exhibits a strong affinity to replace structural Fe(II) in the magnetite coating. The cation exchange process

between Zn and Fe could significantly change the physical and chemical properties of magnetite-coated ZVI, such as the structure, chemical compositions, lattice size, electrical conductivity, redox potential or magnetism. Consequently, Zn^{2+}-doped magnetite-coated ZVI with co-existence of aqueous Fe^{2+} and Zn^{2+} may become inert for nitrate reduction.

The AIM Treatment System

The effect of aqueous Zn^{2+} on the ZVI reactivity was further investigated through conducting flow-through CSTR experiments. In a normal operation of the AIM treatment system, adding aqueous Fe^{2+} into a magnetite-coated ZVI system can facilitate removal reaction rate for nitrate and selenate. Without Fe^{2+} additions, magnetite-coated ZVI cannot effectively remove nitrate or selenate. As shown in Fig. 22 (a) and (b), magnetite-coated ZVI with Fe^{2+} addition effectively removed both nitrate and selenate simultaneously. During the 9-day operation, nitrate could be consistently reduced from 3 mM to 2.6 mM and selenate could be averagely decreased from 0.127 mM to 0.006 mM. The consumption of Fe^{2+} was ~ 0.14 mM, shown in Fig. 22(d). Compared to nitrate and selenate removal, Fe^{2+} usage was relatively small. The ratio of Fe^{2+} usage to both nitrate and selenate removal was around 0.26. The results implied that adding Fe^{2+} into a magnetite-coated ZVI system could reduce activation energy of chemical reaction to effectively trigger both nitrate and selenate removal process. Therefore, Fe^{2+} was essential in the AIM treatment system to enhance the reaction kinetics and help form the right iron oxide for sustaining the system reactivity.

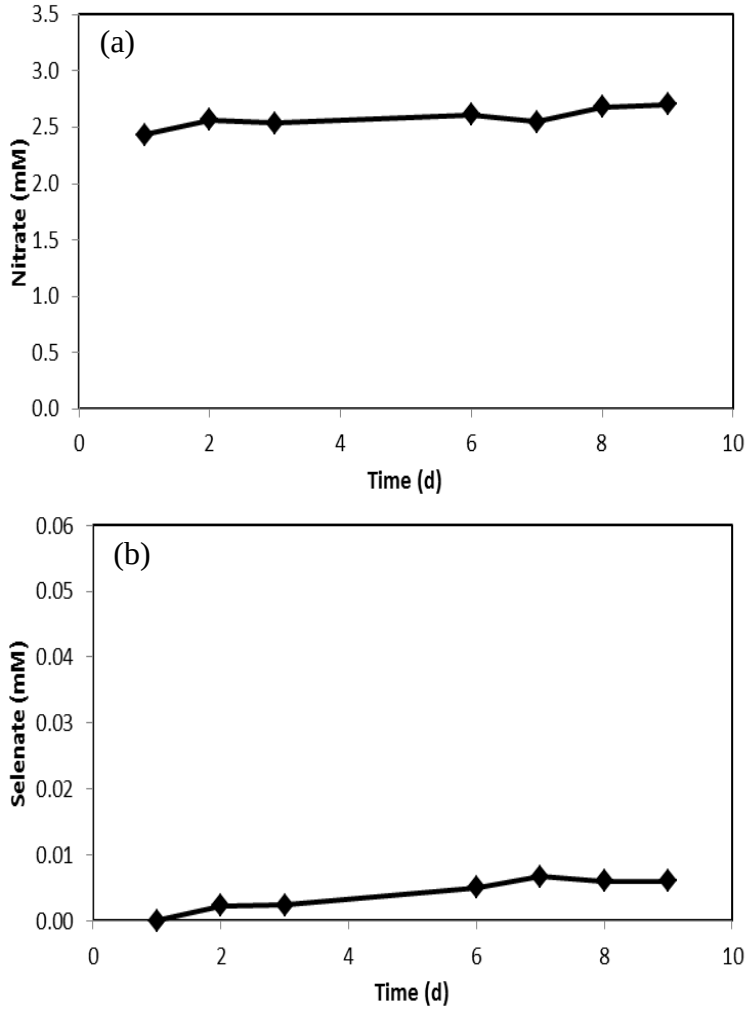

Figure 22. Time course of (a) nitrate, (b) selenate, (c) pH and (d) Fe^{2+} in the flow-through CSTR treatment system with magnetite-coated ZVI system (5% w/v) and 0.6 mM Fe^{2+} dosage for treating simulated wastewater with 3.0 mM nitrate and 0.127 mM selenate.

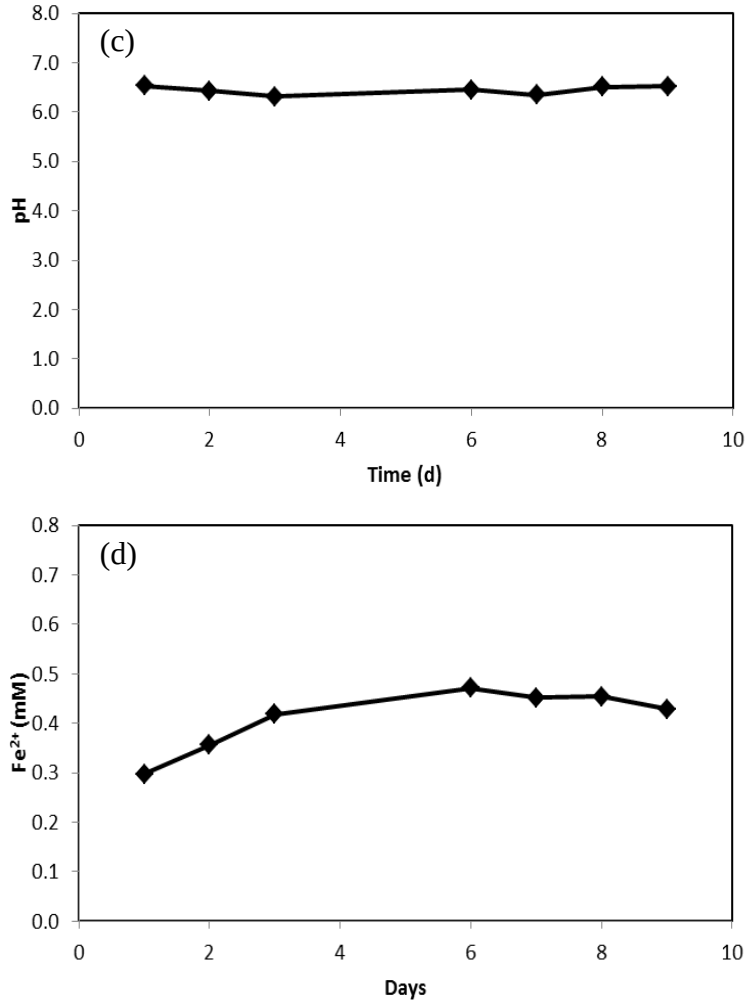

Figure 22. Continued.

Zn^{2+} Effect to the AIM Treatment System

Fig. 23 demonstrated that the removal process of nitrate and selenate by a magnetite-coated ZVI system with the addition of both Fe^{2+} and Zn^{2+}. In this test, 0.1 mM Zn^{2+} and 0.5 mM Fe^{2+} together, instead of 0.6 mM Fe^{2+} as in the test in Fig. 22, was added into the AIM treatment system. The same total metal ion dosage (0.6 mM) is designed to provide better comparison between the tests. With 0.1 mM Zn^{2+} dosage,

nitrate and selenate could be reduced from 3 mM to 2.8 mM, and 0.127 mM to 0.025 mM, respectively. Compared to the AIM treatment system, the removal efficiency of both nitrate and selenate become poorer, but both nitrate and selenate were still being removed. Both nitrate and selenate reduction could cause pH increase, resulting from the release of hydroxyl ions or depletion of protons after redox reaction. Due to less nitrate and selenate removal, pH was slightly lower than the AIM treatment system. Therefore, removal performance of nitrate and selenate might be predicted by the change of pH.

The usage of Fe^{2+} in the system could be dependent on the amount of nitrate and selenate removal. The Fe^{2+} consumption in a magnetite-coated ZVI system with 0.1 mM Zn^{2+} and 0.5 mM Fe^{2+} was averagely ~ 0.11 mM, lower than the AIM treatment system. The results were seemingly reasonable in consideration of less nitrate and selenate removal.

As shown in Fig. 23(d), dissolved Zn^{2+} gradually increased over time from near zero to 0.06 mM at 9^{th} day, indicating that less Zn^{2+} was incorporated into the solid. The disappearance of Zn^{2+} could be also related to nitrate or selenate removal process. Aqueous Zn^{2+} may involve chemical reaction as a reactant, resulting in Zn^{2+} depletion. By the fifth day, Zn^{2+} concentration has increased from 0.006 mM to 0.055 mM, but both nitrate and selenate removal was not significantly changed. The weak quantitative relationship between Zn^{2+} consumption and nitrate and selenate reduction implied that Zn^{2+} might not directly participate in the chemical reaction for both nitrate and selenate removal.

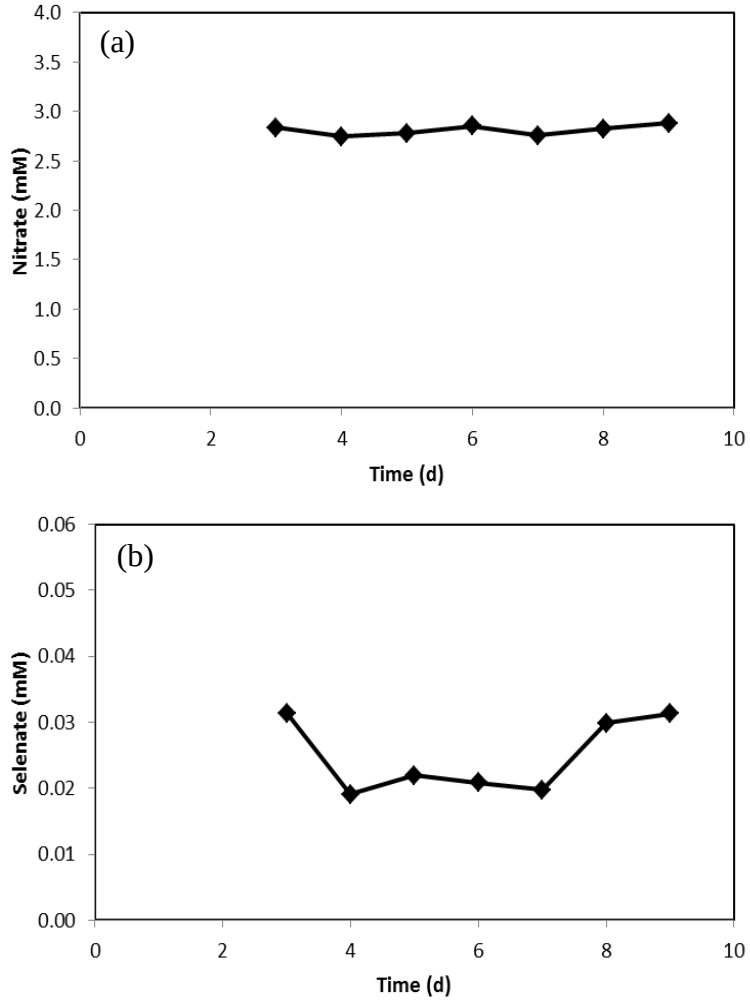

Figure 23. Time course of (a) nitrate, (b) selenate, (c) pH, (d) Fe^{2+} and (e) Zn^{2+} observed in the effluent or reactor (for pH) in a flow-through CSTR treatment system with magnetite-coated ZVI system (5% w/v) + 0.5 mM Fe^{2+} and 0.1 mM Zn^{2+} dosages (0.6 mM in total) for treating simulated wastewater with 3.0 mM nitrate and 0.127 mM selenate.

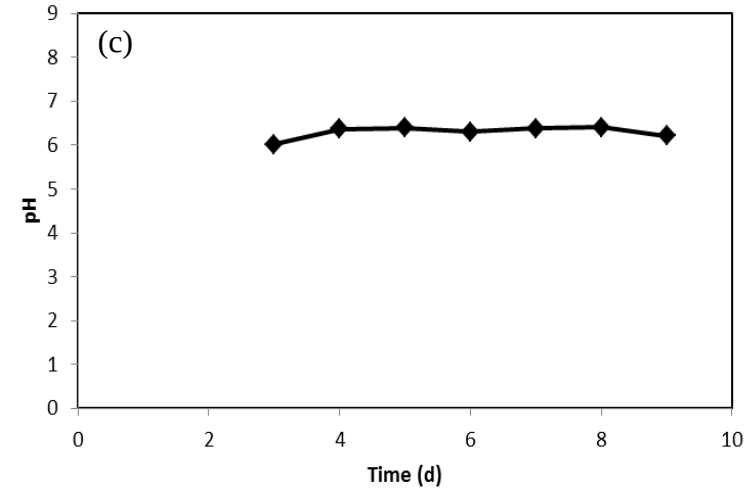

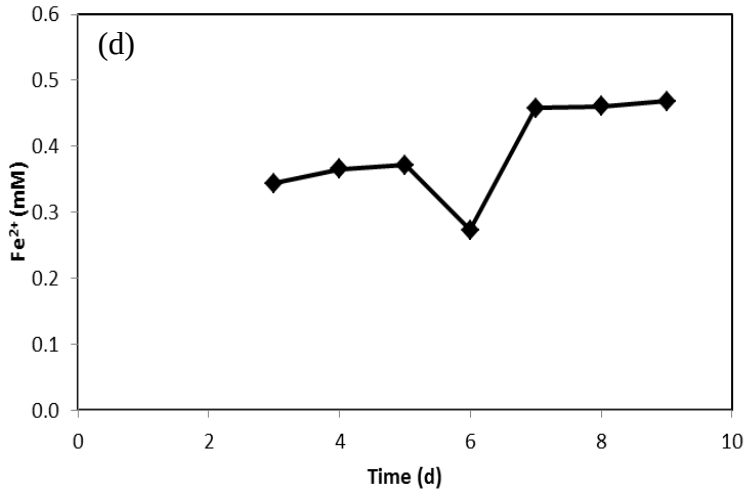

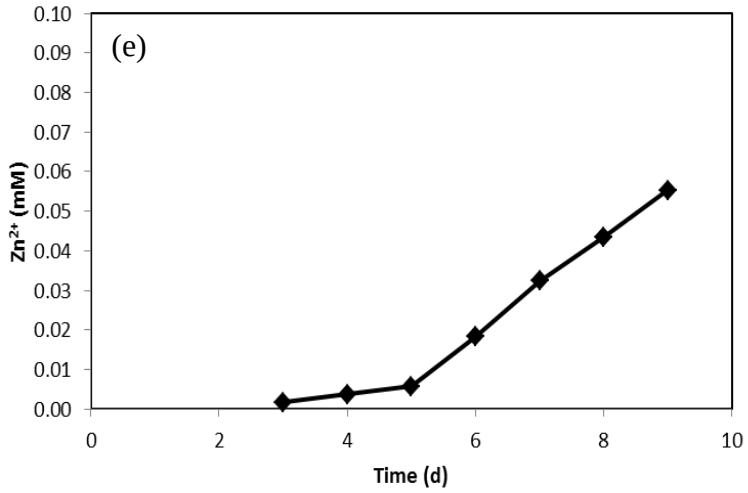

Figure 23. Continued.

With the 0.3 mM Zn^{2+} + 0.3 mM Fe^{2+} combination, nitrate removal in a magnetite-coated ZVI system was further limited, as shown in Fig. 24(a). Nitrate removal decreased to less than 4.3%. Selenate removal also became poorer, but still at over 70% removal on average. The results showed that increased Zn^{2+} dosage in the AIM treatment system could negatively affect the reactivity of magnetite-coated ZVI for both nitrate and selenate removal, which is consistent with observations from batch tests with Zn^{2+}-doped magnetite-coated ZVI and with a magnetite-coated ZVI + aqueous Zn^{2+}system. During test period of 17 days, nitrate removal was nearly invariable, suggesting that nitrate removal could be strongly affected by aqueous Zn^{2+} in the system. Selenate removal efficiency, however, changed more significantly even during the same operational conditions. The removal of selenate could be pertinent to the chemical composition of magnetite-coated ZVI with mixed Fe(II), Fe(III) and Zn(II). The chemical composition of magnetite-coated ZVI could evolve during the reaction as nitrate and selenate reduction trigger formation of new iron oxides and thus affecting the isomorphic substitution between Zn and Fe, and the interfacial chemistry between the solid/liquid interfaces.

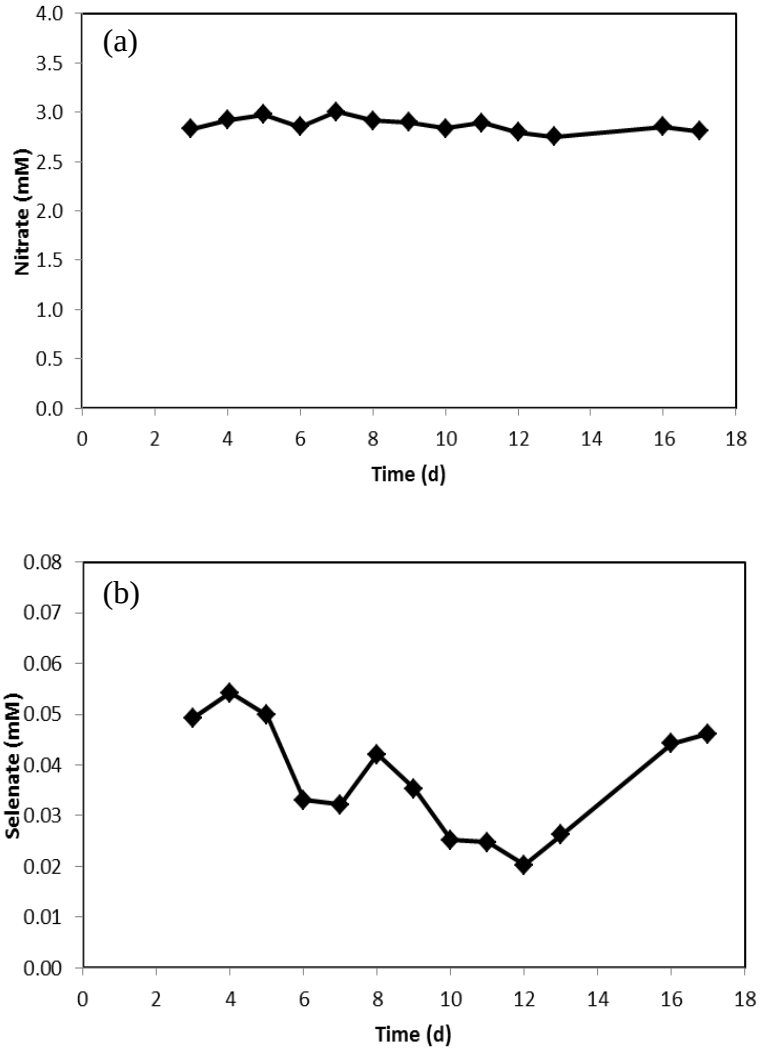

Figure 24. Time course of (a) nitrate, (b) selenate, (c) pH, (d) Fe^{2+} and (e) Zn^{2+} changes in a flow-through CSTR treatment system with magnetite-coated ZVI media (5% w/v) and 0.3 mM Fe^{2+}+ 0.3 mM Zn^{2+} dosages (0.6 mM in total) for treating wastewater with 3.0 mM nitrate and 0.127 mM selenate.

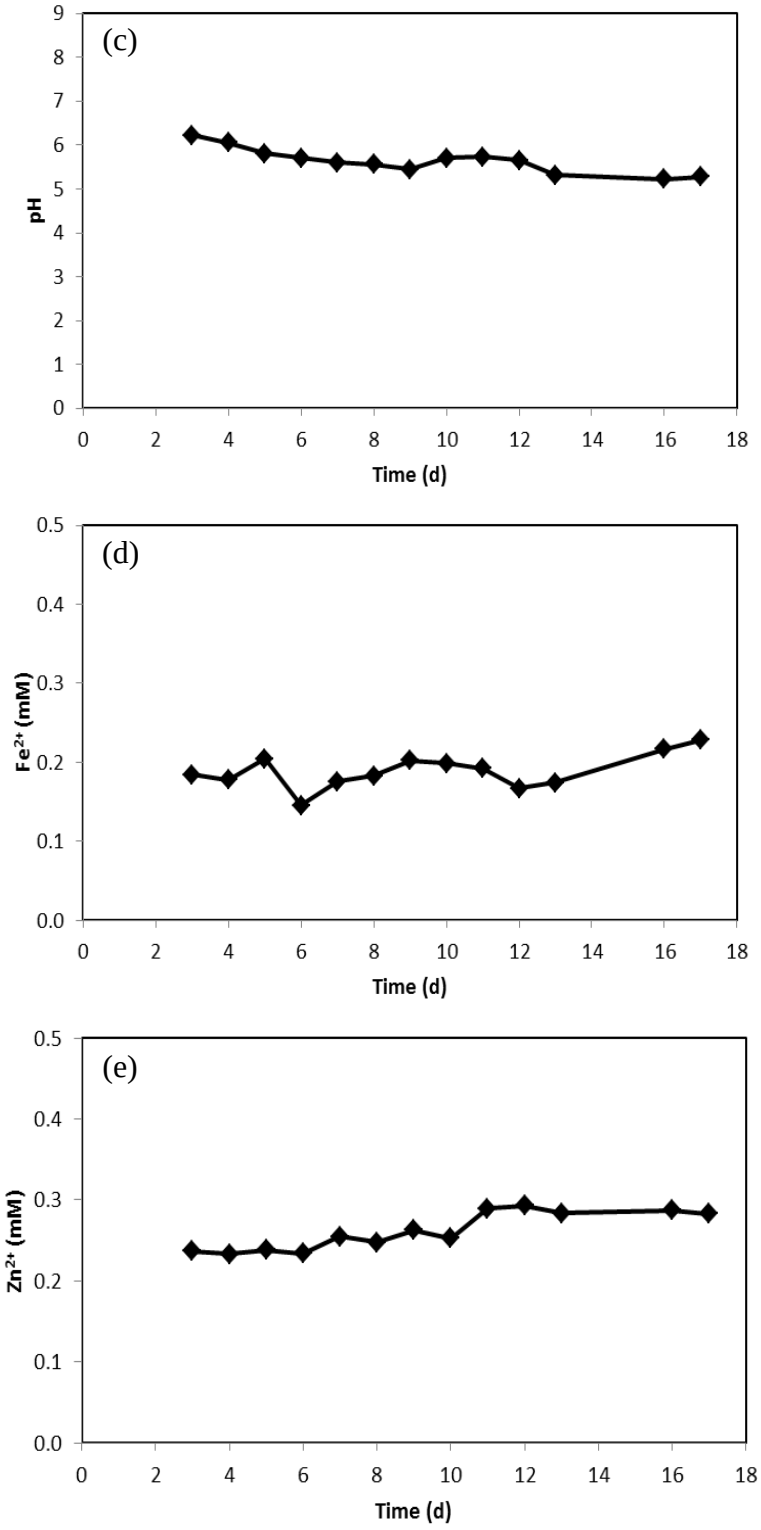

Figure 24. Continued.

Fe^{2+} consumption was averagely at ~ 0.11 mM, the same as in the 0.1 mM Zn^{2+} test, as shown in Fig. 24(d). The average Zn^{2+} usage was about 0.04 mM. Although less Zn^{2+} was consumed during the reaction, aqueous Zn^{2+} was still continuously incorporated into the solid phase. It has to be noted that because the CSTR experimental design, the media of the later tests were inherited from the previous tests, thus the oxide coating on the ZVI grains could have already been saturated with Zn from earlier tests, thus resulting in less Zn^{2+} consumption in the later tests.

Summary

Nitrate removal could be strongly affected by both structural Zn(II) and aqueous Zn^{2+} in a magnetite-coated ZVI system. Zn^{2+}-doped magnetite-coated ZVI in the absence of Fe^{2+} or Zn^{2+} addition could not provide any removal capacity for nitrate reduction. For a Zn^{2+}-doped magnetite-coated ZVI system, even with externally added Fe^{2+} or Zn^{2+}, would remain non-reactive for nitrate removal. For selenate reduction, however, the Zn^{2+}-doped magnetite-coated ZVI media remain a reasonable high reactivity, although it still decrease somewhat compared to a pure magnetite-coated ZVI media. Thus, this study showed that the Zn^{2+}-doped magnetite-coated ZVI media might be able to achieve selective inhibition for nitrate over selenate reduction. Furthermore, the inhibition of nitrate removal could be also achievable in a magnetite-coated ZVI system with Zn^{2+} additions. With more Zn^{2+} additions, the removal performance of nitrate became less efficient. Like nitrate, selenate removal was decreased with increased Zn^{2+}. The use of Zn^{2+} as a supplementary reagent in the activated iron media treatment system may be

valuable to overcome nitrate challenge currently encountered in some commercial applications of ZVI-based technologies.

CHAPTER VI ELECTRICAL CONDUCTIVITY EVALUATION FOR THE REACTIVITY OF ACTIVATED IRON MEDIA

Introduction

The reactivity of ZVI media is important for achieving desired contaminant removal when the ZVI-based technologies are applied to treat wastewater. ZVI as a reductant will be consumed over time to provide electrons for various redox reactions when the target contaminants and various reactive oxidants in the water are reduced by ZVI. Maintaining a sufficient amount of ZVI in the treatment system is essential to sustain high performance during the operation. When treating simple wastewater with known reactive constituents (including target contaminants), the consumption of ZVI can be approximately estimated by adding the demands of electrons for each occurred reduction reactions by assuming that all electrons are derived from ZVI. In real applications of using the ZVI-based technologies to treat more complicated industrial wastewaters (e.g., the flue-gas-desulfurization wastewater), however, a reliable estimate of ZVI consumption might not be attainable due to unknown or changing water quality variables (e.g., reactive oxidants such as persulfate in the FGD wastewater) associated with wastewater complexities. Even with sufficient iron content in the system, the reactions for pollutant reductions may be ceased if the surface of ZVI is coated with a passive metal oxide layer that could act as an electron barrier and block electron transfer through the solid/liquid interface.

In the ZVI-based technologies, the main mechanism responsible for contaminant removal is redox reduction. When a redox reaction occurs, a reductant (e.g., Fe^0) provides electrons to transform an oxidant (e.g., selenate), through which the oxidant is reduced to a lower oxidation state [e.g., Se(-II)] and the reductant is oxidized to a higher oxidation state (e.g., Fe_3O_4). Since the core mechanism involves electron transfer between reactants, the electrical or electronic properties of the relevant materials (e.g., the activated iron media) could play a key role in determining the reactivity of the media for a specific redox transformation. For a ZVI-based reactive system, the electrical properties of the ZVI media might determine how effective the media could provide electrons to the target contaminants. It can be reasonably assumed that if a ZVI media, often with a surface oxide coating, exhibit higher electron conductivity, the media could be more reactive since electrons from ZVI core could migrate more easily to the solid liquid interface to support reduction of target contaminants (such as selenate). Conversely, a ZVI media coated with a passive iron oxide would exhibit poor electrical reactivity and thus low reactivity with respect to mediating reduction reaction for contaminant treatment.

Electrical conductivity (EC) not only is an important electronic property to understand material's electronic conduction for semiconductor application but also a significant water quality parameter to determine liquid's ability to conduct electrical current in solution. The common application of EC in water is to investigate the salinity in solution. When charged dissolved ions are present in a solution, the ions can facilitate electron transport in the solution in the presence of an electric field. In the ZVI-based

technology, the electrical conductivity of the media is largely determined by the physical-chemical properties of the outer oxide coating of the ZVI grains. In the fluidized reactor system, the charge carriers responsible for the electrical current between anodes and cathodes could include the moving dissolved ions (e.g., Na+ and Cl-). If the ZVI media is reactive, however, the media particles could also serve as the electron carriers, obtaining electrons from the cathode and releasing to the anode, thus contributing in part to the overall electrical current when EC is measured. Therefore, in a fluidized activated iron media, the moving media that can efficiently obtain and release electrons, in theory could increase the electrical conductivity of the system. Among many potential factors that might affect the EC, the property of the media, in particularly, the outer layer of the iron oxide coating on ZVI media is the most important factor. A passive oxide layer could inhibit any electron transfer between the media particles and the electrodes or among the discrete media particles when they collide or come into contact with each other. As a result, no EC enhancement will be observed when measuring the fluidized system if the media is passivated (or "dead"). The mixing intensity in the reactor will also affect the EC. Intensive mixing could increase the contact between the media and the electrodes or collisions among media, which might increase the rate of electron migration. Based on these theoretical analysis, it can be inferred that the electrical conductivity in the fluidized AIM treatment system could in a certain way reflect the reactivity of the media for carrying out the desired redox reaction and contaminant destruction.

The purpose of this study is to develop the theory and explore the feasibility of using EC as a parameter to evaluate the reactivity of an activated iron media treatment system. For the study, we study the EC behavior in a fluidized activated iron media system for nitrate reduction under various conditions with an aim to understand the nature of EC and correlated it with the quality or reactivity of the media. For the purpose, experiments were conducted to profile the EC changes in a reactor filled with inert solution of NaCl vs. with an oxidizing solution of $NaNO_3$. In addition, flow-through experiments were conducted to study the EC responses before and after redox reactions of nitrate reduction by a magnetite-coated ZVI system. This study will be the first research to discuss the importance of EC on the reactivity of magnetite-coated ZVI for impaired water treatment.

Materials and Methods

Materials

The chemicals, the preparation of magnetite-coated ZVI and batch experiments were mostly the same as the previous chapters. In addition, NaCl (J.T Baker) was used to prepare a 500 mM stock solution for electrical conductivity tests. For a flow-through CSTR experiments, 325-mesh ZVI grains, which reported a nominal particle size of less than 44 μm in diameter, were used for both ZVI and magnetite-coated ZVI tests in reactor. Commercial magnetite was purchased from Alpha Chemicals.

The Fluidized Reactor

A stainless steel reactor (Fig. 25) with 2 L reaction mixing zone was painted with an electrically-insulated painting layer to avoid any electrical conduction by the steel

reactor body. The painted reactor was used to conduct both batch and flow-through treatment experiments. To completely fluidize the iron media in the reactor, an overhead mixer with adjustable speed was operated at about 1000 rpm. In the batch experiments, ZVI, commercial magnetite and magnetite-coated ZVI were used to study how different media will affect the behavior of the EC and ORP parameters under DI, 0.2 mM NaCl or 0.2 mM $NaNO_3$ solutions. For the flow-through reactor system experiments, the AIM treatment system with 0.1 mM and 0.2 mM Fe^{2+} additions was operated for treating a simulated wastewater spiked with 3.0 mM nitrate. The feed flow rate was controlled at 1 L per hour, corresponding to a hydraulic retention time of 2 hr. Changes of the EC and ORP parameters were recorded over time during the.

Analytical Methods

The analytical methods for pH, Fe^{2+} and NO_3^- analyses were also described in previous chapters. Cl^- was measured using the IC (Dionex DX-500) method under a similar condition to the NO_3^- method. Cations suppressor (CERS-4mm) with CS-18 separation column were used for cations analysis of Na^+ and NH_4^+. EC was measured by a conductivity meter (YSI 3100 model) with a YSI 3252 EC probe.

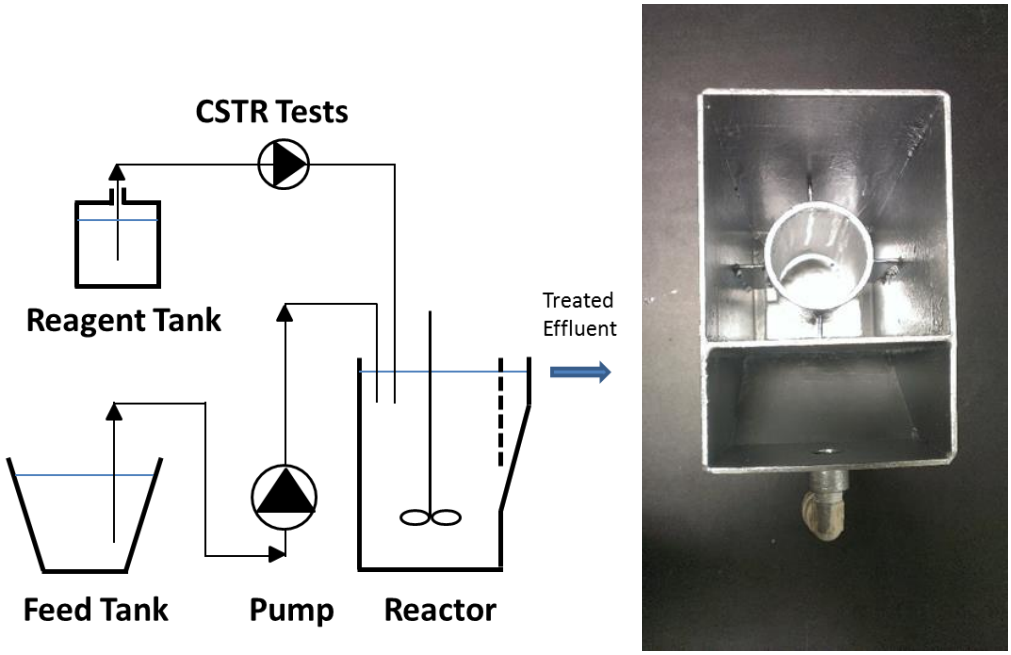

Figure 25. Schematic representation (left) of the flow-through CSTR treatment system (not to scale) and the photo (right) of the reactor with 2 L reaction zone.

Results and Discussions

Concentration Effect on EC

NaCl Solution

EC in NaCl solution was strongly proportional to the concentration of NaCl, shown in Fig. 26. The results showed that increased dissolved ions in liquid could positively contribute elevated ionic strength, resulting in the increase of EC in water. Like pure NaCl solution, adding commercial magnetite or magnetite-coated ZVI into NaCl solution exhibited the similar increase pattern of EC. Therefore, magnetite and magnetite-coated ZVI could not promote extra EC in NaCl solution. In contrast, ZVI could significantly provide additional EC in NaCl solution. EC was enhanced to 147.5 µS/cm with the difference of 21.9 µS/cm more than pure NaCl solution. The increase of

EC may be pertinent to the iron corrosion process by Cl^-, resulting from a strong electrical field generation to draw ions from the iron grains due to transitory adsorption on the surface of iron or iron oxide film (Foley, R.T., 1970). The results demonstrated that Na^+ and Cl^- could not effectively interact with both commercial magnetite and magnetite-coated ZVI for positive EC contribution in a static condition.

$NaNO_3$ Solution

Fig. 27 showed the variation of EC in $NaNO_3$ solution with magnetite-coated ZVI, ZVI and commercial magnetite. Like in NaCl solution, EC in pure $NaNO_3$ solution and $NaNO_3$ solution with the solid media of magnetite-coated ZVI, ZVI and magnetite would be linearly proportional to the concentration of $NaNO_3$ solution. Magnetite could show the same EC pattern with pure $NaNO_3$ solution as well as with pure NaCl solution, suggesting that magnetite could not effectively interact with both NaCl and $NaNO_3$ solutions to supply additional EC in liquid. However, both ZVI and magnetite-coated ZVI could stimulate EC with increased $NaNO_3$ concentration. Compared with pure 1 mM $NaNO_3$ solution, the increases of EC in ZVI and magnetite-coated ZVI in 1 mM $NaNO_3$ solution were around 13.7 µS/cm and 12.9 µS/cm, respectively. The results implied that the ion of Cl^- could facilitate electron transport on outer sphere of ZVI more than the ion of NO_3^-. In addition, the EC enhancement in $NaNO_3$ solution with magnetite-coated ZVI could indicate that magnetite-coated ZVI could actively interact with NO_3^- to accelerate electron transfer kinetics because of negligible EC increase in NaCl solution. Consequently, enhanced EC by co-existence of magnetite-coated ZVI and ZVI in $NaNO_3$ solution may provide a strong evidence to demonstrate that the

degree of interaction between ionic molecules and iron/iron oxides could determine the intensity of electron transport associated with electronic properties of iron/iron oxides to alter EC in solution.

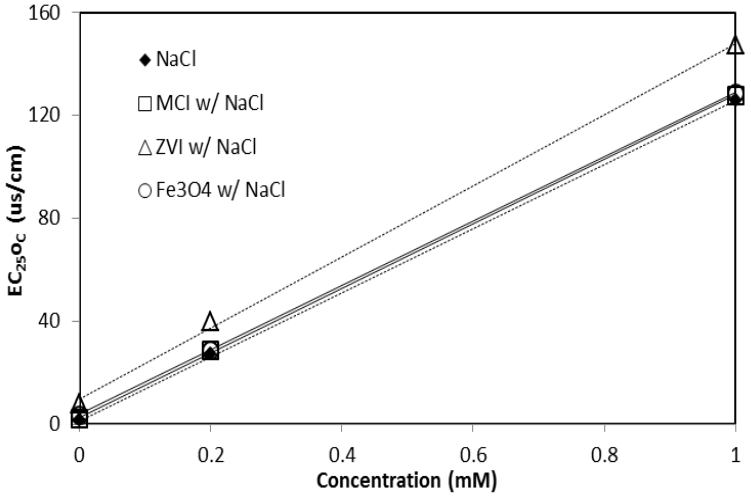

Figure 26. EC evaluation in different concentration of NaCl solution for magnetite-coated ZVI (MCI), ZVI and magnetite (Fe_3O_4).

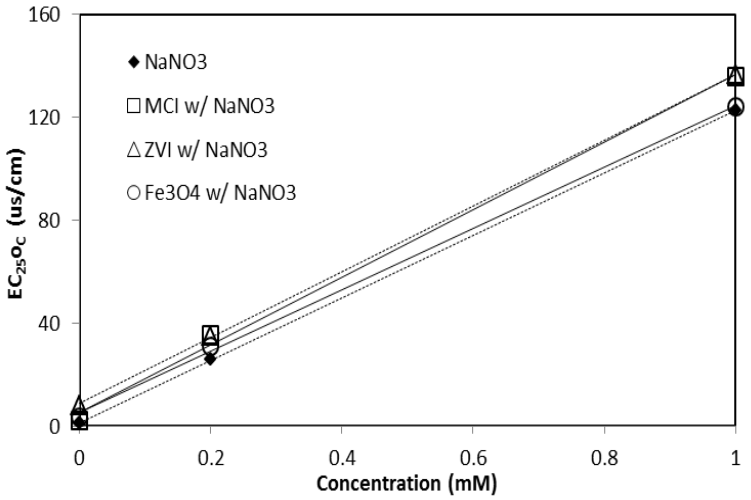

Figure 27. EC evaluation in different concentration of $NaNO_3$ solution for magnetite-coated ZVI (MCI), ZVI and magnetite (Fe_3O_4).

Mixing Speed Effect

NaCl Solution

Fig. 28(a) showed that EC measurement as a response to increased mixing intensity in the reactor filled with DI or 0.2 mM NaCl solution with the media of ZVI, commercial magnetite or magnetite-coated ZVI. With increased mixing speeds, EC with the DI water only increased slightly from 1.0 µS/cm under static condition (at 0 rpm) to 3.0 µS/cm under intensive mixing (at 900 rpm), suggesting that fast moving water increase electron conduction between the electrodes, which is expected. When ZVI, magnetite, or magnetite-coated ZVI was added into the water, EC of the mixed suspension from a static to intensive mixing condition increased from 8.1 µS/cm to 12.7 µS/cm, 3.7 µS/cm to 11.1 µS/cm and 1.7 µS/cm to 10.5 µS/cm, respectively. It has to be noted that under static condition, the solid media are settled at the bottom and thus contribute zero to EC. Therefore, ZVI, magnetite and magnetite-coated ZVI in the system contributes to 4.6 µS/cm, 7.4 µS/cm, and 8.8 µS/cm in EC, respectively. This test confirm our hypothesis that the presence of media in a fluidizing system could contribute to the EC. Magnetite-coated ZVI and magnetite are both superior to ZVI in elevating EC. In dry mode with fresh surface, ZVI should exhibit good electrical conductivity. The low EC increase with ZVI media under the test condition might be due to the formation of a passive oxide layer on the ZVI surface.

In pure 0.2 mM NaCl solution, EC was enhanced with increased mixing speed from 26.8 µS/cm to 28.9 µS/cm. The net increase in EC due to mixing was around 2.0 µS/cm, which is similar to the one with DI water. Na^+ and Cl^- in water has high mobility,

potentially moving at hundreds of meter per second. Thus the mixing speed has little impact on the EC. The slight increase in EC might be due to the thin film layer attached to the electrode surface. At high mixing speed, the stagnant layer could be thinner, thus EC could be increased. The changes of EC in 0.2 mM NaCl with ZVI, magnetite, or magnetite-coated ZVI at 900 rpm mixing speed were -7.4 µS/cm, 2.5 µS/cm and 10.3 µS/cm, respectively. The negative effect of ZVI to EC in a NaCl solution might be attributed to the potential interactions between ZVI surface and Cl-. Cl^- could transitorily adsorb onto the ZVI surface or form a surface complex with Fe as an Fe-Cl complex, resulting in the decrease of EC with less Cl^- ions in water (Foley, R.T., 1970). Compared with ZVI and magnetite, magnetite-coated ZVI is the most effective in promoting EC in a NaCl solution. Unlike ZVI and magnetite, the magnetite coating on the ZVI might possess distinct electronic properties with non-stoichiometric Fe(II)/Fe(III), structural defects and holes, which might provide effective sites for hosting mobile electrons or positive charge carriers that could enhance EC.

With DI water, ORP would be increased from -60 mV to -8 mV with increased mixing speeds (Fig. 28(b)), which might be attributed to the increased DO introduced by mixing. With ZVI or magnetite in the water, ORP increased from -174.7 mV to -168.2 mV and -141.9 mV to -86.6 mM, respectively. ZVI can maintain low ORP but magnetite lack such capacity, which is expected as ZVI is a reducing agent and magnetite is chemically inert. In contrast, magnetite-coated ZVI could create and maintain a strong reducing environment with ORP decreased from -121.6 mV to -221 mV. The observed increase in ORP before 200 rpm mixing speed might be attributed to the fact that at 200

rpm, most of the media are settled at the bottom of the reactor and as such, dissolved oxygen diffused from air prevails in determining the ORP in the liquid phase.

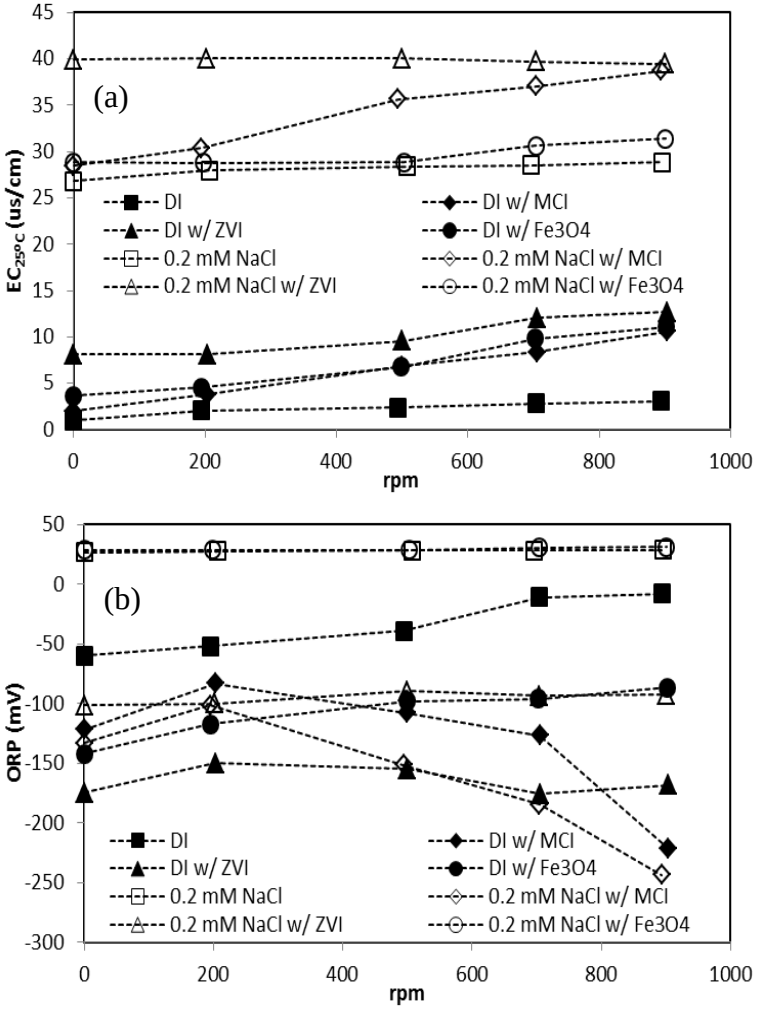

Figure 28. Changes of (a) EC and (b) ORP as a function of the mixing speed in the reactor filled with DI water or with 0.2 mM NaCl solution with the addition of magnetite-coated ZVI (MCI), ZVI, or magnetite (Fe_3O_4).

$NaNO_3$ Solution

With mixing with $NaNO_3$ solution, EC in ZVI, magnetite and magnetite-coated ZVI were all enhanced with accelerated mixing speeds (in 29(a)). The increases of EC in pure $NaNO_3$ solution and $NaNO_3$ solution with ZVI, magnetite and magnetite-coated ZVI in 900 rpm mixing speed were around 3.3 µS/cm, 8.9 µS/cm, 3.3 µS/cm and 14.0 µS/cm, respectively. Due to the similarity of EC change with pure solution, commercial magnetite could not contribute effective EC to the aqueous system, implying that pure magnetite could be inert with nitrate. Compared with NaCl solution, ZVI could provide positive EC instead of negative EC with increased mixing speeds, suggesting that unlike Cl^-, NO_3^- could not adsorbed on the surface of ZVI and could not form a chemical complex with Fe to reduce EC. In contrast, NO_3^- could initiatively interact with the ZVI grains to enhance electron transport for the EC increase. In addition, magnetite-coated ZVI was significantly active in $NaNoO_3$ solution. The enhancement of EC in $NaNO_3$ solution was greatly higher than in NaCl solution, indicating that magnetite-coated ZVI may proactively come in contact with NO_3^- to excite internal electrons with movements to promote electrical conductivity of magnetite-coated ZVI, corresponding to the increase of EC in liquid.

ORP was nearly invariable in pure $NaNO_3$ solution with increased mixing speeds, shown in Fig. 29(b). NO_3^- could be a predominant oxidant other than dissolved oxygen. With adding magnetite into $NaNO_3$ solution, ORP was gradually increased with increased mixing speeds. The increase of ORP from -7.4 mV to 56.4 mV suggested that the surface of magnetite could be oxidized by dissolved oxygen to form an oxidizing

ferric oxide, such as hematite, maghemite or lepidocrocite. Furthermore, due to no ORP change in NaCl solution, NO_3^- could facilitate the oxidization process of magnetite other than Cl^- for the increase of ORP in the system. Unlike magnetite, ORP in $NaNO_3$ solution with ZVI would be decreased from -242.2 mV to -264.5 mV. The pattern of ORP change in $NaNO_3$ solution was as similar as in DI solution, suggesting NO_3^- may not actively react to ZVI to produce reducing iron products but dissolved oxygen could dominantly play an important role in the oxidation process of ZVI with the accompanied reducing iron byproducts in liquid or on the surface of ZVI, resulting in the decrease of ORP. Moreover, magnetite-coated ZVI could significantly exhibit the particular reducing power with increased mixing speed more than ZVI. ORP in $NaNO_3$ solution with magnetite-coated ZVI would be varied from -121.7 mV to -255.0 mV. Therefore, magnetite-coated ZVI in a well-circulated environment could certainly produce reducing products for ORP reduction. The results indicated that magnetite-coated ZVI could be a powerful reducing iron oxide media on both inert solution of NaCl and oxidizing solution of $NaNO_3$ in a completely mixing system to create a strong reducing environment for redox reaction.

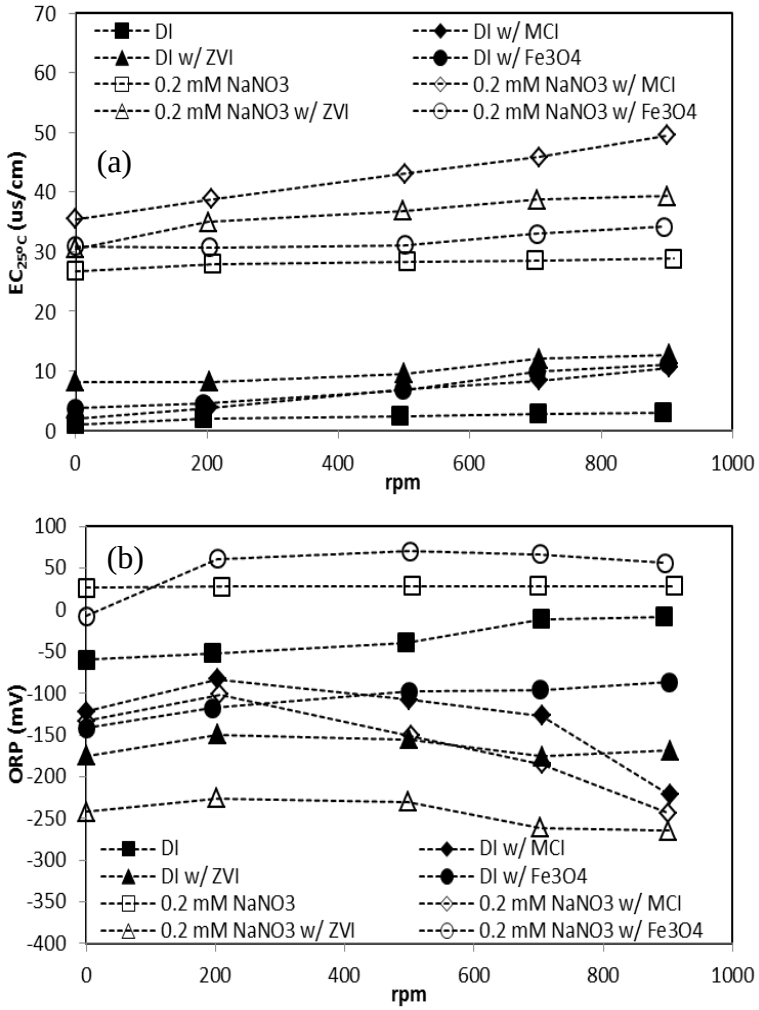

Figure 29. Changes of (a) EC and (b) ORP as a function of the mixing speed in the reactor filled with DI water or with 0.2 mM $NaNO_3$ solution with the addition of magnetite-coated ZVI (MCI), ZVI, or magnetite (Fe_3O_4).

Reactivity of Magnetite-Coated ZVI

Batch experiment had proved that magnetite-coated ZVI could create a reducing environment in a well-mixed condition and could increase EC up to 14 µS/cm in $NaNO_3$ solution without redox reaction for nitrate reduction. To investigate the effect of EC for the reactivity of magnetite-coated ZVI, CSTR experiments were conducted. In pure DI

solution with magnetite-coated ZVI, EC was changed between 34.9 µS/cm to 40.6 µS/cm, shown in Fig. 30(a). In addition, EC in the filtered DI solution was varied from 31.9 µS/cm to 35.7 µS/cm. The EC difference between the mixed solution (DI solution with magnetite-coated ZVI) and the filtered solution was the contribution from the solid media of magnetite-coated ZVI. Therefore, magnetite-coated ZVI could provide additional EC from 3.1 µS/cm to 6.4 µS/cm in DI solution with a well-mixed environment, shown in Fig. 30(b).

In 3 mM $NaNO_3$ solution, a pure magnetite-coated ZVI system exhibited limited removal capacity for nitrate reduction, shown in Fig. 31(a). pH was changed between 8.9 and 9.1. The results showed that magnetite-coated ZVI could not effectively remove nitrate in an alkaline condition. EC in the mixed and filtered solution were varied between 393.4 µS/cm and 396.6 µS/cm and between 382.1 µS/cm and 393.5 µS/cm, respectively. Thence, the EC contribution from magnetite-coated ZVI was between 2.7 µS/cm and 11.7 µS/cm but mostly distributed between 2.7 µS/cm and 6.1 µS/cm. The results suggested that magnetite-coated ZVI in both DI and $NaNO_3$ solution without any occurrences of contaminant reduction process could supply extra EC up to 11.7 µS/cm into the system. Consequently, the EC contribution of magnetite-coated ZVI in CSTR experiments was similar as in batch experiments, and magnetite-coated ZVI could consistently maintain its electronic properties in both anaerobic and aerobic environments.

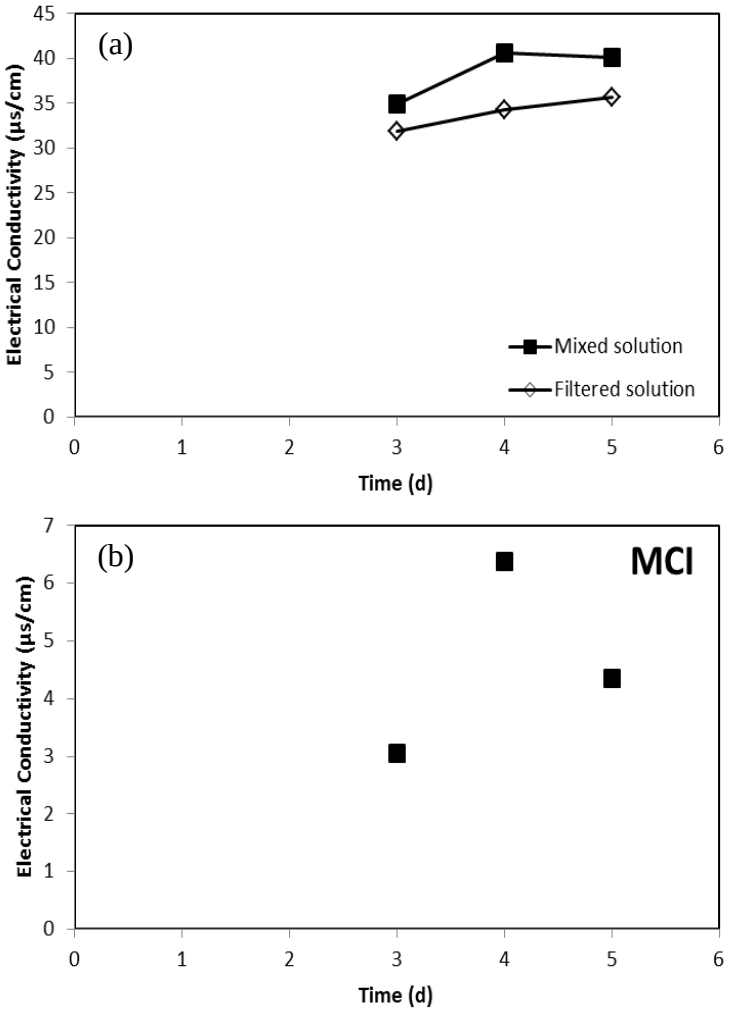

Figure 30. Changes of the electrical conductivity over time in a flow-through CSTR treatment system filled with magnetite-coated ZVI media. (a) total electrical conductivity as measured in the liquid suspension, and (b) electrical conductivity contributed by the magnetite-coated ZVI (MCI) particles ($EC_{MCI}=EC_{tot} - EC_{sol}$).

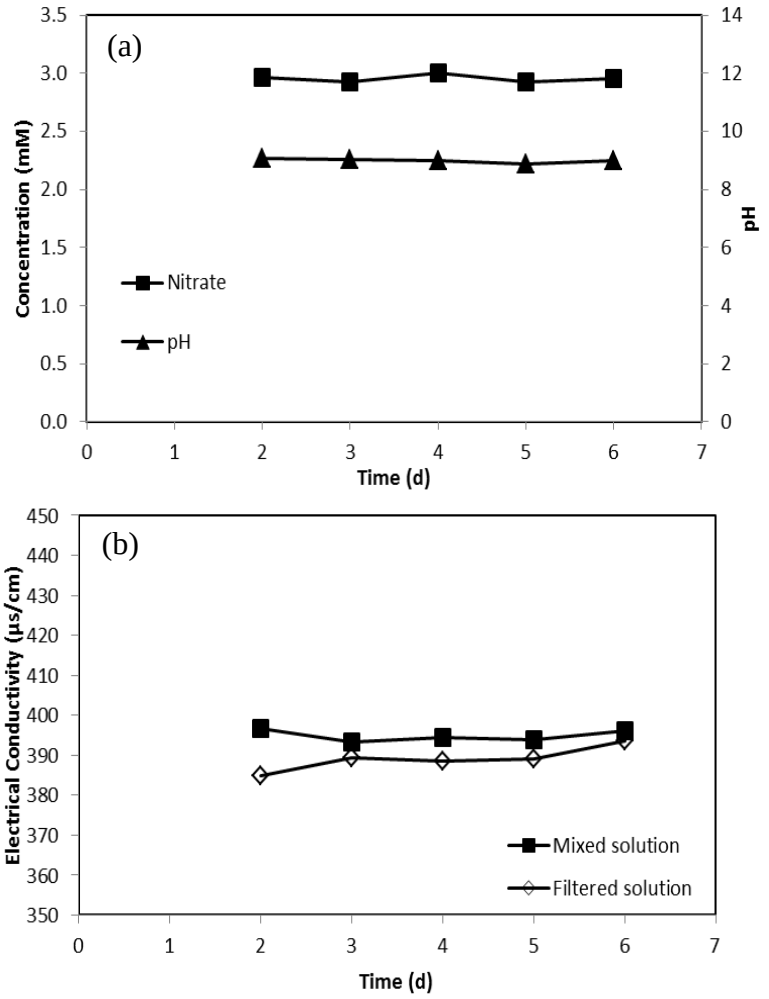

Figure 31. Changes of the electrical conductivity over time in a flow-through CSTR treatment system filled with magnetite-coated ZVI media and operated to treat a wastewater with 3.0 mM nitrate. (a) nitrate and pH changed over time; (b) total electrical conductivity as measured in the liquid suspension; and (c) electrical conductivity contributed by the magnetite-coated ZVI (MCI) particles ($EC_{MCI}=EC_{tot} - EC_{sol}$).

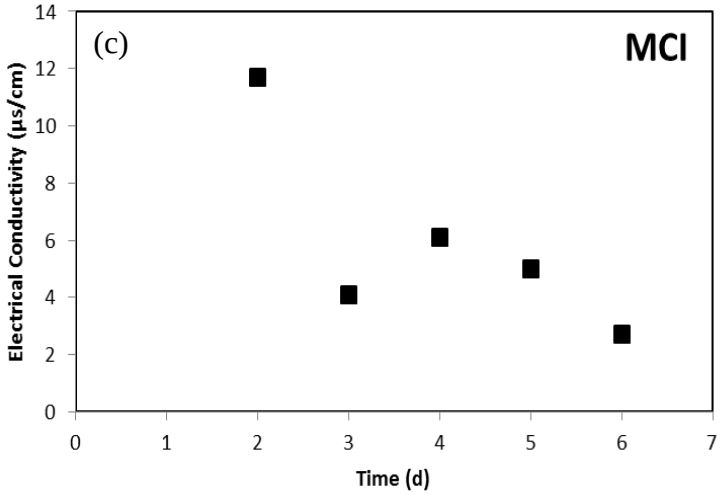

Figure 31. Continued.

With adding 0.1 mM Fe^{2+} into a magnetite-coated ZVI system, however, nitrate could be effectively reduced in the system with complete Fe^{2+} consumption, shown in Fig. 32(a). pH was stably kept aounrd netrual between 7.2 and 7.5 after nitrate reduction for 18 days CSTR operation. With nitrate reduction, EC in the mixed and filtered solution were varied between 368.1 µS/cm and 377.2 µS/cm and between 320.2 µS/cm and 359.1 µS/cm, respectively. Therefore, the EC contribution from magnetite-coated ZVI was between 10.9 µS/cm and 52.3 µS/cm with average EC of 30.2 µS/cm, shown in Fig. 32(b) and (c). The decrease of EC in the mixed and filter solution suggested that the reduction product of nitrate, ammonia, exhibited less electrical conductivity than nitrate. Furthermore, the redox reaction for nitrate reduction can transform the oxidant of nitrate to the lower reducing nitrogen compound. The electrons from magnetite-coated ZVI were transferred to the molecule of nitrate and nitrate will be reduced to ammonia. The process of electron transfer between magnetite-coated ZVI and nitrate could affect

electronic properties of magnetite-coated ZVI when nitrate was reduced by magnetite-coated ZVI. Consequently, the process of electron transport between chemical species could be reflected in the change of EC in the system. Compared with inert reaction for nitrate in both batch and experiment, EC was increased up to 52.3 µS/cm more than 14 µS/cm when nitrate could be reduced in a magnetite-coated ZVI system with 0.1 mM Fe^{2+} additions. The results implied that the high enhancement of EC from magnetite-coated ZVI could represent that the redox reaction could be occurring when magnetite-coated ZVI would be losing electrons to oxidants that would gain electrons for chemical reduction.

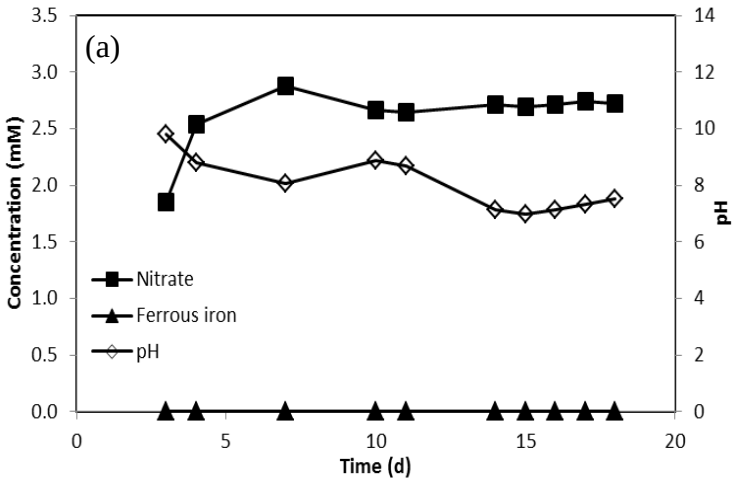

Figure 32. Changes of the electrical conductivity over time in a flow-through CSTR treatment system filled with magnetite-coated ZVI media and operated with the addition of 0.10 mM Fe^{2+} to treat a wastewater with 3.0 mM nitrate. (a) nitrate, Fe^{2+} and pH changed over time; (b) total electrical conductivity as measured in the liquid suspension; and (c) electrical conductivity contributed by the magnetite-coated ZVI (MCI) particles ($EC_{MCI}=EC_{tot} - EC_{sol}$).

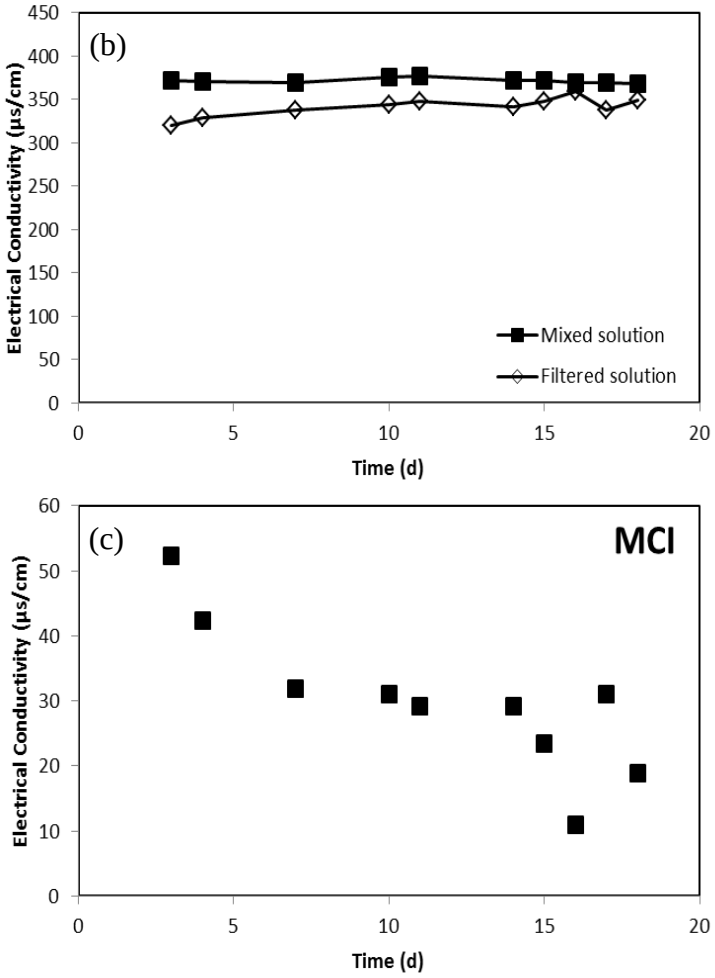

Figure 32. Continued.

Increased Fe^{2+} dosage could facilitate nitrate reduction in a magnetite-coated ZVI system, shown in Fig. 33(a). Although the removal efficiency of nitrate was similar, nitrate in 0.2 mM Fe^{2+} dosage could be reduced 0.12 mM more than in 0.1 mM Fe^{2+} dosage. The results showed that a magnetite-coated ZVI with Fe^{2+} addition could effectively reduce nitrate, and Fe^{2+} consumption may be proportionally pertinent to nitrate reduction. pH was maintained between 7.7 and 8.0 in a neutral environment after nitrate reduction for 18 days CSTR operation. EC in the mixed and filtered solution were

changed between 366.8 µS/cm and 395.6 µS/cm and between 320.0 µS/cm and 371.2 µS/cm, respectively. Consequently, the EC contribution from magnetite-coated ZVI was between 22.8 µS/cm and 64.6 µS/cm with average EC of 33.0 µS/cm, shown in Fig. 33(b) and (c). With 0.2 mM Fe^{2+} additions, EC contributed from magnetite-coated ZVI could be more stable than 0.1 mM Fe^{2+} additions. The results suggested that more nitrate reduction could lead to more electron transfer between magnetite-coated ZVI and nitrate, resulting in higher EC output from magnetite-coated ZVI.

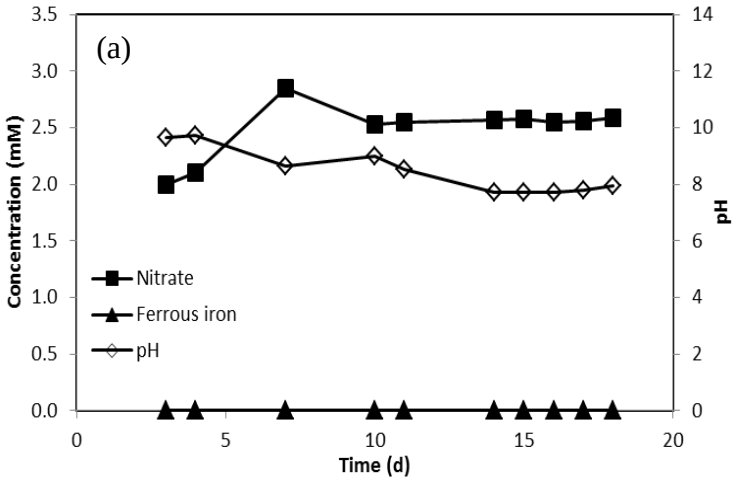

Figure 33. Changes of the electrical conductivity over time in a flow-through CSTR treatment system filled with magnetite-coated ZVI media and operated with the addition of 0.10 mM Fe^{2+} to treat a wastewater with 3.0 mM nitrate. (a) nitrate, Fe^{2+} and pH changed over time; (b) total electrical conductivity as measured in the liquid suspension.

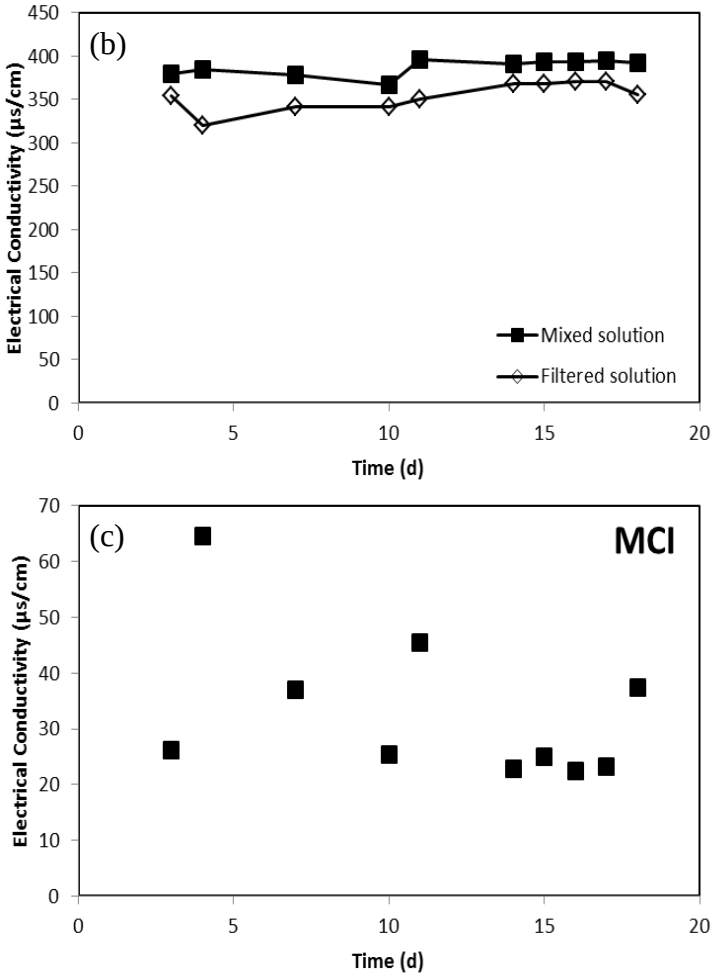

Figure 33. Continued.

Summary

The solid media in a fluidized reactor can contribute to the electrical conductivity of a mixed suspended liquid. In the presence of high total dissolved salts (e.g., 1 mM), dissolved cations and anions in the water contribute most to the the EC and the moving suspended media play a minor role in determining the EC. The physical chemical properties of media will determine how effective the suspended media contribute to the electrical conductivity. Our tests confirmed that under comparable conditions, highly

reactive magnetite-coated ZVI resulted in higher net increase in electrical conductivity of the reaction mixture than in the presence of an inert media. Virgin ZVI media resulted in poorer electrical conductivity than magnetite-coated ZVI, which corroborate the role of magnetite coating in promoting electron conduction and also the reactivity. The magnetite coating on ZVI also show superior EC than commercial magnetite (without ZVI in core). Thus it can be inferred that the reactive magnetite coating possess distinct physical and chemical properties from that of the commercial magnetite crystalline.

This study pioneer an innovative effort to assess the reactivity of a ZVI-based media. Through the tests, we proved that EC is viable parameter for evaluate the quality and maybe even the quantity of the ZVI media for supporting redox reaction. The work open up a new horizon and toolbox for future progress in understanding the interfacial chemistry involved a media system deployed for environmental applications.

CHAPTER VII SUMMARY

This research demonstrated that adding metal ions of Mn^{2+} or Zn^{2+} as a supplementary reagent into an activated iron media treatment system could significantly affect the system performance for both nitrate and selenate removal. The reaction kinetics for particular contaminant removal could be greatly enhanced with the augment of selected metal ions, such as Fe^{2+}, Mn^{2+} or Zn^{2+} in the AIM treatment system. The results inferred that both aqueous and structural metal ions could play an important role in shaping the reactivity of the activated iron media, through altering the composition and its physico-chemical properties of the metal oxide phase in the media. The so-call magnetite coating we created in the activated iron media are in fact an inverse spinel structure with mixed Fe(II)/Fe(III) oxides that possess high flexibility to incorporate metal ions including Mn^{2+} and Zn^{2+} without significantly changing its overall structure, or an isomorphic substitution. The incorporation of these metal impurities, however, did affect the overall reactivity of the system. The influence could vary depending on the specific target reactants, thus achieving selective reactivity for the media, for example, poor reactivity for nitrate, but reasonably high selenate reactivity. Such capacity could be employed to achieve selective removal of priority contaminants in a wastewater. When applied in treating heavy metal contaminated industrial wastewater with high nitrate presence, an AIM treatment system assisted with Zn^{2+} as the supplementary reagent could result in the desirable results of removing heavy metal but without reducing nitrate to ammonia.

The solid media in a fluidized reactor can contribute to the electrical conductivity of a mixed suspended liquid. The physical chemical properties of media will determine how effective the suspended media contribute to the electrical conductivity. The magnetite coating on ZVI showed superior EC capacity than either virgin ZVI or commercial magnetite (without ZVI in core). The EC study pioneers an innovative effort to assess the reactivity of a ZVI-based media. Through the tests, we proved that EC is viable parameter for evaluate the quality and maybe even the quantity of the ZVI media for supporting redox reaction. The work open up a new horizon and toolbox for future progress in understanding the solid state and interfacial chemistry involving a media system deployed for environmental applications.

REFERENCES

Alowitz, M.J., Scherer, M.M., 2002. Kinetics of nitrate, nitrite, and Cr(VI) reduction by iron metal. Environmental Science & Technology 36, 299-306.

APHA-AWWA-WEF, Standard methods for the examination of water and wastewater, 22nd ed., American Public Health Association, Washington, DC, 2012.

Cantrell, K.J., Kaplan, D.I., Wietsma, T.W., 1995. Zero-valent iron for the in situ remediation of selected metals in groundwater. Journal of Hazardous Materials 42, 201-212.

Chan, Y.T., Kuan, W.H., Chen, T.Y., Wang, M.K., 2009. Adsorption mechanism of selenate and selenite on the binary oxide systems. Water Research 43, 4412-4420.

Chen, L., Jin, S., Fallgren, P.H., Swoboda-Colberg, N.G., Liu, F., Colberg, P.J.S., 2012. Electrochemical depassivation of zero-valent iron for trichloroethene reduction. Journal of Hazardous Materials 239-240, 265-269.

Costa, R.C.C., Lelis, M.F.F., Oliveira, L.C.A., Fabris, J.D., Ardisson, J.D., Rios, R.R.V.A., Silva, C.N., Lago, R.M., 2006. Novel active heterogeneous Fenton system based on Fe3−xMxO4 (Fe, Co, Mn, Ni): The role of M^{2+} species on the reactivity towards H_2O_2 reactions. Journal of Hazardous Materials 129, 171-178.

Dahlberg, D., Ivanovic, J., Hassel, B., 2016. Toxic levels of ammonia in human brain abscess. Journal of Neurosurgery 124, 854-860.

Das, S., Jim Hendry, M., Essilfie-Dughan, J., 2013. Adsorption of selenate onto ferrihydrite, goethite, and lepidocrocite under neutral pH conditions. Applied Geochemistry 28, 185-193.

Della Rocca, C., Belgiorno, V., Meriç, S., 2007. Overview of in-situ applicable nitrate removal processes. Desalination 204, 46-62.

Dhaouadi, H., Ghodbane, O., Hosni, F., Touati, F., 2012. Mn_3O_4 nanoparticles: synthesis, characterization, and dielectric properties. ISRN Spectroscopy 2012, 8.

Dutrizac, J.E., Dinardo, O., Kaiman, S., 1981. Selenate analogues of jarosite-type compounds. Hydrometallurgy 6, 327-337.

Foley, R.T., 1970. Role of the chloride ion in iron corrosion, Corrosion 26, 58-70.

Fu, F., Lu, J., Cheng, Z., Tang, B., 2016. Removal of selenite by zero-valent iron combined with ultrasound: Se(IV) concentration changes, Se(VI) generation, and reaction mechanism. Ultrasonics Sonochemistry 29, 328-336.

Gonzalez, C.M., Hernandez, J., Peralta-Videa, J.R., Botez, C.E., Parsons, J.G., Gardea-Torresdey, J.L., 2012. Sorption kinetic study of selenite and selenate onto a high and low pressure aged iron oxide nanomaterial. Journal of Hazardous Materials 211-212, 138-145.

Görg, B., Schliess, F., Häussinger, D., 2013. Osmotic and oxidative/nitrosative stress in ammonia toxicity and hepatic encephalopathy. Archives of Biochemistry and Biophysics 536, 158-163.

Hassett, D.J., McCarthy, G.J., Kumarathasan, P., Pflughoeft-Hassett, D., 1990. Synthesis and characterization of selenate and sulfate-selenate ettringite structure phases. Materials Research Bulletin 25, 1347-1354.

Hayashi, H., Kanie, K., Shinoda, K., Muramatsu, A., Suzuki, S., Sasaki, H., 2009. pH-dependence of selenate removal from liquid phase by reductive Fe(II)–Fe(III) hydroxysulfate compound, green rust. Chemosphere 76, 638-643.

Henderson, A.D., Demond, A.H., 2007. Long-term performance of zero-valent iron permeable reactive barriers: a critical review. Environmental Engineering Science 24, 401-423.

Huang, C.-P., Wang, H.-W., Chiu, P.-C., 1998. Nitrate reduction by metallic iron. Water Research 32, 2257-2264.

Huang, Y.H., Peddi, P.K., Tang, C., Zeng, H., Teng, X., 2013. Hybrid zero-valent iron process for removing heavy metals and nitrate from flue-gas-desulfurization wastewater. Separation and Purification Technology 118, 690-698.

Huang, Y.H., Peddi, P.K., Zeng, H., Tang, C.-L., Teng, X., 2012a. Pilot-scale demonstration of the hybrid zero-valent iron process for treating flue-gas-desulfurization wastewater: Part I. Water Science and Technology 67, 16-23.

Huang, Y.H., Peddi, P.K., Zeng, H., Tang, C.-L., Teng, X., 2012b. Pilot-scale demonstration of the hybrid zero-valent iron process for treating flue-gas-desulfurization wastewater: Part II. Water Science and Technology 67, 239-246.

Huang, Y.H., Tang, C., Zeng, H., 2012c. Removing molybdate from water using a hybridized zero-valent iron/magnetite/Fe(II) treatment system. Chemical Engineering Journal 200-202, 257-263.

Huang, Y.H., Zhang, T.C., 2002. Kinetics of nitrate reduction by iron at near neutral pH. Journal of Environmental Engineering 128, 604-611.

Huang, Y.H., Zhang, T.C., 2004. Effects of low pH on nitrate reduction by iron powder. Water Research 38, 2631-2642.

Huang, Y.H., Zhang, T.C., 2005. Enhancement of nitrate reduction in Fe^0 -packed columns by selected cations. Journal of Environmental Engineering 131, 603-611.

Huang, Y.H., Zhang, T.C., 2006a. Nitrite reduction and formation of corrosion coatings in zerovalent iron systems. Chemosphere 64, 937-943.

Huang, Y.H., Zhang, T.C., 2006b. Reduction of nitrobenzene and formation of corrosion coatings in zerovalent iron systems. Water Research 40, 3075-3082.

Huang, Y.H., Zhang, T.C., Shea, P.J., Comfort, S.D., 2003. Effects of oxide coating and selected cations on nitrate reduction by iron metal. Journal of Environmental Quality 32, 1306-1315.

Hwang, Y.H., Kim, D.G., Shin, H.S., 2011. Mechanism study of nitrate reduction by nano zero valent iron. Journal of Hazardous Materials 185, 1513-1521.

Jordan, N., Ritter, A., Foerstendorf, H., Scheinost, A.C., Weiß, S., Heim, K., Grenzer, J., Mücklich, A., Reuther, H., 2013. Adsorption mechanism of selenium(VI) onto maghemite. Geochimica et Cosmochimica Acta 103, 63-75.

Kapoor, A., Viraraghavan, T., 1997. Nitrate removal from drinking water—review. Journal of Environmental Engineering 123, 371-380.

Lemly, A.D., 2004. Aquatic selenium pollution is a global environmental safety issue. Ecotoxicology and Environmental Safety 59, 44-56.

Liang, X., Zhong, Y., Tan, W., Zhu, J., Yuan, P., He, H., Jiang, Z., 2012. The influence of substituting metals (Ti, V, Cr, Mn, Co and Ni) on the thermal stability of magnetite. Journal of Thermal Analysis and Calorimetry 111, 1317-1324.

Luo, H., Jin, S., Fallgren, P.H., Colberg, P.J.S., Johnson, P.A., 2010. Prevention of iron passivation and enhancement of nitrate reduction by electron supplementation. Chemical Engineering Journal 160, 185-189.

Martínez, M., Giménez, J., de Pablo, J., Rovira, M., Duro, L., 2006. Sorption of selenium(IV) and selenium(VI) onto magnetite. Applied Surface Science 252, 3767-3773.

Moore, A., Young, T., 2005. Chloride Interactions with Iron Surfaces: Implications for Perchlorate and Nitrate Remediation Using Permeable Reactive Barriers. Journal of Environmental Engineering 131, 924-933.

Morita, M., Uemoto, H., Watanabe, A., 2007. Reduction of Selenium Oxyanions in Wastewater Using Two Bacterial Strains. Engineering in Life Sciences 7, 235-240.

Morrison, S.J., Mushovic, P.S., Niesen, P.L., 2006. Early Breakthrough of Molybdenum and Uranium in a Permeable Reactive Barrier. Environmental Science & Technology 40, 2018-2024.

Noubactep, C., Meinrath, G., Merkel, B.J., 2005. Investigating the Mechanism of Uranium Removal by Zerovalent Iron. Environmental Chemistry 2, 235-242.

Olegario, J.T., Yee, N., Miller, M., Sczepaniak, J., Manning, B., 2010. Reduction of Se(VI) to Se(-II) by zerovalent iron nanoparticle suspensions. Journal of Nanoparticle Research 12, 2057-2068.

Peak, D., Sparks, D.L., 2002. Mechanisms of Selenate Adsorption on Iron Oxides and Hydroxides. Environmental Science & Technology 36, 1460-1466.

Perrin, D.D., 1962. The hydrolysis of manganese(II) ion. Journal of the Chemical Society, 2197-2200.

Pettine, M., Gennari, F., Campanella, L., Casentini, B., Marani, D., 2012. The reduction of selenium(IV) by hydrogen sulfide in aqueous solutions. Geochimica et Cosmochimica Acta 83, 37-47.

Powell, B.A., Fjeld, R.A., Kaplan, D.I., Coates, J.T., Serkiz, S.M., 2004. $Pu(V)O^{2+}$ adsorption and reduction by synthetic magnetite (Fe_3O_4). Environmental Science & Technology 38, 6016-6024.

Rangroo Thrane, V., Thrane, A.S., Wang, F., Cotrina, M.L., Smith, N.A., Chen, M., Xu, Q., Kang, N., Fujita, T., Nagelhus, E.A., Nedergaard, M., 2013. Ammonia triggers neuronal disinhibition and seizures by impairing astrocyte potassium buffering. Nat Med 19, 1643-1648.

Robertson, W.D., Vogan, J.L., Lombardo, P.S., 2008. Nitrate Removal Rates in a 15-Year-Old Permeable Reactive Barrier Treating Septic System Nitrate. Ground Water Monitoring & Remediation 28, 65-72.

Rovira, M., Giménez, J., Martínez, M., Martínez-Lladó, X., de Pablo, J., Martí, V., Duro, L., 2008. Sorption of selenium(IV) and selenium(VI) onto natural iron oxides: Goethite and hematite. Journal of Hazardous Materials 150, 279-284.

Scott, T.B., Allen, G.C., Heard, P.J., Randell, M.G., 2005. Reduction of U(VI) to U(IV) on the surface of magnetite. Geochimica et Cosmochimica Acta 69, 5639-5646.

Siantar, D.P., Schreier, C.G., Chou, C.-S., Reinhard, M., 1996. Treatment of 1,2-dibromo-3-chloropropane and nitrate-contaminated water with zero-valent iron or hydrogen/palladium catalysts. Water Research 30, 2315-2322.

Soares, M.I.M., 2000. Biological denitrification of groundwater. Water, Air, & Soil Pollution 123, 183-193.

Soda, S., Kashiwa, M., Kagami, T., Kuroda, M., Yamashita, M., Ike, M., 2011. Laboratory-scale bioreactors for soluble selenium removal from selenium refinery wastewater using anaerobic sludge. Desalination 279, 433-438.

Statham, T.M., Stark, S.C., Snape, I., Stevens, G.W., Mumford, K.A., 2016. A permeable reactive barrier (PRB) media sequence for the remediation of heavy metal and hydrocarbon contaminated water: A field assessment at Casey Station, Antarctica. Chemosphere 147, 368-375.

Su, C., Puls, R.W., 2004. Nitrate Reduction by Zerovalent Iron: Effects of Formate, Oxalate, Citrate, Chloride, Sulfate, Borate, and Phosphate. Environmental Science & Technology 38, 2715-2720.

Su, C., Puls, R.W., 2007. Removal of added nitrate in the single, binary, and ternary systems of cotton burr compost, zerovalent iron, and sediment: Implications for groundwater nitrate remediation using permeable reactive barriers. Chemosphere 67, 1653-1662.

Su, C., Suarez, D.L., 2000. Selenate and selenite sorption on iron oxides: an infrared and electrophoretic study. Soil Science Society of America Journal 64, 101-111.

Szlachta, M., Chubar, N., 2013. The application of Fe–Mn hydrous oxides based adsorbent for removing selenium species from water. Chemical Engineering Journal 217, 159-168.

Tang, C., Huang, Y., Zhang, Z., Chen, J., Zeng, H., Huang, Y.H., 2016. Rapid removal of selenate in a zero-valent iron/Fe_3O_4/Fe^{2+} synergetic system. Applied Catalysis B: Environmental 184, 320-327.

Tang, C., Huang, Y.H., Zeng, H., Zhang, Z., 2014a. Promotion effect of Mn^{2+} and Co^{2+} on selenate reduction by zero-valent iron. Chemical Engineering Journal 244, 97-104.

Tang, C., Huang, Y.H., Zeng, H., Zhang, Z., 2014b. Reductive removal of selenate by zero-valent iron: The roles of aqueous Fe^{2+} and corrosion products, and selenate removal mechanisms. Water Research 67, 166-174.

Waychunas, G.A., Xu, N., Fuller, C.C., Davis, J.A., Bigham, J.M., 1995. Proceedings of the 8th international conference on X-ray absorption fine structure XAS study of AsO_4^{3-} and SeO_4^{2-} substituted schwertmannites. Physica B: Condensed Matter 208, 481-483.

Wilkin, R.T., Puls, R.W., Sewell, G.W., 2003. Long-term performance of permeable reactive barriers using zero-valent iron: Geochemical and Microbiological Effects. Ground Water 41, 493-503.

Xing, X., Li, M., Yuan, L., Song, M., Ren, Q., Shi, G., Meng, F., Wang, R., 2016. The protective effects of taurine on acute ammonia toxicity in grass carp Ctenopharynodon idellus. Fish & Shellfish Immunology 56, 517-522.

Xu, J., Hao, Z., Xie, C., Lv, X., Yang, Y., Xu, X., 2012. Promotion effect of Fe^{2+} and Fe_3O_4 on nitrate reduction using zero-valent iron. Desalination 284, 9-13.

Yang, G.C.C., Lee, H.-L., 2005. Chemical reduction of nitrate by nanosized iron: kinetics and pathways. Water Research 39, 884-894.

Yang, S., He, H., Wu, D., Chen, D., Liang, X., Qin, Z., Fan, M., Zhu, J., Yuan, P., 2009. Decolorization of methylene blue by heterogeneous Fenton reaction using $Fe_3{-}xTixO_4$ ($0 \leq x \leq 0.78$) at neutral pH values. Applied Catalysis B: Environmental 89, 527-535.

Yoon, I.-H., Kim, K.-W., Bang, S., Kim, M.G., 2011. Reduction and adsorption mechanisms of selenate by zero-valent iron and related iron corrosion. Applied Catalysis B: Environmental 104, 185-192.

Young, G.K., Bungay, H.R., Brown, L.M., Parsons, W.A., 1964. Chemical reduction of nitrate in water. Journal (Water Pollution Control Federation) 36, 395-398.

Zawislanski, P.T., Zavarin, M., 1996. Nature and rates of selenium transformations: a laboratory study of kesterson reservoir soils. Soil Science Society of America Journal 60, 791-800.

Zhang, M., Wang, H., Jin, S., Fallgren, P.H., Colberg, P.J.S., 2016. Electrochemically enhanced reduction of trichloroethene by passivated zero-valent iron. Journal of Environmental Chemical Engineering 4, 599-604.

Zhang, N., Lin, L.-S., Gang, D., 2008. Adsorptive selenite removal from water using iron-coated GAC adsorbents. Water Research 42, 3809-3816.

Zhang, Y., Amrhein, C., Frankenberger Jr, W.T., 2005a. Effect of arsenate and molybdate on removal of selenate from an aqueous solution by zero-valent iron. Science of The Total Environment 350, 1-11.

Zhang, Y., Wang, J., Amrhein, C., Frankenberger, W.T., 2005. Removal of selenate from water by zerovalent iron. Journal of Environmental Quality 34, 487-495.